ՀՀ ԳԻՏՈՒԹՅՈՒՆՆԵՐԻ ԱԶԳԱՅԻՆ ԱԿԱԴԵՄԻԱ
ՖԻԶԻԿԱԿԱՆ ՀԵՏԱԶՈՏՈՒԹՅՈՒՆՆԵՐԻ ԻՆՍՏԻՏՈՒՏ

Ազիզբեկյան Հրայր Հրանտի

ԼԱՆԴԱՈՒ-ԶԵՆԵՐԻ ԵՎ ԴԵՄԿՈՎ-ԿՈՒՆԻԿԵԻ ՈՉ ԳԾԱՅԻՆ ԵՐԿՎԻՃԱԿ ՄՈԴԵԼՆԵՐԸ

Ատենախոսություն

Ա.04.21 - «Լազերային ֆիզիկա» մասնագիտությամբ
ֆիզիկա-մաթեմատիկական գիտությունների թեկնածուի
գիտական աստիճանի համար

Գիտական ղեկավար՝
Պրոֆ. Արթուր Իշխանյան

ԵՐԵՎԱՆ – 2017

NATIONAL ACADEMY OF SCIENCE OF ARMENIA

INSTITUTE FOR PHYSICAL RESEARCH

Hrayr AZIZBEKYAN

NONLINEAR TWO-STATE LANDAU-ZENER AND DEMKOV-KUNIKE MODELS

A thesis in physics

submitted for the degree of doctor of philosopy

Specialization: A.04.21– Laser Physics

Scientific supervisor:

Prof. Artur ISHKHANYAN

YEREVAN – 2017

CONTENTS

ACKNOWLEDGMENTS

It is a great pleasure for me to thank those who made this thesis possible.

First of all, I would like to express the deepest appreciation to my supervisor, Prof. Artur Ishkhanyan for his invaluable assistance, numerous hours of inspiring talks and patience. Without his persistent support and decisive contributions, I would have not finished this project. I am very grateful to my supervisors Prof. Jocelyn Hanssen and Prof. Bedros Joulakian for their advices and valuable comments and I am also indebted to Prof. Bedros Joulakian for the good care of me as well as of all the small and big administrative issues arising during my PhD study in France.

I would like to thank all of my coauthors as well as colleagues from the Atom Optics Group of the Institute of Physical Research of Armenian National Academy of Sciences for fruitful discussions and successful collaboration for many years. Special thanks to Dr. Ruzan Sokhoyan and Dr. Vazgen Ghazarian for endless stimulating discussions and for constant friendly care. Also I would like to share the credit of my work with Mr. Ashot Manukyan for his sincere interest and guidance in my work and in general.

With immense gratitude I thank all the teachers and professors I met for being my source of strength, knowledge and inspiration, and for supporting me through this difficult path of becoming a researcher, I would like to mention separately Dr. Avetik Grigoryan and Prof. Mikael Grigoryan for the deep changes they made in my formation and my scientific perception.

And finally, I would like to show my sincere appreciation to my family and friends, who always been there for me whenever I need them, for the encouragement they give to keep me going and their love to empower me. And … thank you Astghik Shahkhatuni.

This research project would not have been possible without the financial assistance of French Embassy in Armenia for Grant No. 2006-3849 as Boursier du Gouvernement Français, Lorraine Graduate School of Chemistry and Molecular Physics, Armenian National Science and Education Fund (ANSEF Grant No. 2009-PS-1692), International Science and Technology Center (ISTC Grant N. A-1241), Federal Agency for Education of Russian Federation and Armenian "Luys" Educational Foundation

INTRODUCTION

In 2011 the scientific community celebrated the 50th anniversary of the demonstration of second harmonic generation (SHG) of light by a ruby laser pulse in a quartz crystal [1]. This discovery immediately became a hot focus of physics research and intense interest was observed over the next decades. Alongside with the development of various types of lasers, SHG set the foundation of nonlinear optics as a separate branch of physics. Nicolas Bloembergen much contributed in formulation of the main approaches of the theory of nonlinear optics and the development of laser physics [2-5], and his study led to an award of Nobel Prize in physics in 1981 (shared with Arthur Schawlow and Kai Siegbahn). SHG was also one of the major topics of physics research in Armenia since 1967. Particularly, the phenomenon was intensively studied in the Institute for Physical Research of Armenian National Academy of Sciences, Yerevan State University, Yerevan Physics Institute and Laser-Techniques R&D Company.

Development of the theory of SHG is still of high importance. Despite of focused attention and intensive efforts in this field [1-13], there is no systematic method to construct *uniformly valid* analytical solutions to the basic set of equations governing the process in the first approximation. Forced by significant mathematical singularities hidden in the governing equations, the analytical discussions are usually limited to very specific approximations applicable to limited ranges of involved parameters (nonlinear susceptibility, phase mismatch and spatial coordinate). However, recent breakthrough in the theory of molecule formation via photoassociation [14-17] and Feshbach resonance [18-23] of cold atoms in degenerate quantum gases led to a substantial progress in the understanding of the corresponding nonlinear mathematical problem. The suggested new methods and approaches could be applied for investigation of the SHG in different types of nonlinear media.

More detailed, the object of our study is the second harmonic generation in optical materials with specific dependence of $\chi^{(2)}(x)$ nonlinearity, for which no analytical solutions were possible to obtain so far. The behavior of the system for two types of nonlinear media is investigated: the basic resonance-crossing models of Landau-Zener [24-27] and Demkov-Kunike [28, 29]. The choice of

these specific configurations is caused by the desire to achieve as high conversion efficiency as possible. It is well known that in the linear case the Landau-Zener crossing allows up to 100% transition to the second state, and it was expected that the conversion coefficient (i.e., transfer of the energy from the fundamental wave to the second harmonic) will be high for nonlinear Landau-Zener model as well.

The Landau-Zener configuration is characterized by a phase mismatch that linearly varies in the direction of the propagation of the fundamental mode in an infinite medium with constant nonlinearity. However, the Landau-Zener model is overly idealized; hence, we consider other configurations promising high conversion efficiency that are close to real physical situations. Among the term-crossing models known from the linear theory, the Demkov-Kunike model is the most realistic one, since it implies nonlinear bell-shaped localization of the nonlinearity and a phase mismatch of finite variation that quasi-linearly crosses the resonance. This is a rather good approximation for a finite length nonlinear medium.

In the present study, we systematically examine the weak and strong interaction regimes of resonance crossing both for Landau-Zener and Demkov-Kunike models. The principal results are obtained by applying rather counterintuitive methods; however, we succeeded in developing simple approaches and derived compact analytical solutions for the problem under consideration for both of the chosen configurations. It turns out that in the limit of weak interaction the proposed solution is represented as a transformed solution of the corresponding system of linear equations. As regards the opposite limit of strong coupling, here the dynamics of the system is more complicated. The results show that in this regime the solution to the problem is written using a two-term ansatz involving three variational parameters. This ansatz can be applied to treat other configurations.

The obtained results indeed confirm that a Landau-Zener transition is able to provide complete conversion. However, our solution shows that for the Demkov-Kunike model it is impossible to transfer the whole energy of the system to the second-harmonic wave, as it is the case for the Landau-Zener model. Still, very high conversion coefficient is predicted.

The developed method and the obtained results are general and can be applied to many analogous problems because the involved type of the quadratic nonlinearity is generic for all the

bosonic field theories. For instance, the results are applicable in photoassociation of an atomic Bose–Einstein condensate, in controlling the scattering length of an atomic condensate by means of Feshbach resonance, and generally in field theories involving a Hamiltonian with a 2:1 resonance.

The results of this study allow various practical applications, such as optimal design of nonlinear frequency converters and doublers, including the proper choice of nonlinear crystal and its dimensions, the best phase matching configuration and the design of optical cavity, which are modern and widespread problems of practical importance in situations ranging from research and development of telecommunication systems to optical tool design where understanding of dynamics of phenomenological flow of the process in physically realized conditions is needed.

In ***Chapter 1*** we demonstrate that under certain conditions the behavior of second harmonic generation in a quadratic-nonlinear medium and the dynamics of ultracold atom-molecule formation in electromagnetic fields during photoassociation and Feshbach resonance are mathematically equivalent and can be described by the same set of two coupled nonlinear differential equations of the first order.

Using an exact nonlinear Volterra integral equation, we show that the linear two-state problem with normalization $1/4$ is an analog to the nonlinear two-state problem. Further, we define and discuss several models for the problem and examples of their physical interpretations. The importance and unique role of Landau-Zener (LZ) and Demkov-Kunike (DK) models for investigation of level crossing problems are discussed.

In ***Chapter 2*** we analyze a quadratic-nonlinear version of the Landau–Zener problem. In cold molecule formation the model describes the case, when the Rabi frequency is constant and the detuning linearly-in-time crosses the resonance. Two different approximations are proposed for weak and strong interaction regimes. In the weak interaction limit, using an exact third-order nonlinear differential equation for the molecular state probability or second harmonic waves' intensity, we propose an approximation written as the solution of the corresponding linear problem with modified parameters.

Considering the strong interaction regime, we propose an approximation written as a sum of two functions, namely, a solution of a limit fourth-order polynomial equation and a scaled solution

to the analogous linear Landau-Zener problem with modified parameters. We derive an expression for the final intensity of the second harmonic at the exit from the medium (or for final transition probability to the molecular state, if photoassociation terminology is used).

In ***Chapter 3*** we examine the spatial dynamics of second harmonic generation or the temporal dynamics of the atom-molecular system for Demkov-Kunike model. In cold molecule formation the model is defined by quasi-linear-in-time term-crossing detuning and bell-shaped pulse. We extend the approach developed for the case of the Landau-Zener model and propose an ansatz for the weak interaction regime as a scaled solution to the corresponding linear problem with some effective parameters. We also suggest an analytical expression for the scaling parameter, assuming that the parameters involved in the solution of the linear problem are not modified.

Further, we demonstrate that the approximate expression for the molecular state probability in the case of strong coupling can be effectively written as a sum of two terms; a solution of the limit first-order nonlinear differential equation and a scaled solution to the linear DK problem with fitting parameters defined through a variational procedure. We conclude by presenting a unified description of weak, intermediate, and strong nonlinearity regimes of the large-detuning case.

The main results of this dissertation have been published in 3 articles in peer reviewed journals, 3 conference proceedings and 2 conference abstracts. These results are as follows:

- A compact analytical theory describing the dynamics of the physical system with high accuracy and applicable for the whole range of input Landau-Zener parameter's variation is constructed for quadratic-nonlinear two-state problem for the Landau-Zener model.
- A variational approach is developed for the Landau-Zener model for the strong interaction regime. The results reveal a remarkable observation that in this coupling limit the resonance crossing is mostly governed by the nonlinearity while the coherent oscillations coming up soon after the resonance has been crossed are principally of linear nature.
- A two-term ansatz is proposed, describing the dynamics within the nonlinear Demkov-Kunike model. The proposed approximation, written as a scaled solution to the linear problem associated to the nonlinear one we treat, contains fitting parameters which are determined through a variational procedure. We suggested analytic expressions for the

parameters. The absolute error of the constructed approximation is less than $3 \cdot 10^{-5}$ for the final transition probability while at certain time points it might increase up to 10^{-3}.

- Three distinct interaction regimes (weak, moderate and strong coupling) of dynamics are shown to occur in a nonlinear Demkov-Kunike level crossing process at large final detuning.

CHAPTER 1. THE NONLINEAR TWO-STATE PROBLEM, BASIC MATHEMATICAL APPROACHES

In the present chapter we define and analyze the general properties and the applicability range of the basic quadratic-nonlinear two-state problem we consider in the present thesis.

We demonstrate that under certain conditions the second harmonic generation in a quadratic-nonlinear optical medium, as well as the dynamics of ultracold atom – molecule transitions in quantum degenerate gases subject to laser photoassociation or magnetic Feshbach-resonance are in the first approximation mathematically equivalent and can be treated in the framework of this basic quadratic-nonlinear two-state problem.

The governing set of equations for this problem is represented by two coupled nonlinear differential equations of the first order involving two input functions, the pair of which is referred to as configuration. The physical meaning of the functions involved in a configuration for the two processes, second harmonic generation and cold atom association, is discussed and the physical quantities standing for these functions in each case are mentioned. Several particular configurations, referred to as models, known from the linear theory are listed and the importance of Landau-Zener and Demkov-Kunike models for investigation of level crossing problems is discussed.

A Volterra integral equation of the second kind for the second state's probability is derived for models with constant and variable amplitudes. General properties of the derived equation are discussed. It is noted that the equation may provide a systematic way to attack the nonlinear problem in the case of small enough Landau–Zener parameter.

It is shown that the linear two-state problem with normalization $1/4$ *is an analog to the nonlinear two-state problem under consideration, namely, it is shown that in the limit of vanishing nonlinearity the solution to the nonlinear problem tends to the solution of this linear problem. The solutions of the associated linear two-state problem in terms of the Gauss hypergeometric functions are presented.*

1.1. Second harmonic generation. A basic nonlinear two-state problem.

Second harmonic generation in a quadratic nonlinear medium is the first nonlinear optical effect observed soon after the invention of powerful sources of coherent light radiation, the lasers. The phenomenon was widely explored due to the many interesting applications. Besides of its practical use, SHG as a basic nonlinear process can be used to demonstrate many characteristics of nonlinear optics like intensity dependence, phase-sensitivity, etc. Besides, the analytical solutions of SHG are applicable in various fields of physics as well and therefore are of wide interest.

The creation of second harmonic, corresponding to the elementary process of the creation of a new quantum with double energy by the annihilation of two light quanta was first observed by Franken and co-workers [1]. Although in the radiofrequency and microwave range of the electromagnetic spectrum the multiple photon absorption and harmonic generation have been observed much earlier, but it is for the optical region, that phase relationships between the waves propagating in the nonlinear medium play especially important role.

The optical response of a material is expressed in terms of the induced polarization $\mathbf{P}$. For a linear material the relation between the polarization and the electric field $\mathbf{E}$ of the incident radiation is linear: $\mathbf{P} = \varepsilon_0 \chi^{(1)} \mathbf{E}$, where $\chi^{(1)}$ is the linear susceptibility.

In nonlinear optics, the response of the material can be described as a Taylor expansion of the material polarization $\mathbf{P}$ in powers of the electric field $\mathbf{E}$:

$$\mathbf{P} = \varepsilon_0 \sum_n \chi^{(n)} \mathbf{E}_n = \varepsilon_0 \chi^{(1)} \mathbf{E} + \varepsilon_0 \chi^{(2)} \mathbf{E}^2 + \varepsilon_0 \chi^{(3)} \mathbf{E}^3 + \ldots, \tag{1.1}$$

where $\chi^{(n)}$ corresponds to the tensor of the n-th order nonlinear process. For most practical applications that consider a specific nonlinear process in a well defined direction, the tensor can be reduced to a single effective nonlinear coefficient. For the second harmonic generation, we consider only second order term and the resulting nonlinear polarization is:

$$P_k^{\mathrm{NL}} = \varepsilon_0 \chi_{ijk}^{(2)} E_i E_j, \tag{1.2}$$

where P_k^{NL} are components of material polarization ($k = x, y, z$). The harmonic input field is given by

$$E_i = A_i e^{-i\omega t} + c.c., \tag{1.3}$$

where A_i is a field amplitude at a given position, and ω is the frequency.

The resulting second order non-linear polarization is:

$$P_k^{\mathrm{NL}} = \varepsilon_0 \chi_{ijk}^2 (A_i A_j e^{-i2\omega t} + A_i^* A_j^* e^{i2\omega t} + A_i A_j^* + A_i^* A_j). \quad (1.4)$$

As we can see the non-linear polarization contains a component that radiates at twice the frequency of the input light. There is also another component at frequency zero, characterizing an effect known as optical rectification. Further we will ignore this DC electrical field and discuss only the second harmonic.

In most of materials second harmonic generation cannot be observed due to the important symmetry aspect of the Taylor expansion. All even-order coefficients must disappear for media with inversion symmetry, since the symmetry inversion operation $\vec{r} \to -\vec{r}$ changes sign of $\vec{P} \to -\vec{P}$ and $\vec{E} \to -\vec{E}$, but leaves the inversion-symmetric media unaffected, which is possible only when $\chi^{(n)} = 0$ for even n. Therefore, second harmonic generation can be observed only in a very specific class of nonlinear media, since most materials have inversion symmetry.

The rough estimate of the light intensity required for observation of harmonic generations is the following. The intensity of a higher order scattering process will be smaller than the scattering in the next lower order process by a factor

$$\left(\frac{E_l}{E_{at}}\right)^2 \sim \left(\frac{eEa}{(W_0 - W_n)^2}\right)^2 \quad (1.5)$$

if the scattering is due to electric dipole-type transitions [3]. E_l is the electric field in the light wave and $E_{at} \approx 3\times10^8 V/cm$ is a measure of the average atomic electric field acting on valence electrons, a is the atomic radius, and $W_0 - W_n$ is the average excitation energy of the atom. In practice nonlinear effects are observable for $(E_l / E_{at})^2 \sim 10^{-10}$ or $E_l \approx 3\times10^3 V/cm$, which corresponds to light intensity of $0.25 MW/cm^2$, that is available even in unfocused laser beams.

Because of the relative strength of the nonlinear coefficients it is logical that the first nonlinear optical process to be discovered was second-harmonic generation, in which a small fraction of the incident laser light is converted into light at twice the incident frequency (Fig. 1.1).

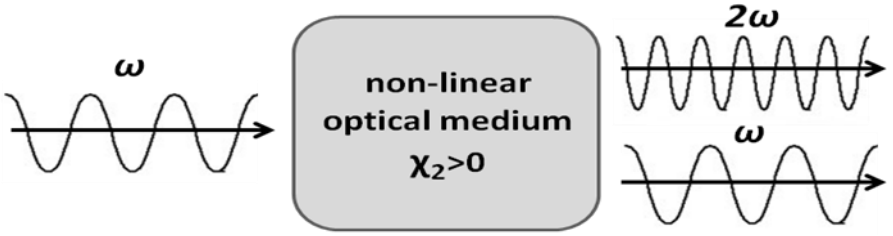

Figure 1.1. Second harmonic generation in a nonlinear medium.

Let us consider the relatively simple case, the generation of second harmonic for plane waves. The limit of plane wave can be achieved in practice when a laser beam is wide enough to neglect focusing effects. The plane wave with wave vector $\vec{k}_\omega$ of incident light with frequency ω *is* proportional to $e^{-i\vec{k}_\omega \vec{r}}$. For simplicity we assume $\vec{k}_\omega = (0,0,k_{z,\omega})$, that is the fundamental and second harmonic beam propagate in the positive z direction. The nonlinear polarization creates a dipole emitter that radiates at twice the fundamental frequency at every position in the non-linear crystal, and at every time the relative phase of these dipoles is given by the non-linear polarization generated by the fundamental wave:

$$\left(e^{ik_{z,\omega}z}\right)^2 = e^{i2k_{z,\omega}z}. \tag{1.6}$$

The plane waves emitted in the forward direction are plane-waves at double the frequency and have the form $e^{-ik_{z,2\omega}z}$. The overall efficiency of this process in the forward direction is obtained by adding all contributions from different positions. This leads to the following integral that gives the conversion efficiency per unit length of the process (in terms of intensity):

$$\eta = \frac{1}{\mathrm{L}^2}\left|\int_o^L e^{i2k_\omega z} e^{-ik_{2\omega}z}\,dz\right|^2 = \frac{1}{\mathrm{L}^2}\left|\int_o^L e^{i\Delta k z}\,dz\right|^2 = \left(\frac{\sin(\Delta k L/2)}{\Delta k L/2}\right)^2, \tag{1.7}$$

where L, thickness of nonlinear medium, extends from $z=0$ to $z=L$, $\Delta k = 2k_\omega - k_{2\omega}$ is the wave vector mismatch of the process. The maximum value $\eta = 1$ is obtained, when $\Delta k = 0$.

In the limits of coupled-plane wave approach and the approximation of slowly varying envelopes, the equations describing two interacting waves with amplitudes A_1 and A_2 propagating

in the positive direction of a spatial t axis in a nonlinear medium are as follows [3]

$$\begin{cases} \dfrac{dA_1^*}{dz} = +i\dfrac{2\omega^2 K}{k_1 \cos^2\alpha_1} A_2^* A_1 e^{+i(2k_1-k_2)z}, \\ \dfrac{dA_2}{dz} = -i\dfrac{4\omega^2 K}{k_2 \cos^2\alpha_2} A_1^2 e^{+i(2k_1-k_2)z}. \end{cases} \tag{1.8}$$

The detailed derivation of this set of equations from Maxwell's equations is given in Appendix 1. The theory can be applied to a wide variety of phenomena where nonlinearities play a role. It should be noted that several assumptions are made throughout the treatment, e.g., only monochromatic waves with perfectly defined propagation vector are considered.

The intrinsic nonlinear properties of electrons and ions bound in atoms, molecules, and dense media can be connected with the macroscopic properties of Maxwell's field quantities in nonlinear dielectrics. This permits a detailed description of the coherent nonlinear scattering processes in terms of macroscopic, nonlinear susceptibilities. The interaction between coherent light waves leads to a rigorous solution which shows that it is possible for the idealized cases to convert power completely from some frequencies to others.

The set (1.8) of two coupled nonlinear equations is encountered in many processes, and its canonical representation (Zener's form) we adopt is as following:

$$\begin{cases} i\dfrac{da_1}{dt} = U(t)e^{-i\delta(t)} a_2 \bar{a}_1, \\ i\dfrac{da_2}{dt} = \dfrac{U(t)}{2} e^{i\delta(t)} a_1 a_1. \end{cases} \tag{1.9}$$

The system describes interacting waves with amplitudes a_1 and a_2, propagating in the positive direction of a spatial t-axis, $\bar{a}_1$ is the complex conjugate to a_1, the real function $U(t)$ is proportional to the second-order optical susceptibility of the medium (usually variable) $\chi^{(2)}(t)$, and $\delta(t)$ is the phase difference between the waves involved, i.e., its *derivative* is the wave number mismatch: $\delta_t = 2k_1 - k_2$. Below, we put $\delta(t) = 2\delta_0 t$, thus adopting the notation $2\delta_0 = 2k_1 - k_2$; the factor 2 before δ_0 is introduced here just for convenience. The initial conditions considered below is $a_1(-\infty) = 1$, $a_2(-\infty) = 0$, so that we assume that there is no seed of second harmonic at the

entrance into the medium.

System (1.9) assumes a lossless medium. In accordance with that, the system possesses a motion integral which expresses the conservation of the field power flow, or, equivalently, the number of particles (photons) involved in the frequency conversion process. We normalize this integral to unity:

$$|a_1|^2 + 2|a_2|^2 = \text{const} = 1, \tag{1.10}$$

so that $p = |a_2|^2$ effectively acts as a measure of the conversion efficiency.

1.2. Photoassociation and Feshbach resonance of ultracold atoms

Quantum degenerate gases (Bose-Einstein condensates and Fermi-gases) of ultracold atoms and molecules have become a dynamically developing research domain due to recent experimental and theoretical achievements (see, e.g., [30-34]). The domain essentially rests on two fascinating discoveries. At first Steven Chu, Claude Cohen-Tannoudji, William D. Phillips developed methods to cool and trap atoms with laser light [35-37]. Afterwards, in 1995, based on this discovery and further theoretical and experimental advancements, three groups could experimentally observe Bose-Einstein condensation (BEC) by cooling alkali atoms (rubidium at JILA - Eric A. Cornell and Carl E. Wieman, sodium at MIT - Wolfgang Ketterle, lithium at Rice University - Randall G. Hulet) confined in traps to ~10^{-7} K [38-40] (the phenomenon of condensation at ultra-low temperatures was theoretically predicted by Satyendra Nath Bose and Albert Einstein in 1924-1925 [41, 42]). Both discoveries were highly appreciated and researchers were awarded Nobel Prizes in Physics in 1997 and 2001 correspondingly.

BEC can be considered as a state of matter of dilute gases of weakly interacting bosons confined and cooled to temperatures near absolute zero. A large fraction of bosons will occupy the lowest possible energy state, and many fascinating quantum effects can then be observed on a macroscopic scale. The BEC not only proved Einstein's proposed theory, but also opened large possibilities to study quantum mechanics, and in particular, the theory of matter based on wavelike properties of elementary particles. In quantum mechanics all particles with mass m and temperature T can be characterized as wave packets with the de Broglie wavelength $\lambda_{dB} = \sqrt{2\pi\hbar^2/(mk_BT)}$. By decreasing temperature of atoms, it is possible to make λ_{dB} comparable with the interatomic separation and achieve overlapping of atoms. In this case, bosonic atoms become indistinguishable; the wave nature of each atom is coherent with that of every other and a gas of atoms with the same quantum-mechanical state forms a BEC. Quantum-mechanical waves extend across the sample of condensate and microscopic becomes macroscopic. Due to realization of BEC in dilute ultracold gases of neutral alkali-metal atoms many important nonlinear phenomena occurring in many-body quantum systems can be tested experimentally.

A further even more appealing step was to create molecular BEC [43-46], since due to the complex internal structure of molecules the new range of properties and thus new important applications can be observed and studied, for instance, processes referred as "superchemistry" [47], quantum computation and information processing [48, 49], high precision molecular spectroscopy and precision measurements [50-54].

Standard laser cooling techniques used for atoms only freezes the centre-of mass motion of a quantum object and therefore are inefficient in the case of molecules, since molecules possess rotational and vibrational degrees of freedom. Several approaches are developed to overcome this problem. The most widely used ones are the optical laser photoassociation, when excited molecule is formed by two colliding atoms interacting with a laser field [14-17, 55] and magnetic Feshbach resonance, which occurs when the energy of a bound molecular state is equal to the total energy of a colliding pair of atoms, which can lead to atom-molecule transitions during collision [18-23]. Consequently, the Raman photoassociation and magnetic Feshbach resonance have become the standard tools to create cold molecules starting from ultracold atomic gases [48, 56, 57].

The above-discussed photo- and magneto-association processes based upon the two-mode association scheme for an effective quantum two-state system are also described by the set of coupled equations (1.9). In this case a_1 and a_2 represent the free atomic and bound molecular states' probability amplitudes, respectively. In photoassociation, $U(t)$ is the Rabi frequency, and $\delta(t)$ is the detuning modulation function, defined as the integral of the frequency detuning. The Rabi frequency is proportional to the amplitude of the laser field, and the detuning δ_t is defined as $\delta_t = \omega_{21} - \omega_L(t)$, where ω_{21} is the frequency corresponding to the atom-molecule transition, and ω_L is the frequency of the laser field. The system once again describes a lossless process, and the equation (1.10) is the normalization to unity of the total number of particles.

Thus, all three above discussed processes are governed by the same set of equations (1.9), and hereafter we will refer to it as a basic nonlinear two-state problem. This nonlinear two-state problem was always in the center of attention and was studied from various sides and by different groups of researchers [58-69]. We will discuss and analyze various approximations and models

proposed for this system.

In the table below we brought parameters of the canonical representation (so called Zener's form) of the problem for the processes we analyze; second harmonic generation, cold molecule formation via photoassociation and magnetic Feshbach resonance. Using this table, mathematical approximations and conclusions made for one set of parameters can be transferred to other processes and physical parameters.

Table 1. Definition of parameters of the canonical representation (Zener's form) for second harmonic generation, photoassociation and Feshbach resonance.

	Second Harmonic Generation	**Photoassociation**	**Feshbach Resonance**
U	second order nonlinear susceptibility	Rabi frequency of laser field	square root of the magnetic-field width of the resonance
δ_t	phase mismatch	frequency detuning	magnetic field
a_1	fundamental wave's amplitude	atomic state's probability amplitude	atomic state's probability amplitude
a_2	second harmonic wave's amplitude	molecular state's probability amplitude	molecular state's probability amplitude
$p = \lvert a_2 \rvert^2$	conversion efficiency	transition probability	transition probability
t	spatial coordinate	temporal coordinate	temporal coordinate

1.3. Volterra integral equation for the models with constant and variable field amplitude

In the present section we derive, following the lines of [58], a Volterra integral equation [70] written for arbitrary field configuration that will play an important role in further developments. The integral equation is obtained using the Fubini method [70] that in its turn is based on the formal application of the Lagrange's method of constant variation.

First, we obtain some useful relations that straightforwardly follow from (1.9). We multiply the equations of system (1.9) by each other and get the equation

$$-a_{1t}a_{2t} = \frac{U^2}{2} a_2 a_1 |a_1|^2 . \tag{1.11}$$

Then we divide the first equation of the system (1.9) by the complex conjugated second equation that gives us the following relation:

$$-\frac{a_{1t}}{\bar{a}_{2t}} = 2\frac{a_2}{\bar{a}_1} \;\Rightarrow\; a_{1t} = -2\frac{a_2}{\bar{a}_1}\bar{a}_{2t} . \tag{1.12}$$

By putting (1.12) into (1.11) we get the equation

$$|a_{2t}|^2 = \frac{U^2}{4}|a_1|^4 . \tag{1.13}$$

This equation can be straightforwardly obtained by taking modulus square of the second equation of (1.9).

Now, we turn to the modulus and arguments of the complex amplitudes $a_{1,2}$

$$\begin{aligned} a_1 &= r_1(t)e^{i\theta_1(t)} , \\ a_2 &= r_2(t)e^{i\theta_2(t)} . \end{aligned} \tag{1.14}$$

Equation (1.13) written in the new variables has the following form

$$\left(\frac{dr_2}{dt}\right)^2 + r_2^2\left(\frac{d\theta_2}{dt}\right)^2 = \frac{U^2}{4}(1-2r_2^2)^2 . \tag{1.15}$$

Note that in the variables (1.14) the normalization condition is written as

$$r_1^2 + 2r_2^2 = 1 . \tag{1.16}$$

We introduce the following notations:

$$p = r_2^2,\ q = 2r_2^2 \frac{d\theta_2}{dt}. \tag{1.17}$$

In the new notations equation (1.15) is rewritten as follows:

$$\left(\frac{dp}{dt}\right)^2 + q^2 = U^2(1-2p)^2 p\,. \tag{1.18}$$

First we discuss, following [58], the constant-amplitude case $U = U_0 = \text{const}$. In this case, for the derivative of equation (1.15) we have

$$U_0{}^2\left(1-2r_2^2\right)r_2 = -\left(\ddot{r}_2 + r_2\dot{\theta}_2^2 + \frac{r_2^2}{\dot{r}_2}\dot{\theta}_2\ddot{\theta}_2\right) \tag{1.19}$$

(here, the dot indicates the derivative with respect to time).

Now via elimination of one of the dependent variables of the system (1.9) and using (1.10) we obtained the following nonlinear equations of the second order:

$$a_{1tt} + \left(i\delta_t - \frac{U_t}{U}\right)a_{1t} - \frac{U^2}{2}\left(1-2|a_1|^2\right)a_1 = 0\,, \tag{1.20}$$

$$a_{2tt} + \left(-i\delta_t - \frac{U_t}{U}\right)a_{2t} + U^2\left(1-2|a_2|^2\right)a_2 = 0\,. \tag{1.21}$$

In the case of constant amplitude, equation (1.21) is simplified:

$$a_{2tt} - i\delta_t a_{2t} + U_0{}^2\left(1-2|a_2|^2\right)a_2 = 0\,. \tag{1.22}$$

Using (1.14) we obtain the following useful relations:

$$a_{2t} = e^{i\theta_2}\left(\dot{r}_2 + ir_2\dot{\theta}_2\right), \tag{1.23}$$

$$a_{2tt} = e^{i\theta_2}\left(\ddot{r}_2 + 2i\dot{r}_2\dot{\theta}_2 + ir_2\ddot{\theta}_2 - r_2\dot{\theta}_2^2\right). \tag{1.24}$$

After substituting the relations (1.23)-(1.24) and (1.19) into the equation (1.22) we arrive at the equation

$$\left(i - \frac{2r_2^2\dot{\theta}_2}{2r_2\dot{r}_2}\right)\left(4r_2\dot{r}_2\dot{\theta}_2 + 2r_2^2\ddot{\theta}_2\right) = i\delta_t\left(2r_2\dot{r}_2 + 2r_2^2\dot{\theta}_2\right). \tag{1.25}$$

In notations (1.17), this equation is written as

$$\frac{\dot{q}}{\dot{p}}\left(\dot{p} + i\dot{q}\right) = \delta_t\left(\dot{p} + i\dot{q}\right) \quad \Leftrightarrow \quad \dot{q} = \delta_t\,\dot{p}\,. \tag{1.26}$$

After differentiation of (1.18) and taking into account (1.26) we obtain an equation:

$$\frac{d^2q}{dt^2} - \frac{\delta_{tt}}{\delta_t}\frac{dq}{dt} + \delta_t^2 q = \frac{U_0^2\delta_t}{2}(1-8p+12p^2), \tag{1.27}$$

which can be solved using the variation of constants method. It can easily be seen that the general solution of the homogeneous part of the equation (1.27) [if we equate to zero the right-hand side of the equation (1.27)] has the following form:

$$q = C_1\cos(\delta(t)) + C_2\sin(\delta(t)), \tag{1.28}$$

and the Wronskian of the fundamental solutions $W = q_1q_{2t} - q_2q_{1t}$ is equal to δ_t, hence the general solution of the inhomogeneous equation (1.27) can be written as

$$q(t) = \cos(\delta(t))\left(C_1 - \int_{t_0}^{t}\sin(\delta(x))\frac{U_0^2}{2}(1-8p(x)+12p^2(x))dx\right) +$$

$$\sin(\delta(t))\left(C_2 + \int_{t_0}^{t}\cos(\delta(x))\frac{U_0^2}{2}(1-8p(x)+12p^2(x))dx\right). \tag{1.29}$$

In the force of the relation (1.26) the differentiation of this equation leads to an integro-differential equation

$$\frac{dp}{dt} = -C_1\sin(\delta(t)) + C_2\cos(\delta(t)) + \cos(\delta(t))\int_{t_0}^{t}\cos(\delta(x))\frac{U_0^2}{2}(1-8p(x)+12p^2(x))dx +$$

$$\sin(\delta(t))\int_{t_0}^{t}\sin(\delta(x))\frac{U_0^2}{2}(1-8p(x)+12p^2(x))dx. \tag{1.30}$$

The constants $C_{1,2}$ should be determined from initial conditions. Below we consider the case, when the molecular state probability p satisfies the initial condition $p(t_0) = 0$, i.e. at the beginning of the process the condensate was completely atomic.

After integrating the equation (1.30) we obtain the equation

$$p(t) = -C_1S_\delta(t) + C_2C_\delta(t) + \frac{U_0^2}{2}\int_{t_0}^{t}\cos(\delta(x))\left(\int_{t_0}^{x}\cos(\delta(y))(1-8p(y)+12p^2(y))dy\right)dx +$$

$$\frac{U_0^2}{2}\int_{t_0}^{t}\sin(\delta(x))\left(\int_{t_0}^{x}\sin(\delta(y))(1-8p(y)+12p^2(y))dy\right)dx, \tag{1.31}$$

where we introduced the following notations:

$$C_\delta(t) = \int_{t_0}^{t} \cos\big(\delta(x)\big)dx\,,\quad S_\delta(t) = \int_{t_0}^{t} \sin\big(\delta(x)\big)dx\,. \tag{1.32}$$

Finally, the integration by parts leads (1.31) to a nonlinear ***Volterra integral equation*** of the second kind [58]

$$p(t) = -C_1 S_\delta(t) + C_2 C_\delta(t) + \frac{U_0^2}{2}\int_{t_0}^{t} K(t,x)(1-8p(x)+12p^2(x))dx\,, \tag{1.33}$$

where the kernel $K(t,x)$ is given by the expression

$$K(t,x) = \big(C_\delta(t) - C_\delta(x)\big)\cos\big(\delta(x)\big) + \big(S_\delta(t) - S_\delta(x)\big)\sin\big(\delta(x)\big). \tag{1.34}$$

After working out the first term of the integrand in (1.33) we finally arrive at the following Volterra integral equation of the second kind:

$$p(t) = f(t) - 4U_0^2\int_{t_0}^{t} K(t,x)(p(x) - \frac{3}{2}p^2(x))dx\,, \tag{1.35}$$

where the forcing function f is given by the expression

$$f(t) = -C_1 S_\delta(t) + C_2 C_\delta(t) + \frac{U_0^2}{4}\big(C_\delta^2(t) + S_\delta^2(t)\big). \tag{1.36}$$

Thus, we have shown that for all the models defined by the constant amplitude $U = U_0 = \text{const}$ (and arbitrary detuning $\delta_t(t)$) the probability of molecular state p satisfies Volterra integral equation (1.33) of the second kind.

Now we derive, following [58], an integral equation for the models with arbitrary varying amplitude $U(t)$ and detuning $\delta_t(t)$. It can be easily seen that the initial system (1.9) can be reduced to an equivalent system with constant field amplitude. Indeed, consider the following transformation of the independent variable t:

$$z(t) = \int_{t_0}^{t} \frac{U(t')}{U_0}dt'\,. \tag{1.37}$$

Since $U(t)$ is a sign preserving function, $z(t)$ is a monotonic function and the mapping (1.37) is one-to-one.

The latest statement is a consequence of the class property theorem. In order to prove this we consider any integrable class of the nonlinear two-level problem. It is clear that in any class one can always find a representative for which the amplitude is constant:

$$U^*(z) = U_0 = \text{const}\,. \tag{1.38}$$

Indeed, let a representative of a class be given by an amplitude $U(t)$ and detuning $\delta_t(t)$. Thus, the other representatives of the class will be determined by the formulas, where we consider $t(z)$ transformation:

$$U^*(z) = U(t)\frac{dt}{dz}, \tag{1.39}$$

$$\delta_z^*(z) = \delta_t(t)\frac{dt}{dz}. \tag{1.40}$$

On the function $t(z)$ we impose the condition that (1.38) must be satisfied. From (1.39) one can easily determine the function $z(t) \equiv t^{-1}(z)$ that is given by the formula (1.37). From the formula (1.38)-(1.40) it follows that

$$\delta_z^*(z(t)) = \delta_t(t)\frac{U^*(z(t))}{U(t)} = \delta_t(t)\frac{U_0}{U(t)}. \tag{1.41}$$

Thus, hereafter when we write « z » we refer to the variable for which the initial system of equations is written in the form

$$\begin{cases} i\dfrac{da_1^*(z)}{dz} = U_0 e^{-i\delta^*(z)} a_2^*(z)\bar{a}_1^*(z)\,, \\ i\dfrac{da_2^*(z)}{dz} = \dfrac{U_0}{2} e^{i\delta^*(z)} a_1^{*2}(z) \end{cases} \tag{1.42}$$

[$\delta^*(z)$ should be determined from (1.41)]. The differential equation for the probability, written in terms of the variable z, takes the following form:

$$p_{zzz}^* - \frac{\delta_{zz}^*}{\delta_z^*} p_{zz}^* + \left[\delta_z^{*2} + 4U_0^2(1-3p^*)\right]p_z^* + \frac{U_0^2}{2}\frac{\delta_{zz}^*}{\delta_z^*}\left(1-8p^*+12p^{*2}\right) = 0\,. \tag{1.43}$$

Since the present study is mostly dedicated to the strong interaction limit, we make an important remark, concerning this limit. The nonlinear terms in Eq. (1.43) are proportional to the

field intensity U_0^2. Hence, one may expect that the strong nonlinearity regime corresponds to high field strengths.

Using the results of the previous section, in particular the formula (1.32)-(1.34), one can write an integral equation equivalent to (1.43):

$$p^*(z) = C_1 C_\delta^*(z) + C_2 S_\delta^*(z) + \frac{U_0^2}{2}\int_{z_0}^{z} K^*(z,z')\left(1 - 8p^*(z') + 12p^{*2}(z')\right)dz', \tag{1.44}$$

where

$$C_\delta^*(z) = \int_{z_0}^{z} \cos\left(\delta^*(z')\right)dz',\ S_\delta^*(z) = \int_{z_0}^{z} \sin\left(\delta^*(z')\right)dz', \tag{1.45}$$

$$K(z,z') = \left(C_\delta^*(z) - C_\delta^*(z')\right)\cos\left(\delta^*(z')\right) + \left(S_\delta^*(z) - S_\delta^*(z')\right)\sin\left(\delta^*(z')\right), \tag{1.46}$$

and the forcing function $f^*(z)$ is now defined by the expression

$$f^*(z) = C_1 C_\delta^*(z) + C_2 S_\delta^*(z) + \frac{U_0^2}{4}\left(C_\delta^{*2}(z) + S_\delta^{*2}(z)\right). \tag{1.47}$$

Now, in the formula (1.44)-(1.47) we return to the physical variable *t* and obtain an integral equation written for a physical model defined by arbitrary amplitude and detuning:

$$p(t) = C_1 C_\delta(t) + C_2 S_\delta(t) + \frac{U_0^2}{2}\int_{t_0}^{t} K(t,t')\frac{U(t')}{U_0}\left(1 - 8p(t') + 12p^2(t')\right)dt', \tag{1.48}$$

where

$$C_\delta(t) = \int_{t_0}^{t} \cos\left(\delta(t')\right)\frac{U(t')}{U_0}dt',\ S_\delta(t) = \int_{t_0}^{t} \sin\left(\delta(t')\right)\frac{U(t')}{U_0}dt', \tag{1.49}$$

$$K(t,t') = \left(C_\delta(t) - C_\delta(t')\right)\cos\left(\delta(t')\right) + \left(S_\delta(t) - S_\delta(t')\right)\sin\left(\delta(t')\right). \tag{1.50}$$

And the forcing function should be written as

$$f(t) = C_1 C_\delta(t) + C_2 S_\delta(t) + \frac{U_0^2}{4}\left(C_\delta^2(t) + S_\delta^2(t)\right). \tag{1.51}$$

Let us now compare the nonlinear and linear problems. In the integral equation (1.48) whole nonlinearity is "concentrated" in the term

$$\frac{U_0^2}{2}\int_{t_0}^{t} K(t,t')\frac{U(t')}{U_0}(12p^2(t'))dt'.$$

It is then understood that the linear analog of the integral equation (1.48) is the equation

$$p_L(t) = C_1 C_\delta(t) + C_2 S_\delta(t) + \frac{U_0^2}{2}\int_{t_0}^{t} K(t,t')\frac{U(t')}{U_0}\left(1-8p_L(t')\right)dt'. \tag{1.52}$$

By means of differentiation of (1.52) it can be easily shown that it is equivalent to the following differential equation of the third order:

$$\begin{aligned} p_{Ltt} - \left(\frac{\delta_{tt}}{\delta_t} + 2\frac{U_t}{U}\right)p_{Ltt} + \left[\delta_t^2 + 4U^2 - \left(\frac{U_t}{U}\right)_t + \frac{U_t}{U}\left(\frac{\delta_{tt}}{\delta_t} + \frac{U_t}{U}\right)\right]p_{Lt} + \\ + \frac{U^2}{2}\left(\frac{\delta_{tt}}{\delta_t} - \frac{U_t}{U}\right)\left(1-8p_L\right) = 0. \end{aligned} \tag{1.53}$$

It is known that the canonical *linear* two-state problem is written as [71, 72]:

$$\begin{cases} i\dfrac{da_{1L}}{dt} = U(t)e^{-i\delta(t)}a_{2L}, \\ i\dfrac{da_{2L}}{dt} = U(t)e^{i\delta(t)}a_{1L}, \end{cases} \tag{1.54}$$

where index "L" emphasizes the linearity of the system. Its first integral is the quantity:

$$|a_{1L}|^2 + |a_{2L}|^2 = I_L = \text{const}. \tag{1.55}$$

From system (1.54) one obtains an equation for the second state's probability $\tilde{p}_L = |a_{2L}|^2$:

$$\begin{aligned} \tilde{p}_{Ltt} - \left(\frac{\delta_{tt}}{\delta_t} + 2\frac{U_t}{U}\right)\tilde{p}_{Ltt} + \left[\delta_t^2 + 4U^2 - \left(\frac{U_t}{U}\right)_t + \frac{U_t}{U}\left(\frac{\delta_{tt}}{\delta_t} + \frac{U_t}{U}\right)\right]\tilde{p}_{Lt} + \\ + \frac{U^2}{2}\left(\frac{\delta_{tt}}{\delta_t} - \frac{U_t}{U}\right)\left(4I - 8\tilde{p}_L\right) = 0. \end{aligned} \tag{1.56}$$

By comparing equations (1.53) and (1.56) we notice that if we apply $I_L = 1/4$ in (1.55) then (1.53) and (1.56) will coincide. Thus, we conclude that system (1.54) is the linear analog of the nonlinear system (1.9) (we stress again that one should keep in the mind the supplementary normalization constraint $I_L = 1/4$).

It is then understood that this linear problem should present a reasonable approximation for the nonlinear problem under consideration in the case of vanishing nonlinearity. An important further extension is that, as we show below, the solution to the linear problem can be appropriately modified to construct a much more advanced approximation to the nonlinear problem. This

extension is achieved by modifying the parameters involved in the linear solution. In the light of these observations, the solutions of the linear problem present a considerable interest for our research. For this reason, here after we discuss the solution of the linear problem for several models which present interest from the physical point of view.

Discussing now the general properties of the derived integral equation (1.35), we note that if the forcing function $f(t)$, and the kernel, $K(t,x)$, are bounded, one may apply the Picard's successive approximations,

$$p_0 = \frac{\lambda}{4} f(t), \qquad p_n = \frac{\lambda}{4} f(t) - 4\lambda \int_{-\infty}^{t} K(t,x)\left(p_{n-1} - \frac{3}{2} p_{n-1}^2 \right) dx, \qquad n \geq 1, \tag{1.57}$$

to construct a sequence of functions $p_n(t)$, which, according to the general theory, converges uniformly everywhere to a limit function $p(t)$ that is the unique solution of the equation. Since the conditions used are quite general, the Volterra integral equation (1.35) or (1.44) may provide a systematic way to attack the nonlinear system (1.9) in the case of small enough Landau–Zener parameter λ.

However, the convergence of Picard's series (1.57) is very slow [58]. To demonstrate this, note that by rearrangement of the terms the Picard's solution can be presented as a power series expansion in λ. This expansion accounts for the orders of the involved terms explicitly. Substituting $p = p_0 + \lambda p_1 + \lambda^2 p_2 + \ldots$ into equation (1.35) and equating coefficients at the same powers of λ we get $p_0 = 0$ and, successively,

$$\lambda: \quad p_1 = \frac{1}{2} \int_{-\infty}^{t} K(t,x) dx, \tag{1.58}$$

$$\lambda^2: \quad p_2 = \frac{1}{2} \int_{-\infty}^{t} K(t,x)(-8p_1) dx, \tag{1.59}$$

$$\lambda^3: \quad p_3 = \frac{1}{2} \int_{-\infty}^{t} K(t,x)(-8p_2 + 12p_1^2) dx, \quad .... \tag{1.60}$$

[Of course, λp_1 is the forcing function of the Volterra equation (1.35): $p_1 = [C_\delta^2(t) + S_\delta^2(t)]/4 = f(t)/4$.] Now, since all the p_i tend to finite, in general nonzero values at $t \to +\infty$ it is understood that any finite sum, being a polynomial in λ, is not restricted at $\lambda \to \infty$. Furthermore, it can even take negative values. For instance, for the Landau–Zener model $p_1 = f(t)/4 \to \pi/4$ at $t \to +\infty$ so that λp_1 starting from $\lambda \approx 0.65$ already exceeds the maximum $1/2$ allowed by the normalization, and the next approximation, $\lambda p_1 + \lambda^2 p_2$, becomes less than

zero when $\lambda > 0.65$.

Thus another approach is preferred. Note first that p_0, p_1 and p_2 satisfy the same equations as the corresponding terms of the expansion in the linear case. Hence, we are leaded to apply to the initial integral equation (1.35) the substitution $p = p_L + u$, p_L being the scaled linear solution (i.e., the linear solution with normalization $I_L = 1/4$). Then we have

$$p_L + u = \frac{\lambda}{2} \int_{-\infty}^{t} K(t,x)[1 - 8(p_L + u) + 12(p_L + u)^2]dx. \tag{1.61}$$

Canceling the terms belonging to the linear problem leads to a new Volterra integral equation of Hammerstein type,

$$u = 6\lambda \int_{-\infty}^{t} K(t,x) p_L^2 dx - 4\lambda \int_{-\infty}^{t} K(t,x)[(1 - 3p_L)u - \frac{3}{2}u^2]dx, \tag{1.62}$$

with changed forcing function that is of the order of λ^3. It is then understood that this forcing function should lead to much faster converging approximations. Indeed, we now try an expansion of the form

$$u = u_0 + \lambda u_1 + \lambda^2 u_2 + \lambda^3 u_3 + \ldots. \tag{1.63}$$

Since $p_L \sim \lambda$ at small λ, we conclude that $u_0 = u_1 = u_2 = 0$. For the next term, however, we get an important result:

$$\lambda^3 u_3 = 6\lambda \int_{-\infty}^{t} K(t,x) p_L^2 dx. \tag{1.64}$$

Noting that $u = \lambda^3 u_3 + O(\lambda^4)$, we finally arrive at a principal result:

$$u \approx 6\lambda \int_{-\infty}^{t} K(t,x) p_L^2 dx. \tag{1.65}$$

This is the desired form of the first correction term. Thus, finally, we obtain that in the first approximation the solution to the nonlinear problem in the weak interaction regime is written as

$$p(t) = p_L(t) + 6\lambda \int_{-\infty}^{t} K(t,x)[p_L(x)]^2 dx. \tag{1.66}$$

This is numerically proven to be a good approximation. For the Landau–Zener model, up to $\lambda < 0.5$ the comparison with the numerical solution to system (1.19) gives practically indistinguishable graphs. And it also works well as a satisfactory first approximation even up to $\lambda \lesssim 1$.

1.4. Various models of medium configuration

As we have seen, the problems of SHG and cold atom photoassociation can be represented as a quadratic-nonlinear quantum two-state problem. The solution of this problem depends on the input functions. In the case of SHG these functions are the nonlinear susceptibility and phase mismatch, that is $U(x)$ and $\delta(x)$, respectively. This pair of U and δ is called configuration model and determines the behavior of the system. These functions may vary in many different ways.

The aim of this work is to analyze the dynamics of the second harmonic generation for optical media with various dependences of nonlinear susceptibility and phase mismatch. The choice of the specific configurations that we apply is not accidental: they represent essentially different physical situations which are of practical interest. We list some useful models and describe their main characteristics. Further we concentrate on the models providing the most effective transition – the resonance crossing models. The Landau-Zener and Demkov-Kunike models are key models for this purpose.

The case of constant nonlinear suscectibility and constant detuning presents the simplest possible configuration:

$$U = U_0, \quad \delta_t = \delta_0. \tag{1.67}$$

This is the Rabi model [71-73]. The exact solutions of the Rabi problem both in the linear and nonlinear cases are known [73, 74]. In the linear case, the conversion efficiency is always an oscillatory, periodic function of the spatial coordinate. In the nonlinear case the solution dramatically differs from this behavior in the exact resonance case $\delta_t = 0$: in this case, the nonlinear conversion efficiency demonstrates monotonic increase.

In practical applications better conversion efficiencies are acheived by application of resonance-crossing models. The most basic and thus the most important model, which has many practical applications, is the model of constant nonlinearity and linearly resonance-crossing detuning known as the Landau-Zener model [24-27] (Fig. 1.2). Configuration functions for this model are given as:

$$U(t) = U_0, \quad \delta_t = 2\delta_0 t. \tag{1.68}$$

We note, that in the case, when the qualitatively most important part of the interaction is being realized in the close vicinity of the resonance any model with non vanishing amplitude and approximately liner-in-variable resonance crossing can be effectively approximated by the Landau-Zener model. For this reason it is considered as a standard reference to be compared with. As we will concentrate in term-crossing models, the LZ model is of crutial interest for this thesis. The methodology for finding the solution for this model will be discussed in detail in the next chapter.

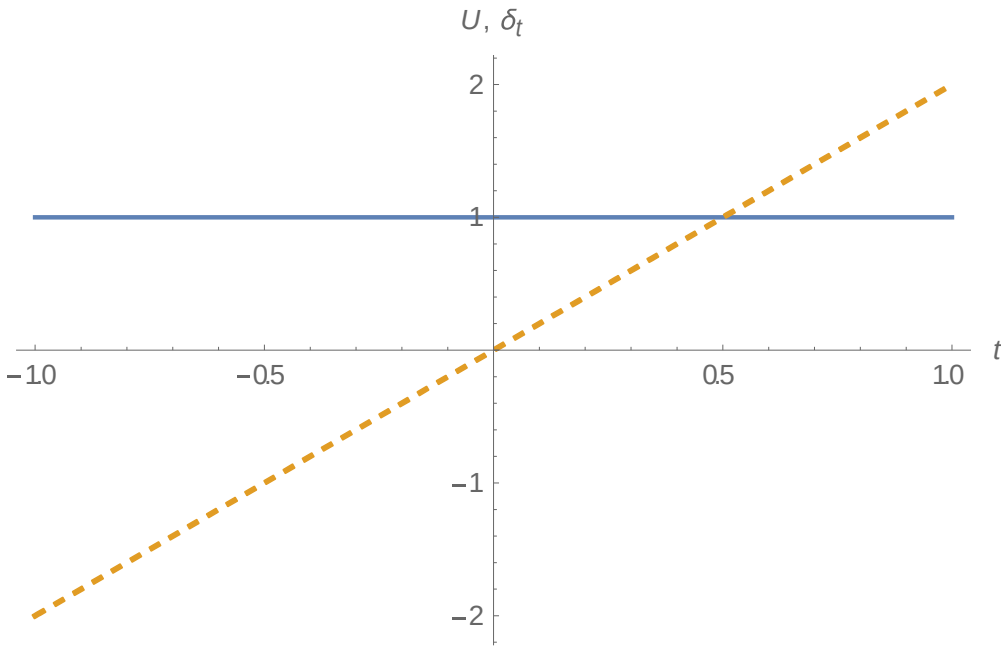

Fig. 1.2. The Landau-Zener model. Solid line is the Rabi frequency, dashed line is the detuning.

Despite its fundamental nature the Landau–Zener term-crossing model describes a very degenerate, physically unrealizable process. For example, in SHG constant nonlinearity means infinite in space nonlinear medium. Similarily, linearely increasing phase mismatch stends for unlimited energy differencies in infinities. From mathematical point of view this divergence leads to considerable troubles in contrast to other models. Nevertheless, this model is proven to be applicable for a wide range of physical conditions.

To overcome the infinite nonlinearity complication, a model of localized nonlinearity can be suggested - the Rosen-Zener model [75] (Fig. 1.3) - which can be considered as a generalisation of

the Rabi model:

$$U(t) = \frac{U_0}{\mathrm{ch}(t/\tau)}, \quad \delta_t(t) = 2\delta_0 . \tag{1.69}$$

Similarity with the Rabi model can be easily verified by tending τ to infinity. Thus, the Rosen-Zener model serves as a physicaly realizable prototype for all *non-crossing* models.

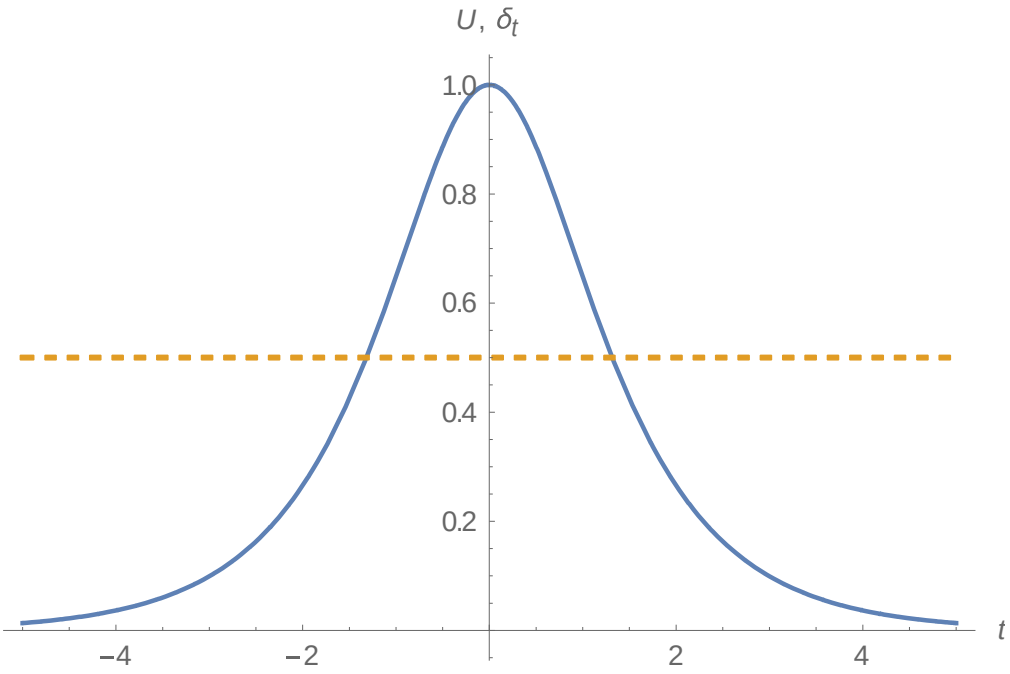

Fig. 1.3. Rosen-Zener model. Solid line is the Rabi frequency, dashed line is the detuning.

Further, there exists a model that has all the virtues of the Landau-Zener model and is free from its shortcomings. Such a model is the first Demkov-Kunike model [28-29] (Fig. 1.4):

$$U(t) = \frac{U_0}{\mathrm{ch}(t/\tau)}, \quad \delta_t(t) = 2\delta_0 \tanh(t/\tau) . \tag{1.70}$$

This model also describes the passage of the system through the resonance, but in this case

$$\lim_{t\to\pm\infty} U(t) = 0, \quad \lim_{t\to\pm\infty} \delta_t(t) = \pm 2\delta_0 , \tag{1.71}$$

($\tau > 0$) and the Rabi frequency given by (1.70) is a quadratic integrable function: this ensures the

satisfaction of the physical constraint that the laser pulse must have finite energy. The first Demkov-Kunike model is a straightforward generalization of the Landau-Zener model. To prove this we fix t, take $\delta_2 = \tilde{\delta}_0 \tau$ and tend the parameter τ to infinity. As a result, we obtain

$$U(t) = U_0, \quad \delta_t = 2\tilde{\delta}_0 t. \tag{1.72}$$

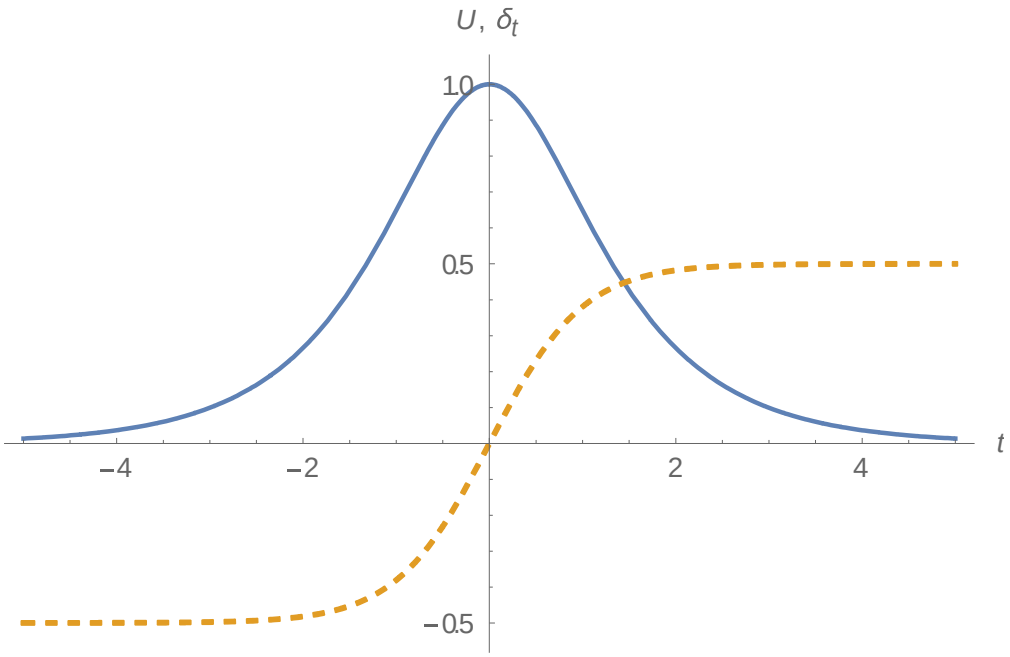

Fig. 1.4. Demkov-Kunike model. Solid line is the Rabi frequency, dashed line is the detuning.

The exponential resonance crossing model by Nikitin [76] is another generalization of the Landau-Zener resonance passage with a following Rabi-like interaction. It is sometimes referred to as an "anti Demkov" model. The model is defined by the following nonlinear susceptibility and phase mismatch:

$$U(t) = U_0, \quad \delta_t = \Delta(1 - e^{-at}), \tag{1.73}$$

where the crossing point is adjusted to coincide with the origin.

Note, that this model differs from the well-known second Nikitin-exponential model [77] with an exponential susceptibility: $U = U_0 e^{-at}$. For the Nikitin model there are two distinct interaction schemes: the so-called Nikitin's positive model (Fig. 1.5) and Nikitin's negative model (Fig. 1.6) with positive and negative a respectively. As we mention above, this model incorporates LZ and Rabi models, obviously near the resonance the phase mismatch behaves as the Landau-

Zener linear detuning, $\delta_t \approx \Delta a t$ [see (1.73)],while for $t \gg 1/a$ and for $t \ll 1/a$ in Nikitin's positive and negative models, respectively, the phase mismatch is practically constant like in the Rabi model.

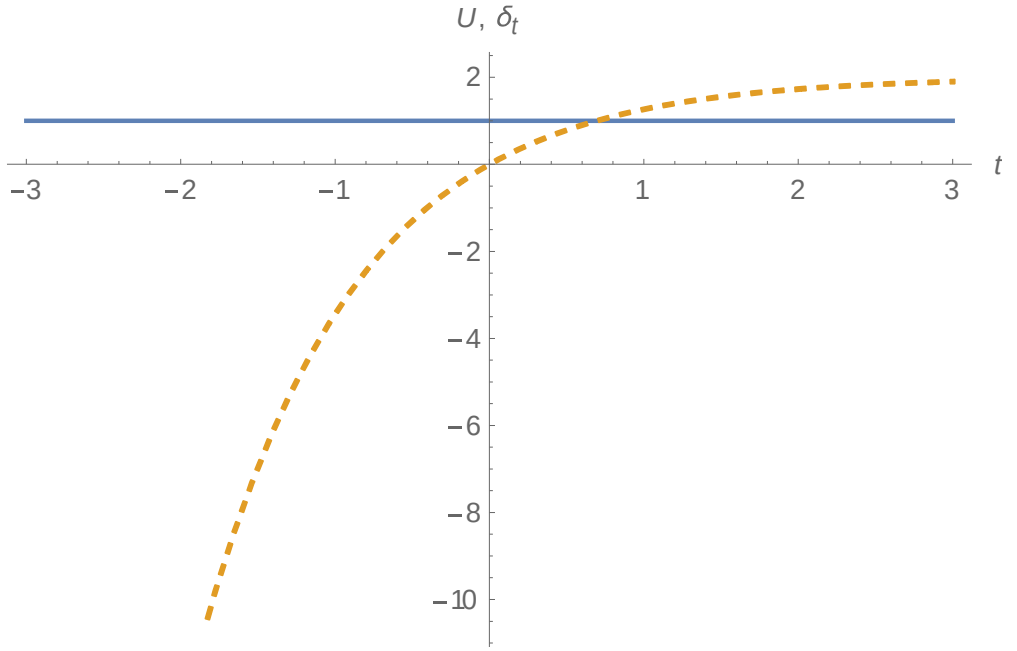

Fig. 1.5. Nikitin's positive model. Solid line is the Rabi frequency, dashed line is the detuning.

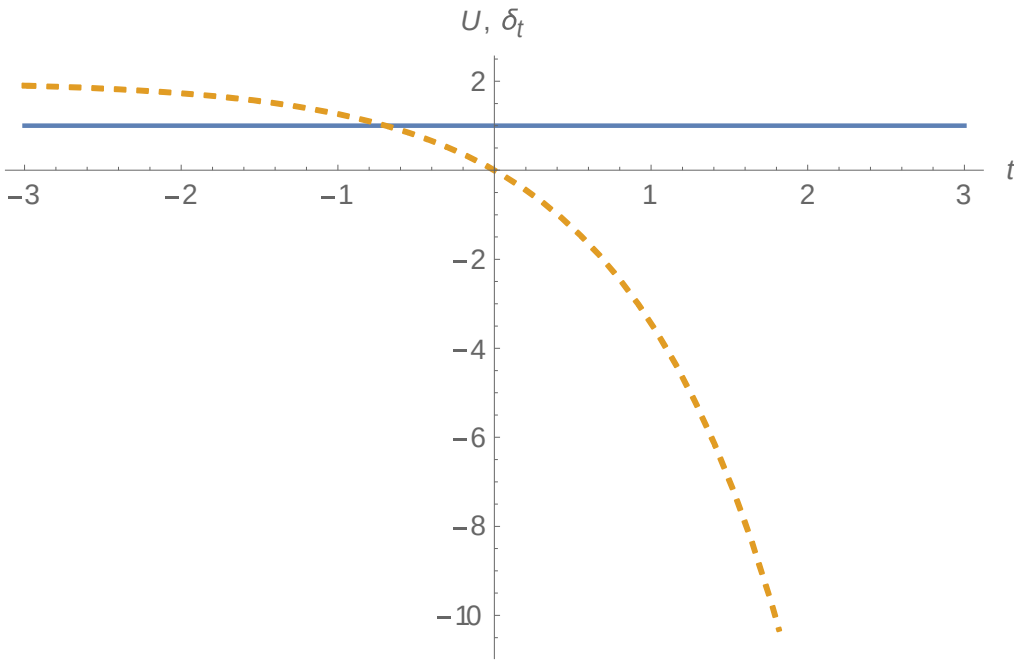

Fig. 1.6. Nikitin's negative model. Solid line is the Rabi frequency, dashed line is the detuning.

For reference and comparison purposes, a few more models with known analytic solutions

for linear two-state problem are listed below.

Figure 1.7 presents the model of two delayed pulses:

$$U = U_{10} e^{-(t-t_1)^2/\tau_1} + U_{20} e^{-(t-t_2)^2/\tau_2}, \quad \delta_t = \delta_0. \tag{1.74}$$

The parabolic-crossing model is represented in the Figure 1.8:

$$U(t) = U_0, \quad \delta_t = \delta_0^2 t^2 - a^2. \tag{1.75}$$

Consideration of multiple crossings leads to several new phenomena. Periodic crossings are one of the most interesting of those (Fig. 1.9):

$$U(t) = U_0, \quad \delta_t = \delta_0 \sin \omega_0 t. \tag{1.76}$$

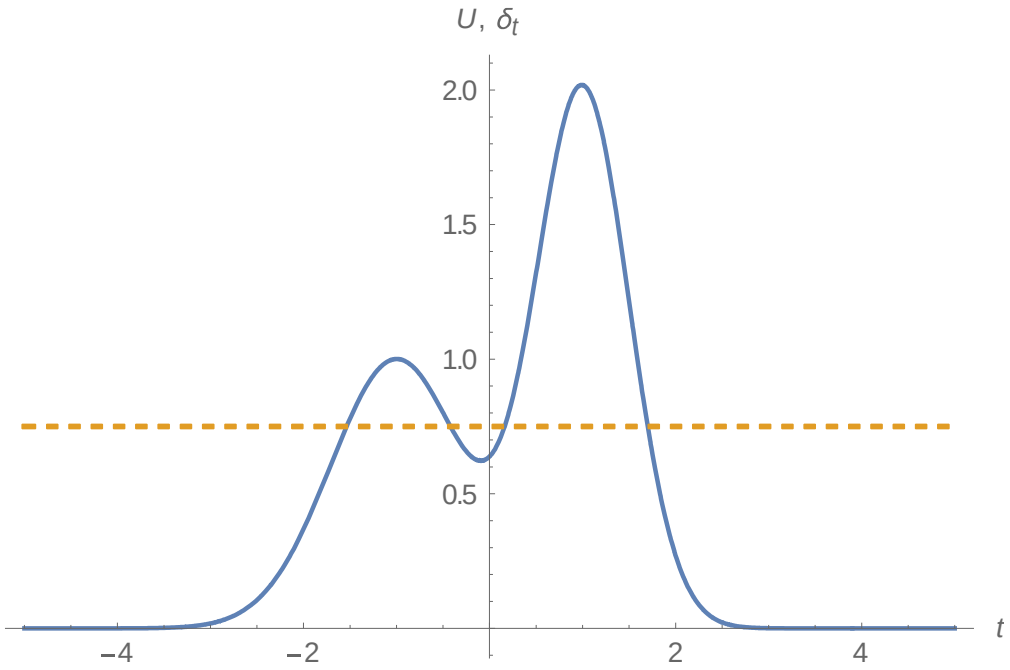

Fig. 1.7. Two delayed pulses. Solid line is the Rabi frequency, dashed line is the detuning

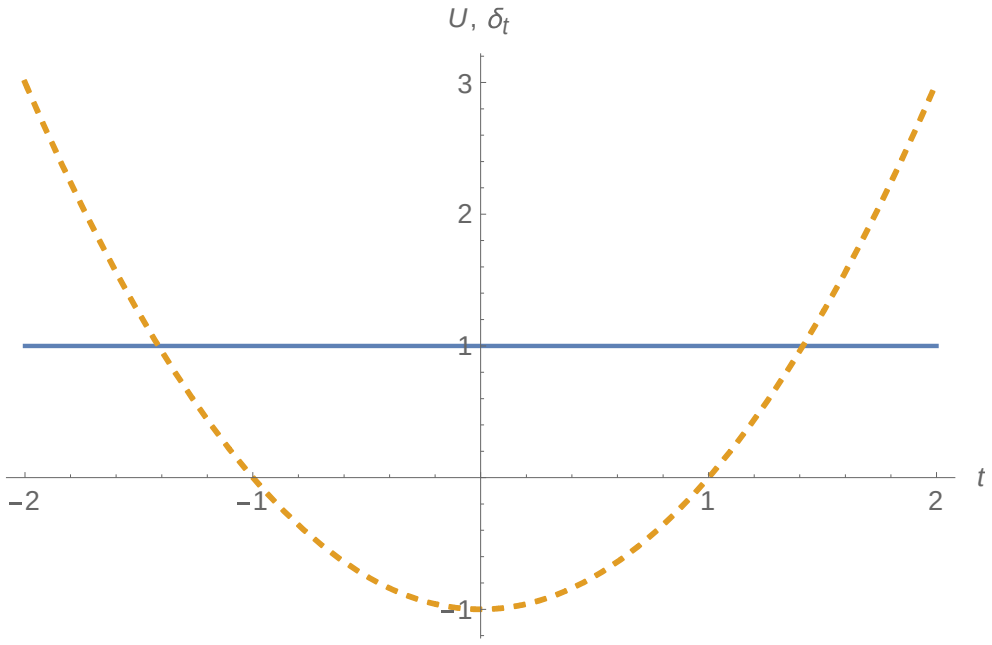

Fig. 1.8. Parabolic model. Solid line is the Rabi frequency, dashed line is the detuning

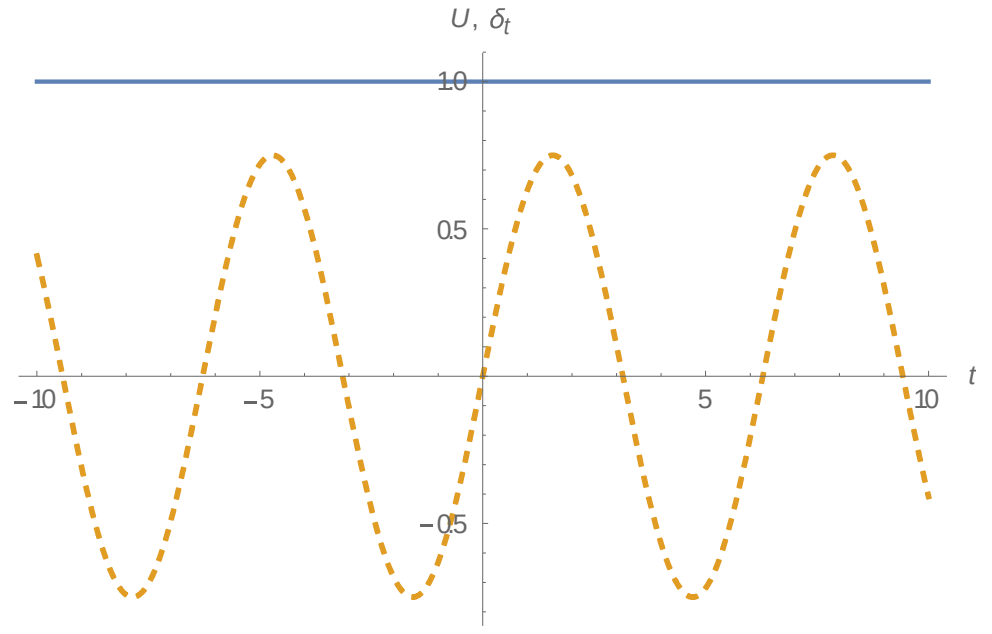

Fig. 1.9. Periodic crossing model. Solid line is the Rabi frequency, dashed line is the detuning

Another nontrivial possibility leading to several new features in the behavior of the system is the bichromatic model involving two laser fields of different color (Fig. 1.10):

$$\begin{aligned} i\frac{da_1}{dt} &= \left(U_1 e^{-i\Delta_1 t} + U_2 e^{-i\Delta_2 t}\right) a_1^* a_2, \\ i\frac{da_2}{dt} &= \frac{\left(U_1 e^{+i\Delta_1 t} + U_2 e^{+i\Delta_2 t}\right)}{2} a_1 a_1 \end{aligned} \qquad (1.77)$$

with $U_{1,2} = \text{const}$, $\Delta_{1,2} = \text{const}$.

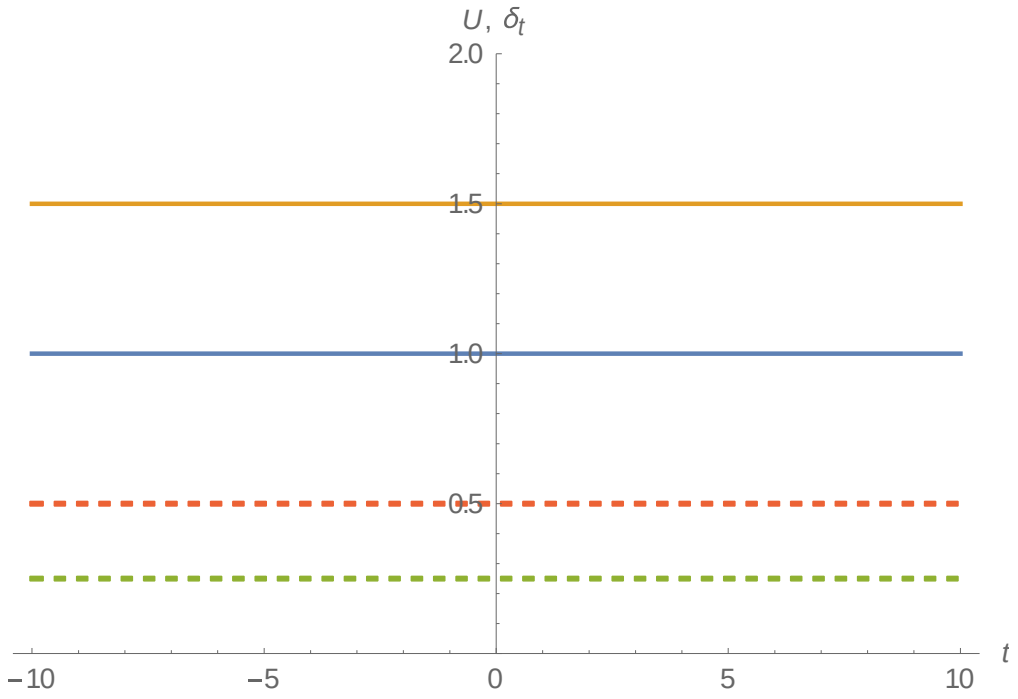

Fig. 1.10. The bichromatic Rabi model. Solid lines are the Rabi frequencies, dashed lines are the detunings $\Delta_{1,2}$.

In this research, we concentrate our discussion on two models: the Landau-Zener and Demkov-Kunike, since these are the ones which provide high conversion efficiency and also they can serve as a basis for discussion of all other resonance-crossing models, i.e., the results obtained for them can be extended to other models. For only several models discussed above the exact analytical solutions are known. The solutions are usually written in terms of hypergeometric functions. Two classes of hypergeometric functions are mainly used: Kummer (confluent) and Gauss hypergeometric functions. The solution for the Landau-Zener model is given in terms of confluent hypergeometric functions ${}_1F_1$ [24, 25]. For the Demkov-Kunike and Rosen-Zener models the exact solution to the linear problem is given in terms of the Gauss hypergeometric functions ${}_2F_1$ [28, 29]. These two models are unified by the circumstance that they originate from the same integrable class [78, 79]. We present here the derivation of the solution for this class.

1.5. Solution of the linear two-state problem in terms of the hypergeometric functions

Consider the familiar linear time-dependent two-state problem (here, for convenience, we skip the index indicating linearity):

$$\begin{cases} i\dfrac{da_1}{dt} = U(t)e^{-i\delta(t)}a_2 \ , \\ i\dfrac{da_2}{dt} = U(t)e^{i\delta(t)}a_1 \ . \end{cases} \tag{1.78}$$

The quantity $|a_1|^2 + |a_2|^2 = \text{const}$ is the first integral of this system.

From the point of view of atom optics the system (1.78) describes interaction of an isolated atom with optical laser radiation [71, 72]. In this case ω_{21} in the definition of the detuning is the frequency that corresponds to the transition between the two levels in the atom.

It is known that the system (1.78) is obtained by application of many approximations. We list them below:

1. The laser field is described classically.
2. The electro-dipole approximation is assumed.
3. The laser radiation is considered to be strictly monochromatic.
4. Quasi-resonant approximation is applied: it is assumed that $\delta_t << \omega_{21}$, hence only two chosen energetic levels of the atom are effectively involved in the interaction.
5. Rotating wave approximation is made: in the obtained equations the rapidly oscillating terms are removed. As a result the shifts of the energetic levels are not taken into account.

By elimination of a_2 from (1.78), an equivalent differential equation of the second order is derived

$$a_{1tt} + \left(i\delta_t - \frac{U_t}{U} \right) a_{1t} + U^2 a_1 = 0 \, . \tag{1.79}$$

Now, our aim is to find such functions $U(t)$ and $\delta(t)$ for which the system (1.78) has an exact analytic solution. Following [78, 79] we look for functions that can be found by reduction of a second order integrable equation, say,

$$u_{xx} + f(x)u_x + g(x)u = 0 \tag{1.80}$$

to (1.79) via transformations of the dependent and independent variables

$$x = x(t) \tag{1.81}$$

$$u(x) = \varphi(x)a_1, \tag{1.82}$$

where the function $x(t)$ that determines the transformation of the independent variable is a complex-valued function of the real variable: $x(t) = a(t) + ib(t)$.

Now, we make an important statement that is known as the theorem of the class property of integrable cases of the two-level problem [78, 79]. Let us consider the formal solution of the system (1.78) depending on the complex variable x, i.e. we make formal change $t \to x$ in the system (1.78) and rewrite it as follows:

$$\begin{cases} i\dfrac{da_1^*(x)}{dx} = U^*(x)e^{-i\delta^*(x)}a_2^*(x), \\ i\dfrac{da_2^*(x)}{dx} = U^*(x)e^{i\delta^*(x)}a_1^*(x). \end{cases} \tag{1.83}$$

Let us suppose, that we managed to find a solution $a_{1,2}^*(x)$ of this system for some functions $U^*(x)$ and $\delta^*(x)$. Then, one can state that *for a model given by the following Rabi frequency*

$$U(t) = U^*(x)\frac{dx}{dt}, \tag{1.84}$$

and detuning

$$\delta_t(t) = \delta_x^*(x)\frac{dx}{dt} \tag{1.85}$$

the solution to the system (1.78) is given by functions $a_{1,2}^*(x(t))$, where $x(t)$ is arbitrary complex-valued function. This statement is known as the class property theorem [78, 79]. It can be easily proved by direct substitution. The only constraint that is imposed on the function $x(t)$ when considering *physical* models is that the Rabi frequency $U(t)$ and the detuning $\delta_t(t)$ must be real functions. Thus the class property permits one to split the set of the integrable models $U(t)$ and $\delta_t(t)$ into a number of independent classes and each of the classes will contain an infinite number of integrable models. The models $\{U^*(x),\ \delta_x^*(x)\}$ are referred to as basic integrable models. Since the class property automatically takes into account the transformation of the independent variable,

hereafter when obtaining integrable models we apply to the equation (1.80) only the transformation of the dependent variable (1.82). This transformation reduces (1.80) to the following equation

$$a_{1xx}^{*}+\left(2\frac{\varphi_x}{\varphi}+f\right)a_{1x}^{*}+\left(\frac{\varphi_{xx}}{\varphi}+f\frac{\varphi_x}{\varphi}+g\right)a_1^{*}=0. \tag{1.86}$$

Now we compare it with the equation

$$a_{1xx}^{*}+\left(i\delta_x^{*}-\frac{U_x^{*}}{U^{*}}\right)a_{1x}^{*}+U^{*2}a_1^{*}=0 \tag{1.87}$$

and demand coincidence of (1.86) and (1.87). This leads to the following system of nonlinear equations:

$$\begin{cases} i\delta_x^{*}-\dfrac{U_x^{*}}{U}=2\dfrac{\varphi_x}{\varphi}+f\ , \\ U^{*2}=\dfrac{\varphi_{xx}}{\varphi}+f\dfrac{\varphi_x}{\varphi}+g\ , \end{cases} \tag{1.88}$$

from which we determine the functions $U^{*}(x)$, $\delta_x^{*}(x)$ and $\varphi(x)$.

Let us now consider the above described scheme, taking as an initial equation the Gauss hypergeometric equation [78-979]:

$$u_{xx}+\left(\frac{\gamma}{x}+\frac{\gamma-(\alpha+\beta+1)}{1-x}\right)u_x-\frac{\alpha\beta}{x(1-x)}u=0. \tag{1.89}$$

In this particular case the system (1.88) is written as

$$\begin{cases} i\delta_x^{*}-\dfrac{U_x^{*}}{U}=2\dfrac{\varphi_x}{\varphi}+\dfrac{\gamma}{x}+\dfrac{\gamma-(\alpha+\beta+1)}{1-x}\ , \\ U^{*2}=\dfrac{\varphi_{xx}}{\varphi}+\left(\dfrac{\gamma}{x}+\dfrac{\gamma-(\alpha+\beta+1)}{1-x}\right)\dfrac{\varphi_x}{\varphi}-\dfrac{\alpha\beta}{x(1-x)}. \end{cases} \tag{1.90}$$

From the structure of (1.90) we conclude that it is worthwhile to make the following choice:

$$\varphi=x^{\mu}(1-x)^{\nu}, \tag{1.91}$$

$$\delta_x^{*}=\frac{\delta_1}{x}+\frac{\delta_2}{1-x}, \tag{1.92}$$

and

$$U^{*}(x)=\frac{U_0^{*}}{x^{k_1}(1-x)^{k_2}}. \tag{1.93}$$

We start the analysis of the system (1.90) with the determination of the values of the parameters $k_{1,2}$ in (1.93). So we multiply the both sides of the second equation of system (1.90) by $x^2(1-x)^2$. After that the right-hand side of it will be a quadratic polynomial in x. From the demand that the left-hand side of it also must be a quadratic polynomial in x we obtain the following constraints on the parameters $k_{1,2}$:

$$0 \le 4 - 2k_1 - 2k_2 \le 2 \quad \Rightarrow \quad 1 \le k_1 + k_2 \le 2. \tag{1.94}$$

Now we multiply the both sides of the same equation by $x^{2+\varepsilon}$, where $\varepsilon > 0$, and tend x to zero. The right-hand side of the equation will tend to zero, and from the demand that the left-hand side of it also must tend to zero we obtain the following inequality:

$$-2k_1 + 2 + \varepsilon > 0. \tag{1.95}$$

In (1.95) we apply the limit transition $\varepsilon \to 0$: as a result, the strict inequality (1.95) will turn to the not strict inequality

$$k_1 \le 1. \tag{1.96}$$

In the same manner one can obtain the condition

$$k_2 \le 1. \tag{1.97}$$

Besides, it follows from the structure of (1.90) that the parameters $k_{1,2}$ adopt only integer and half-integer values.

It can be easily seen that the hypergeometric equation is invariant with respect to the transformation $x \to 1-x$; hence such $\{k_1, k_2\}$ pairs that can be obtained via transposition of the parameters $\{k_1, k_2\}$ are not independent.

Thus, finally, we obtain four independent $\{k_1, k_2\}$ pairs, i.e. four basic models. The detuning is given by the formula (1.92), and the Rabi frequency is defined as

$$\frac{U^*(x)}{U_0} = \frac{1}{x(1-x)}, \ \frac{1}{\sqrt{x}(1-x)}, \ \frac{1}{1-x}, \ \frac{1}{\sqrt{x(1-x)}}. \tag{1.98}$$

Substituting (1.91)-(1.93) into (1.90) we easily obtain the following system of equations:

$$
\begin{aligned}
&\gamma = i\delta_1 + k_1 - 2\mu\,,\\
&\alpha + \beta = -1 - 2\nu + k_2 - i\delta_2 + \gamma\,,\\
&\alpha\beta = -\left[U^{*2}x^2\right]_x\Big|_{x=0} + 2\mu\nu - \nu(i\delta_1 + k_1) + \mu(i\delta_2 - k_2)\,,\\
&\nu(\nu + 1 + i\delta_2 - k_2) + U^{*2}(1-x)^2\Big|_{x=1} = 0\,,\\
&\mu(\mu + 1 - i\delta_1 - k_1) + U^{*2}x^2\Big|_{x=0} = 0
\end{aligned}
\qquad (1.99)
$$

that determine the link between the input and output parameters of the problem.

Applying different forms of transformations $x = x(t)$ to the basic models (1.98) and (1.92) one obtains numerous physical models. Importantly, the last of the derived basic solutions defines a model that we use in this study, the Demkov-Kunike model: the choice $x = (1 + \tanh(t/\tau))/2$ leads to the configuration

$$
U(t) = \frac{U_0}{\mathrm{ch}(t/\tau)}\,,\quad \delta_t(t) = 2\delta_0 \tanh(t/\tau)\,. \qquad (1.100)
$$

Unlike the solution of the Demkov-Kunike problem, the solution of the Landau-Zener problem is given in terms of Kummer confluent hypergeometric function ${}_1F_1$ [24, 25]. However, as we have mentioned previously, the Demkov-Kunike model is a generalization of the Landau-Zener model. This generalization is achieved by a limiting procedure applied to the parameters of the Demkov-Kunike model. When applied to the *solution* of the Demkov-Kunike problem, this procedure is equivalent to coalescence of two singularities of the Gauss hypergeometric function. The Gauss function is then reduced to the Kummer hypergeometric function and thus the solution to the Landau-Zener problem can be obtained from the solution to the Demkov-Kunike problem.

Summary of Chapter 1

In this chapter we presented mathematical representation of a basic nonlinear two-state problem as a set of two coupled nonlinear differential equations of the first order. We have shown that under certain conditions the same mathematical system describes both the dynamics of ultracold atom – molecule transitions during photoassociation and Feshbach resonance and second harmonic generation in a quadratic nonlinear optical medium. Using an exact Volterra integral equation for the second state's probability, we have demonstrated that a linear two-state problem with normalization $I_L = 1/4$ is an analog of the nonlinear two-state problem we study. We have presented the solutions of the associated linear problem in terms of the Gauss hypergeometric functions. Discussing the general properties of the derived Volterra integral equation, we noted that the equation may provide a systematic way to attack the nonlinear problem in the case of small enough Landau–Zener parameter. We have defined and discussed several external field configurations for cold molecule formation and various nonlinear susceptibilities and phase mismatch in an optical medium for second harmonic generation. For further investigation we choose two configurations, which presumably should allow high conversion efficiency: the nonlinear Landau-Zener and Demkov-Kunike models. We presented the solution to the linear Demkov-Kunike problem in terms of the Gauss hypergeometric functions.

CHAPTER 2. NONLINEAR LANDAU-ZENER PROBLEM

We present in detail and analyze a quadratic-nonlinear version of the Landau–Zener problem. If SHG terminology is applied, the Landau-Zener model presents the situation when the phase mismatch varies along the direction of propagation of interacting waves, being a linear function of the spatial coordinate. In cold molecule formation it describes the case, when the Rabi frequency is constant and the detuning linearly crosses the resonance in time. We propose different approximations for various interaction regimes.

For the case of weak interaction we develop a variational approach which enables us to construct an accurate analytic approximation describing the spatial dynamics of second harmonic wave (or the time dynamics of the molecular state) using an exact third-order nonlinear differential equation for second harmonic wave's intensity (or molecular state probability). We show that the constructed approximation written as the solution of the corresponding linear problem with modified parameters quantitatively well describes many characteristics of the dynamics of the system. In particular, it provides a highly accurate formula for the final intensity of the second harmonic (or for the final transition probability to the molecular state).

In the strong interaction regime we reveal a remarkable observation that the resonance crossing is mostly governed by the nonlinearity while the damped coherent oscillations coming up soon after the resonance has been crossed are basically of linear nature. Thus, we propose an approximation, written as a sum of two functions, namely, a solution of a limit fourth-order polynomial equation and a scaled solution to the analogous linear Landau-Zener problem with modified parameters. The constructed approximation turns out to have a larger applicability range (than it was initially expected) covering the whole moderate coupling regime for which the proposed solution accurately describes all the main characteristics of the system's evolution except the amplitude of the coherent oscillation, which is rather overestimated. We also derive an analytic expression for the final intensity of the second harmonic at the exit from the medium (or, equivalenly, for the final transition probability of the molecular state).

Overview

For the sake of generality, in this chapter we use the terminology applied in cold atom association in degenerate quantum gases. As we have mentioned in Chapter 1 *coherent* molecule formation in ultracold gases by applying associating optical or magnetic fields under certain experimental conditions [80, 81] can be described by a basic mean-field time-dependent two-level problem, defined by the following set of coupled *nonlinear* equations (see also [82-86]):

$$i\frac{da_1}{dt} = U(t)\,e^{-i\delta(t)}\bar{a}_1 a_2, \quad i\frac{da_2}{dt} = \frac{U(t)}{2}\,e^{i\delta(t)}a_1 a_1, \tag{2.1}$$

where t is the time, a_1 and a_2 are the atomic and molecular state probability amplitudes, respectively, $\bar{a}_1$ denotes the complex conjugate of a_1. The real functions $U(t)$ and $\delta(t)$ are the characteristics of the applied field. Under the conditions considered in the present research the two techniques, the photoassociation and Feshbach resonance, are mathematically equivalent; for definiteness, in what follows we use the photoassociation terminology. In photoassociation, $U(t)$ is referred to as the Rabi frequency of the associating laser field, and $\delta(t)$ is the frequency detuning modulation function for which the derivative, $\delta_t(t)$, is the detuning of the laser field frequency from that of transition from the atomic state to the molecular one (the alphabetical index denotes differentiation with respect to the mentioned variable).

The theoretical efforts to describe the dynamics of cold molecule formation within photoassociation and Feshbach resonance techniques have mostly been focused on the treatment of the Landau-Zener (LZ) model. In order to achieve high conversion efficiency, one has to apply a level-crossing field configuration [80]. Then, as it is well appreciated, the Landau-Zener model inevitably comes up as a natural starting point for studying such models and serves as a prototype for other level-crossing models. For this reason, this model has been a subject of intensive investigations over the last years (e.g., see Refs. [58-69]). Hwever, despite the large interest to the model, so far there was no reasonable approximation, which accurately describes the behavior of the system during and after the resonance crossing. Our goal was to construct an accurate analytic approximation applicable for characterization of the time evolution of the molecular state probability for the whole variation range of the LZ parameter.

Differential equation for the molecular state probability for the nonlinear LZ model

We treat here the basic case when the evolution of the system starts from the pure atomic state, so that the initial conditions for $p = |a_2|^2$ are

$$p(-\infty) = 0\,, \quad p_t(-\infty) = 0\,, \quad p_{tt}(-\infty) = 0\,, \tag{2.2}$$

System (2.1) describes a lossless process, i.e., conserves the total number of particles, which we choose as normalized to unity:

$$|a_1|^2 + 2|a_2|^2 = \text{const} = 1\,. \tag{2.3}$$

Note that $|a_1|^2 \in [0,1]$, whereas $|a_2|^2 \in [0,1/2]$. After eliminating one of the dependent variables from system (2.1) we obtain the following nonlinear equations of the second order for the atomic and molecular states' probability amplitudes, respectively:

$$a_{1tt} + \left(i\delta_t - \frac{U_t}{U}\right)a_{1t} - \frac{U^2}{2}\left(1 - 2|a_1|^2\right)a_1 = 0\,, \tag{2.4}$$

$$a_{2tt} + \left(-i\delta_t - \frac{U_t}{U}\right)a_{2t} + U^2\left(1 - 2|a_2|^2\right)a_2 = 0\,. \tag{2.5}$$

Hence, instead of the two coupled first-order equations (2.1) one may work with one second-order equation [either (2.4) or (2.5)]. However, it turns out that it is more convenient to deal with one equation, written for the molecular state probability $|a_2|^2$. It can be shown that all other involved variables are then expressed in terms of this quantity.

It can be shown by direct differentiation that the transition probability $p = |a_2|^2$ satisfies the following relations:

$$p_t = a_{2t}^* a_2 + a_2^* a_{2t} = -i\frac{U}{2}(a_1^2 a_2^* e^{i\delta(t)} - a_1^{*2} a_2 e^{-i\delta(t)})\,, \tag{2.6}$$

$$p_{tt} = \frac{U_t}{U}\,p_t + \frac{U^2}{2}(1 - 8p + 12p^2) + \frac{U}{2}\delta_t(a_1^2 a_2^* e^{i\delta(t)} + a_1^{*2} a_2 e^{-i\delta(t)})\,. \tag{2.7}$$

Furthermore, it can be checked by straightforward differentiation that the function

$$Z = a_1^2 a_2^* e^{i\delta(t)} + a_1^{*2} a_2 e^{-i\delta(t)} \tag{2.8}$$

satisfies the relation

$$Z_t = -\delta_t \frac{2p_t}{U}. \tag{2.9}$$

Then, differentiation of equation (2.7) followed by some algebra yields the following nonlinear ordinary differential equation of the third order for the molecular state probability [92]:

$$p_{ttt} - \left(\frac{\delta_{tt}}{\delta_t} + 2\frac{U_t}{U}\right)p_{tt} + \left[{\delta_t}^2 + 4U^2(1-3p) - \left(\frac{U_t}{U}\right)_t + \frac{U_t}{U}\left(\frac{\delta_{tt}}{\delta_t} + \frac{U_t}{U}\right)\right]p_t + \frac{U^2}{2}\left(\frac{\delta_{tt}}{\delta_t} - \frac{U_t}{U}\right)(1-8p+12p^2) = 0. \tag{2.10}$$

It is worth stressing that the normalization condition (2.3) is incorporated in this equation.

The derived equation is considerably simplified for the models with constant field amplitude: $U(t) = U_0$. In this case we have the equation [91,92]

$$p_{ttt} - \frac{\delta_{tt}}{\delta_t}p_{tt} + \left[{\delta_t}^2 + 4U_0^2(1-3p)\right]p_t + \frac{U_0^2}{2}\frac{\delta_{tt}}{\delta_t}(1-8p+12p^2) = 0 \tag{2.11}$$

which can be rewritten in the following factorized form [91]:

$$\left(\frac{d}{dt} - \frac{\delta_{tt}}{\delta_t}\right)\left[p_{tt} - \frac{U_0^2}{2}(1-8p+12p^2)\right] + {\delta_t}^2 p_t = 0. \tag{2.12}$$

This equation serves as a starting point for the development presented below.

For the LZ model, equation (2.12) is written as [91]

$$\left(\frac{d}{dt} - \frac{1}{t}\right)\left[p_{tt} - \frac{\lambda}{2}(1-8p+12p^2)\right] + 4t^2 p_t = 0, \tag{2.13}$$

where we have passed to the dimensionless time, $t \to t/\sqrt{\delta_0}$, and have introduced the conventional LZ parameter

$$\lambda = \frac{{U_0}^2}{\delta_0}. \tag{2.14}$$

The *linear* counterpart of the nonlinear system (2.1) reads

$$i\frac{da_{1L}}{dt} = U_0 e^{-i\delta(t)}a_{2L}, \quad i\frac{da_{2L}}{dt} = U_0 e^{i\delta(t)}a_{1L}. \tag{2.15}$$

Accordingly, for the second state probability $p_L = |a_{2L}|^2$ of the linear problem we have the

equation [compare with Eq. (2.13)]

$$\left(\frac{d}{dt}-\frac{1}{t}\right)\left(p_{Ltt}-\frac{\lambda}{2}(4-8p_L)\right)+4t^2 p_{Lt}=0\,. \tag{2.16}$$

Note that when deriving Eq. (2.16) the normalization constraint $|a_{1L}|^2+|a_{2L}|^2=1$ has been taken into account. This linear differential equation is exactly solvable, and we denote as p_{LZ} the solution which satisfies the initial conditions: $p_L(-\infty)=0$, $p_{Lt}(-\infty)=0$, $p_{Ltt}(-\infty)=0$. This solution can be written in terms of the confluent hypergeometric functions [87]:

$$p_{LZ}(t)=|a_{2LZ}(t)|^2=|C_{01}\cdot F_1+C_{02}\cdot F_2|^2 \tag{2.17}$$

with

$$C_{01}=\sqrt{\lambda e^{-\pi\lambda/4}\cosh(\pi\lambda/4)}\,\frac{i}{2}\,\frac{\Gamma(1/2-i\lambda/4)}{\Gamma(1-i\lambda/4)},\quad C_{02}=\sqrt{\lambda e^{-\pi\lambda/4}\cosh(\pi\lambda/4)}\sqrt{i\delta_0}\,, \tag{2.18}$$

and

$$F_1={}_1F_1(i\lambda/4;1/2;it^2),\quad F_2=t\cdot{}_1F_1(1/2+i\lambda/4;3/2;it^2), \tag{2.19}$$

where Γ is the Euler gamma-function [87] and ${}_1F_1$ is the Kummer confluent hypergeometric function [87]. The limits of p_{LZ} for $t\to 0$ and $t\to+\infty$ are written as

$$\begin{aligned} p_{LZ}(0)&=\frac{1-e^{-\pi\lambda/2}}{2},\\ p_{LZ}(+\infty)&=1-e^{-\pi\lambda}. \end{aligned} \tag{2.20}$$

2.1. Weak interaction regime for the nonlinear LZ model

Now we examine the weak coupling limit of the association process, which corresponds to the weak associating fields with the Rabi frequency being $U_0 < 1$. This limit has been previously discussed by several authors both in the context of photoassociation and Feshbach resonance (see, e.g., [58-69]) and an accurate formula for the final transition probability to the molecular state at $t \to +\infty$ has been proposed [58, 60]. However, the whole time dynamics of the system has not been treated in detail.

In this section, following [88-91], we try to construct an approximate solution of the equation (2.13) using the solution p_{LZ} to the linear equation (2.16). To do this, we consider the linear equation (2.16) with an auxiliary parameter λ^*:

$$\left(\frac{d}{dt}-\frac{1}{t}\right)\left(p_{LZtt}-\frac{\lambda^*}{2}(4-8p_{LZ})\right)+4t^2 p_{LZt}=0, \tag{2.21}$$

and try to approximate the solution to the exact equation (2.13) as follows:

$$p_0 = C^* p_{LZ}(\lambda^*, t). \tag{2.22}$$

As it is seen, apart from a simple pre-factor C^*, we have here introduced an *effective* LZ parameter λ^*. After substituting this expression into the left-hand side of equation (2.13) and taking into account that function $p_{LZ}(\lambda^*, t)$ satisfies equation (2.21), we get some remainder:

$$R = \left(\frac{d}{dt}-\frac{1}{t}\right) r(t), \tag{2.23}$$

where $r(t)$ is the notation for

$$r(t) = C^* \frac{\lambda^*}{2}(4-8p_{LZ}(\lambda^*) - \frac{\lambda}{2}\left(1-8C^* p_{LZ}(\lambda^*)+12(C^* p_{LZ}(\lambda^*))^2\right). \tag{2.24}$$

It is obvious that if the remainder R is identically zero, then the function p_0 given by equation (2.22) is the exact solution to equation (2.13). Hence, it is intuitively understood that a way to proceed is to try to minimize R by means of appropriate choice of λ^* and C^*.

To do this, we first note that, since the function $p_{LZ}(\lambda^*, t)$ is bounded everywhere, the

function R is bounded almost everywhere. The exception is the resonance crossing point $t=0$, where, due to the term $1/t$ in the operator $\left(\frac{d}{dt}-\frac{1}{t}\right)$, in general, R diverges. Therefore, as a first step, we eliminate this divergence, i.e., we require λ^* and C^* to satisfy the equation $r(0)=0$. Explicitly, this equation is written as

$$C^*\frac{\lambda^*}{2}\left(4-8p_{LZ}(\lambda^*,0)\right)-\frac{\lambda}{2}\left(1-8C^*p_{LZ}(\lambda^*,0)+12C^{*2}p_{LZ}(\lambda^*,0)^2\right)=0. \tag{2.25}$$

To find appropriate values of parameters λ^* and C^* we need to introduce one more equation. Of course, in order to construct an approximation as simple as possible, one may first try to avoid variation of both auxiliary parameters and to attempt to get a simpler, one-parametric approximation instead. A natural choice is then to fix $\lambda^*=\lambda$ and vary C^* alone. Equation (2.25) then immediately yields:

$$C^*=\frac{1-\sqrt{1-3P_{LZ}(0)^2}}{6P_{LZ}(0)^2} \tag{2.26}$$

with $P_{LZ}(0)$ given by Eq. (2.20). Numerical examination reveals that this approximation works only for very small λ, of the order of 10^{-2}. For $\lambda=0.25$ the error is about 5% and for $\lambda=1$ it becomes 20%. This result shows that we have to consider two-parametric fit, hence, we do need a second equation to determine the parameters λ^* and C^*.

For derivation of the second equation we write the (exact) solution to the initial equation (2.13) as

$$p=p_0+u \tag{2.27}$$

and examine the exact equation for the correction term u. This equation is written as

$$\left(\frac{d}{dt}-\frac{1}{t}\right)\left(u_{tt}-\frac{\lambda}{2}(-8u+24p_0u+12u^2)+r\right)+4t^2u_t=0. \tag{2.28}$$

Now, considering the correction u as sufficiently small (since the zero-order approximation p_0 is supposed to be sufficiently close to the exact solution) one arrives at the needed second equation:

$$\left(C^*\frac{\lambda^*}{2}(4-8p_{LZ}(\lambda^*,+\infty))-\frac{\lambda}{2}\left(1-8C^*p_{LZ}(\lambda^*,+\infty)+12C^{*2}p_{LZ}(\lambda^*,+\infty)^2\right)\right)+$$
$$\left(2C^*\lambda^*-\frac{\lambda}{2}\right)-\frac{\lambda}{2}p_{LZ}^2(\lambda^*,+\infty)=0. \qquad (2.29)$$

The details of derivation of this equation are presented in Appendix 2.

Thus, the values of parameters λ^* and C^*, for which the function (2.22) approximates the exact solution to equation (2.13) are determined by equations (2.25) and (2.29). One may numerically solve these equations and further compare the proposed approximation (2.22) with the numerical solution to the exact equation (2.13). The comparison is shown on Fig. 2.1. It is seen that the coincidence is quite good – some deviation is observed only for the several first oscillations occurring after resonance-crossing and we see that the deviation becomes visible for relatively large λ: $0.3 \le \lambda \le 1$. In the meanwhile, several important characteristics of the process, such as the final transition probability (at $t \to +\infty$) and the frequency of oscillations are determined with high accuracy. As is seen, it is the amplitude of oscillations that displays significant deviations from the numerical result. However, it can be shown that there exists a modification of the applied variational method which is potent to provide essential improvement of the result.

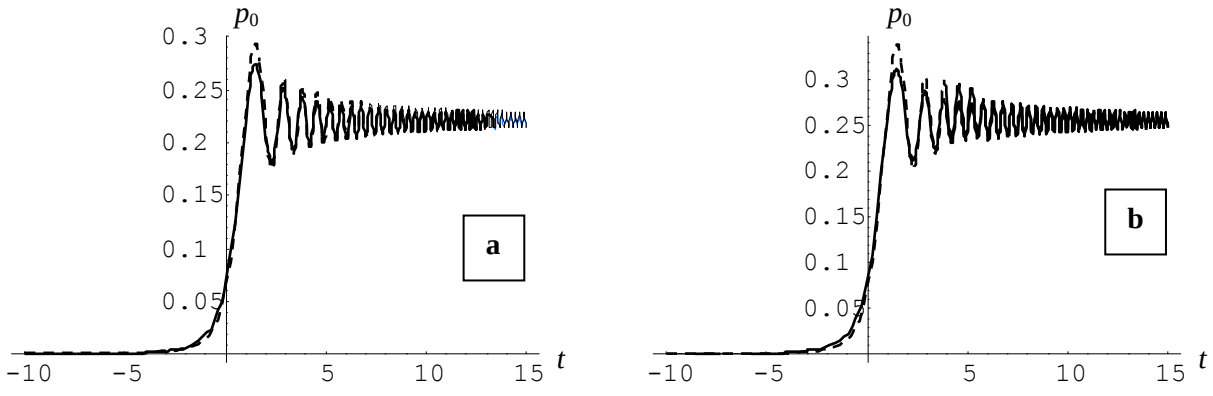

Fig. 2.1. Comparison of the solution (2.22) (dotted lines) with the numerical solution to equation (2.13) (solid lines) at a) $\lambda = 0.25$, b) $\lambda = 0.64$.

The system of equations (2.25) and (2.29) for determination of optimal values of the parameters λ^* and C^* can be solved by approximate methods. In order to do this, we first eliminate C^* from the system. Next, we show that with the increase of λ the function $\lambda^*(\lambda)$ first monotonically increases starting from $\lambda^*(0)=0$ and further monotonically decreases to zero at $\lambda=\sqrt{2}$. The function reaches its maximal value at $\lambda\approx 0.454$. The corresponding auxiliary parameter λ^* then adopts the value $\lambda^*_{\max}\approx 0.124$. A sufficiently good approximation for the function $\lambda^*(\lambda)$ is given by the following formula:

$$\lambda^* = \lambda\left(1-\frac{\lambda}{\sqrt{2}}\right)\frac{1+\lambda/\pi}{1+4\lambda}. \tag{2.30}$$

Comparison of the derived formula with the numerical result is shown in Fig. 2.2. It is seen that the approximation for the interval $\lambda\in[0,1]$ (i.e., the whole weak interaction limit) is rather good. Furthermore, we apply equation (2.30) to calculate the function $C^*(\lambda)$ using equation (2.25). Comparison of the resultant approximation with the numerical result for $C^*(\lambda)$ is shown in Fig. 2.3. As it is seen, the graphs are practically indistinguishable.

An analytic expression for C^* as a function of λ can be constructed starting from equation (2.25) and applying, for example, successive iterations. Indeed, rewrite equation (2.25) in the following form

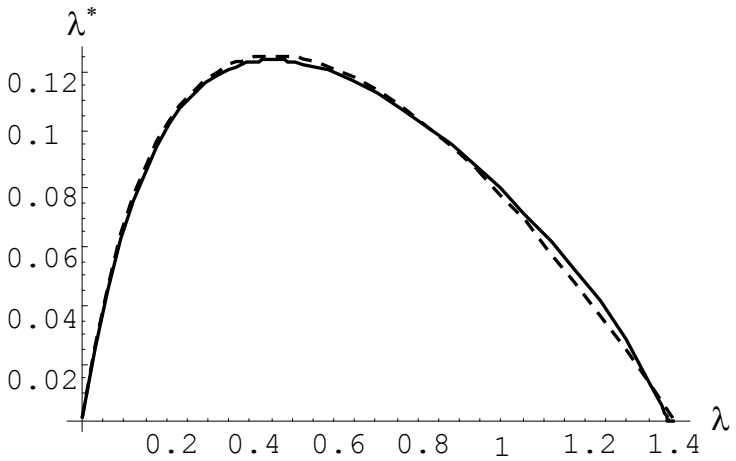

Fig. 2.2. Function $\lambda^*(\lambda)$ [dotted line – formula (2.30)].

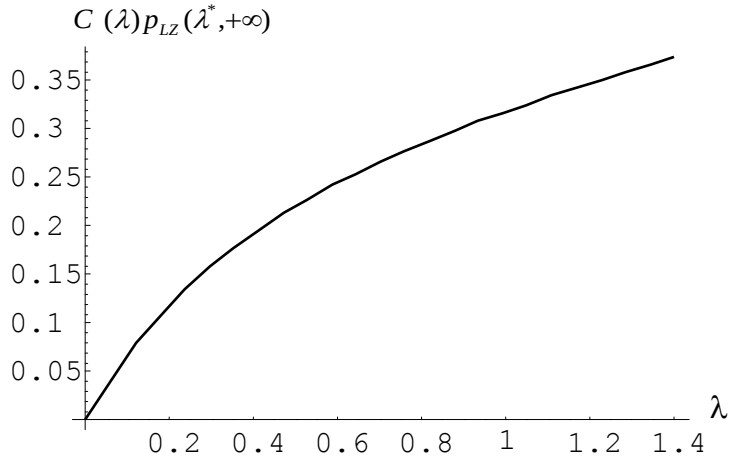

Fig. 2.3. Function $C^*(\lambda)\cdot p_{LZ}(\lambda^*,+\infty)$.

$$C^* = \frac{\lambda/4}{\lambda^* + 2(\lambda-\lambda^*)\ p_{LZ}(\lambda^*,0) - 3\lambda C^* p_{LZ}(\lambda^*,0)^2}. \tag{2.31}$$

Now, as a zero-order approximation we put in the right-hand side of this equation $C^{*(0)}=0$. As a result, we get an expression that is already a good approximation. By applying further iterations, we conclude that an accurate approximation for all $\lambda \le 1$ is given by the formula

$$C^* = \frac{\lambda/4}{\lambda^* + 1.75(\lambda-\lambda^*)\ p_{LZ}(\lambda^*,0)}. \tag{2.32}$$

The graph of this function is visually indistinguishable from the numerical solution. The substitution of $\lambda^*(\lambda)$ from Eq. (2.30) into this formula shows that function $C^*(\lambda)$, in contrast to the function $\lambda^*(\lambda)$, monotonically increases on the segment $\lambda \in [0,1]$.

The final transition probability to the molecular state at $t \to +\infty$ for the weak interaction limit, according to Eq. (2.22), is $p(+\infty) = C^*(\lambda)p_{LZ}(\lambda^*,+\infty)$. It is namely this function that is shown in Fig. 2.3. Note finally that the direct comparison shows that on the whole segment $\lambda \in [0,1]$ expression (2.32) produces a final transition probability that accurately matches the formula derived in Refs. [58, 60].

2.2. Strong interaction regime for the nonlinear LZ model

Now, following [88, 91], we consider the strong interaction regime, i.e., the case when the Landau-Zener parameter is large (equivalently, the field intensity U_0^2 is large enough or the detuning sweep across the resonance is sufficiently slow, that is the sweep rate $2\delta_o$ is small). Hence, the second term in the square brackets in Eq. (2.13) adopts, in general, large value. Since for large t the last term of the equation also adopts large value, we suppose that the leading terms in Eq. (2.13) are the last two so that we neglect, for a while, the term p_{tt} thus arriving at a limit nonlinear equation of the first order. This equation admits two trivial stationary solutions, $p = 1/2$ and $p = 1/6$, and a nontrivial one. Unfortunately, for the initial condition $p(-\infty) = 0$ the nontrivial solution diverges as $t \to +\infty$ [59], hence, it cannot be directly applied as a proper initial approximation. In Ref. [59], an appropriate initial approximation was constructed via combination of the nontrivial solution with the trivial one $p = 1/2$. Using the constructed function as a zero-order approximation, the nonadiabatic transition probability has been calculated and it appeared that the final transition probability is expressed as a power of the Landau-Zener parameter [59, 60] in contrast to the familiar exponential prediction of the linear theory [24-27]. However, this approach is rather complicated and it does not provide a clear treatment of the time dynamics of the association process. Here we make a step forward proposing a much simpler treatment of the problem that gives comprehensive understanding of the whole time evolution of the system [88-91]. To achieve this goal, we use an extended limit equation [88, 91] which differs from that used in Ref. [59] by a term of the form A/t, where A is a constant which is supposed to be small compared with other involved terms in order not to change the leading asymptotes. Due to this modification of the limit equation, we manage to construct a simple two-term approximation that accurately describes the whole time dynamics of the system. Importantly, the constructed solution reveals the main characteristics of the process in a simple and natural manner.

The *extended* limit equation, involving an adjustable constant A, is written as

$$\left(\frac{d}{dt} - \frac{1}{t}\right)\left[-\frac{\lambda}{2}(1 - 8p + 12p^2) + A\right] + 4t^2 p_t = 0. \qquad (2.33)$$

This equation is integrated via transformation of the independent variable followed by interchange of the dependent and independent variables. This results in a polynomial equation of the fourth degree for the limit solution $p_0(t)$:

$$\frac{\lambda}{4t^2} = \frac{C_0 + p_0(p_0-\beta_1)(p_0-\beta_2)}{9(p_0-\alpha_1)^2(p_0-\alpha_2)^2}, \tag{2.34}$$

where C_0 is the integration constant and

$$\alpha_{1,2} = \frac{1}{3} \mp \frac{1}{6}\sqrt{1+\frac{6A}{\lambda}}, \quad \beta_{1,2} = \frac{1}{2} \mp \sqrt{\frac{A}{2\lambda}}. \tag{2.35}$$

For the initial condition $p_0(-\infty) = 0$ it holds $C_0 = 0$. Note that at $A = 0$ the quartic equation (2.34) reduces to a quadratic one since in this case three of the four parameters $\alpha_{1,2}$, $\beta_{1,2}$ become equal, $\alpha_2 = \beta_1 = \beta_2 = 1/2$. The solution of this quadratic equation diverges at $t \to +\infty$. However, for a *positive* A the solution of the quartic equation (2.34) defines a bounded, monotonically increasing function which tends to a finite value less than $1/2$ when $t \to +\infty$ (Fig. 2.4). This solution has all the needed features to be used as an appropriate initial approximation for constructing a solution to the problem. It is thus understood that introduction of the parameter A is, indeed, an essential point.

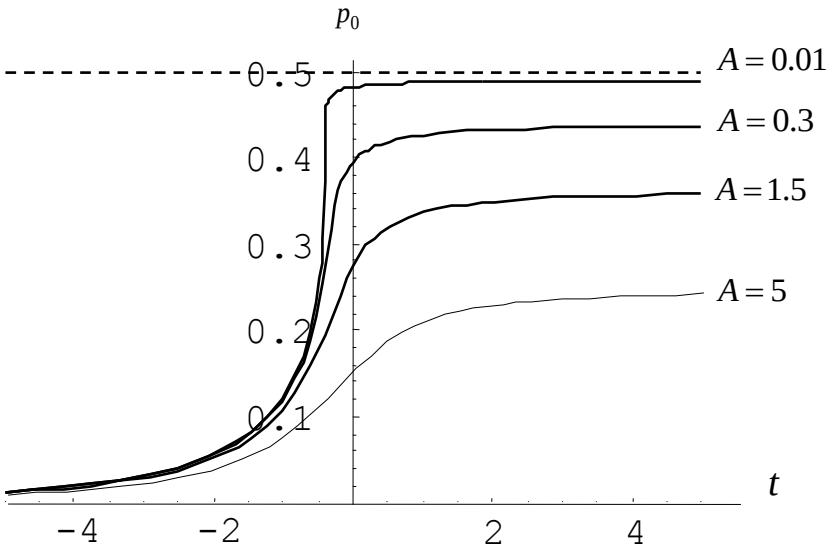

Fig. 2.4. The limit solution $p_0(t)$ for positive $A > 0$ and a fixed λ.

Consider the properties of the limit solution $p_0(t)$ defined by Eq. (2.34) with $C_0 = 0$. The final value $p_0(+\infty)$ is easily found by noting that the left hand-side of Eq. (2.34) goes to zero as $t \to +\infty$. It is then seen that should be $p_0(+\infty) = 0$ or $p_0(+\infty) = \beta_1$ or $p_0(+\infty) = \beta_2$. Since $p_0(t)$ is a monotonically increasing function with $p_0(-\infty) = 0$ and since $\beta_2 > 1/2$, we deduce that $p_0(+\infty) = \beta_1$. In the similar way we find that $p_0(0) = \alpha_1$. Thus,

$$p_0(0) = \frac{1}{3} - \frac{1}{6}\sqrt{1 + \frac{6A}{\lambda}}, \quad p_0(+\infty) = \frac{1}{2} - \sqrt{\frac{A}{2\lambda}}. \tag{2.36}$$

To determine the appropriate value of the parameter A, we substitute $p_0(t, A)$ into the exact equation for the molecular state probability (2.13) and examine the remainder

$$R = \left(\frac{d}{dt} - \frac{1}{t}\right)\left[p_{0tt} - A\right]. \tag{2.37}$$

Obviously, the better the approximation p_0 is the smaller the remainder is. Now note that if $p_{0tt}(0) - A \neq 0$ the remainder diverges at the resonance crossing point $t = 0$ while it is finite for all other points of time. Therefore, we eliminate this divergence by requiring A to obey the equation

$$p_{0tt}(0) - A = 0. \tag{2.38}$$

After some algebra, this equation is rewritten as

$$A = \frac{2}{9\lambda}\left(1 + \frac{1 - 18A/\lambda}{(1 + 6A/\lambda)^{3/2}}\right). \tag{2.39}$$

The approximate solution of the derived equation can be constructed by Newton's successive approximations starting, e.g., from $A = 0$. It turns out that the first approximation is already good enough. Thus, we put $A = 0$ in the right-hand side of the equation and obtain

$$A = \frac{4}{9\lambda}. \tag{2.40}$$

This value of A leads to a good zero-order approximation $p_0(t)$. Numerical simulations show that for large λ this function accurately describes the time evolution of the system in the interval covering the prehistory (up to the resonance point) and an interval after the resonance has

been crossed. However, after that, p_0 misses several essential features of the process. Indeed, for instance, the coherent oscillations between atomic and molecular populations which come up at a certain time point after the resonance has been passed are not incorporated in this solution. Furthermore, the final transition probability at $t \to +\infty$ predicted by p_0 is always lower than what is shown by the numerical solution of the exact equation.

It is understood that the shortcomings of the suggested limit solution are due to the singularity of the procedure we have applied to obtain it. Indeed, we have constructed p_0 by neglecting the term p_{tt} in the square brackets in Eq. (2.13), i.e., the two highest order derivative terms of the equation. Of course, when determining the appropriate value of A via imposing Eq. (2.38), we have taken into account these terms (in fact, to some extent). Yet, this was an indirect procedure and we have convinced that it is not enough.

Therefore, to improve the result, we need a correction that accounts for the second and third order derivatives of p. However, this is not an obvious task because the equation obeyed by the correction term $u \equiv p - p_0$ is still an essentially nonlinear one. Moreover, at an attempt to linearize the exact Eq. (2.13) using p_0 as a zero-order approximation and supposing the correction u to be small as compared with p_0: $u << p_0$, we arrive at a complicated equation with variable coefficients (depending on p_0) the solution of which is not known. We now introduce an approach that enables one to overcome these difficulties. Importantly, the resultant solution not only correctly accounts for the higher order derivate terms in the equation for correction term u but also takes into account, to a very good extent, the nonlinear terms. The constructed solution displays much more improved results. It both accurately treats the oscillations and well fits the final transition probability. For the most part of the variation range of the Landau-Zener parameter $\lambda >> 1$, the resultant graphs are practically indistinguishable from the numerical solution.

Consider a correction u defined as

$$p = p_0 + u\,. \tag{2.41}$$

This function obeys the following exact equation:

$$\left(\frac{d}{dt}-\frac{1}{t}\right)\left(u_{tt}+4\lambda(1-3p_0)u+p_{0tt}-A-6\lambda u^2\right)+4t^2u_t=0. \tag{2.42}$$

Taking into account the initial conditions discussed here, we impose:

$$u(-\infty)=0,\quad u_t(-\infty)=0,\quad u_{tt}(-\infty)=0. \tag{2.43}$$

Since the limit solution $p_0(t)$ is supposed to be a good approximation, the correction u is expected to be small. So, we neglect, for a while, the nonlinear term $-6\lambda u^2$ in Eq. (2.42) thus arriving at a linear equation. Despite the fact that we now have a linear equation, there is only little progress since the solution of the derived equation in the general case of variable $p_0(t)$ is not known. However, note that for constant p_0 one can construct the solution using the scaling transformation

$$u=\frac{A}{2\lambda(1-3p_0)}v. \tag{2.44}$$

As a result, in this case we get a linear Landau-Zener problem for v with an effective Landau–Zener parameter $\lambda^*=\lambda(1-3p_0)$. This observation gives an argument to make a conjecture that the exact solution of Eq. (2.42) can be approximated as:

$$u=C^*\frac{p_{LZ}(\lambda^*,t)}{p_{LZ}(\lambda^*,\infty)}, \tag{2.45}$$

where $p_{LZ}(\lambda^*,t)$ is the solution of the linear Landau-Zener equation with an effective Landau-Zener parameter λ^*:

$$\left(\frac{d}{dt}-\frac{1}{t}\right)\left(p_{LZ\,tt}+4\lambda^*\,p_{LZ}-2\lambda^*\right)+4t^2\,p_{LZ\,t}=0 \tag{2.46}$$

satisfying the initial conditions (2.2). This solution is conveniently written in terms of the Kummer hypergeometric functions.

This proves to be a good conjecture. The numerical simulations show that one can always find C^*, λ^*, and A such that the approximate solution (2.45) accurately fits the numerical solution of Eq. (2.42). Now, in order to derive analytic formulas for fitting parameters C^* and λ^*, we substitute expression (2.45) into the exact Eq. (2.42) and aim at minimization of the remainder

$$R=\left(\frac{d}{dt}-\frac{1}{t}\right)\left\{4\left[\lambda(1-3p_0)-\lambda^*\right]\frac{P_{LZ}(\lambda^*,t)}{P_{LZ}(\lambda^*,\infty)}+\frac{2\lambda^*}{P_{LZ}(\lambda^*,\infty)}+\frac{1}{C^*}\left(p_{0_{tt}}-A\right)-6\lambda C^*\frac{P_{LZ}^2(\lambda^*,t)}{P_{LZ}^2(\lambda^*,\infty)}\right\} \quad (2.47)$$

via appropriate choice of these parameters.

The first term in the curly brackets is a product of two functions. The function $\frac{P_{LZ}(\lambda^*,t)}{P_{LZ}(\lambda^*,\infty)}$ is an increasing (though oscillating) function that starts from zero at $t=-\infty$ and noticeably differs from zero only for time points $t>0$. On the other hand, the function $4[\lambda(1-3p_0)-\lambda^*]$ is a monotonically decreasing function that tends to a large, since λ is a large parameter, final value at $t\to+\infty$ (see Fig. 2.5). It is then understood that this term is highly suppressed if one chooses

$$\lambda^*=\lambda(1-3p_0(+\infty)). \quad (2.48)$$

Note that for $\lambda>>1$ this gives $\lambda^*\approx-\lambda/2$ (2.49)

so that for large λ, λ^* becomes a large *negative* parameter. Interestingly, this choice of λ^* leads to other relevant observations. First, it is known that

$$\lim_{t\to+\infty}P_{LZ}(\lambda^*,t)=1-e^{-\pi\lambda^*}, \quad (2.50)$$

hence, in the case of negative λ^* the function $P_{LZ}(\lambda^*,\infty)$ grows exponentially with $|\lambda^*|$. Consequently, with this choice of λ^* the second term in the curly brackets in Eq. (2.47) is also essentially suppressed. Second, in contrast to positive λ^*, for negative λ^* the Landau-Zener function $P_{LZ}(\lambda^*,t)$ starts to noticeably differ from zero not merely for non-negative time points $t\geq0$ but exclusively for those of the order of or larger than $\sqrt{-\lambda^*/2}$ (see Fig. 2.5).

Hence, the first term in the curly brackets in Eq. (2.47) is even smaller than it was initially expected. Thus, the choice (2.48) essentially suppresses the first two terms in Eq. (2.47).

Regarding the two last terms in Eq. (2.47), one should minimize them with respect to the parameter C^*. This implies the condition

$$\frac{\partial R}{\partial C^*}=\left(\frac{d}{dt}-\frac{1}{t}\right)\left(-\frac{1}{C^{*2}}\left(p_{0_{tt}}-A\right)-6\lambda\frac{P_{LZ}^2(\lambda^*,t)}{P_{LZ}^2(\lambda^*,\infty)}\right)=0. \quad (2.51)$$

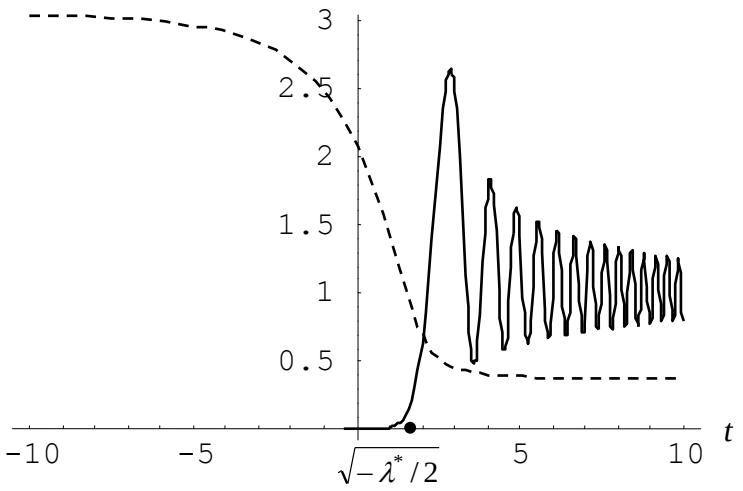

Fig. 2.5. Behavior of functions $4[\lambda(1-3p_0)-\lambda^*]$ (dashed line) and $P_{LZ}(\lambda^*,t)/P_{LZ}(\lambda^*,\infty)$.

Since the last term of this equation is proportional to (large) λ and $\dfrac{P_{LZ}(\lambda^*,t)}{P_{LZ}(\lambda^*,\infty)}$ is an increasing function of time, it is understood that the "worst" point is $t=+\infty$. Hence, we look for minimization at $t=+\infty$. This immediately leads to the following value for C^*:

$$C^* = \sqrt{\frac{A}{6\lambda}}\,. \tag{2.52}$$

This result, together with relation (2.48), is of considerable general importance. Indeed, we see that though we use a solution of a linear equation, $P_{LZ}(\lambda^*,t)$, the parameters of this solution, λ^* and C^*, are essentially changed due to the nonlinear terms involved.

The obtained formulas (2.48) and (2.52) present a rather good approximation. As it can be checked numerically, the solution (2.41), $p=p_0+u$, with p_0 being the exact solution of the limit equation (2.33) and u being a linear Landau-Zener function qualitatively well describes the process. This solution can be then used as an initial approximation for linearization of the initial equation (2.13). However, more elaborate approaches can be suggested. An immediate observation, e.g., is that if we try the approximation (2.41), (2.45) without imposing the initial restriction that the introduced parameter A is already determined by Eq. (2.38), one may modify the latter equation to determine a value of A which will take into account the correction term u. The development of this

approach leads to the following formulas for λ^* and C^*:

$$\lambda^* = -\frac{\lambda}{2} + \lambda \cdot \ln\left(1 + \frac{1}{\lambda}\right), \tag{2.53}$$

$$C^* = \frac{1}{4\lambda} + \frac{1}{27\lambda^3}. \tag{2.54}$$

These formulas define a fairly good approximation. Indeed, starting already from $\lambda = 3$, the produced graphs (Fig. 2.6) are practically indistinguishable from the numerical solution of the exact Eqs. (2.1). The derived approximation notably improves the accuracy of the previous approximation of Ref. [59]. However, importantly, it is applicable far beyond the strong interaction limit and provides a sufficiently good description also for intermediate regime of moderate field intensities (or sweeping rates) down to $\lambda = 1$ and even slightly less ($0.95 < \lambda < 1$) (Fig. 2.7). Though in this regime the predicted amplitude of oscillations differs from that displayed by the numerical solution, it is seen from Fig. 2.7 that the approximation correctly describes many properties of the system's time evolution including the effective transition time, the final transition probability, and the period of atom-molecule oscillations.

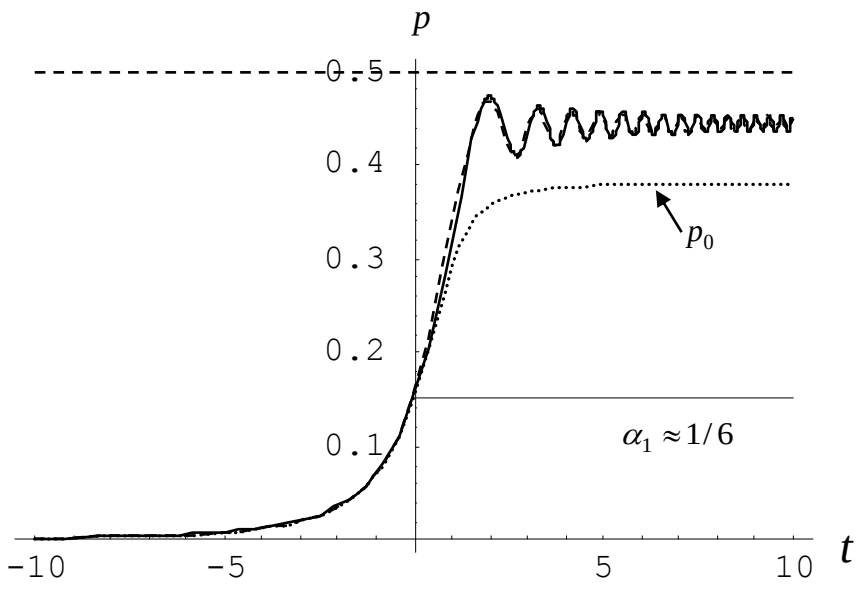

Fig. 2.6. Molecular state probability vs. time at $\lambda = 4$ (dashed line – approximate solution with parameters (2.40), (2.53), and (2.54), dotted line – limit solution). It is seen that in the strong coupling limit $\lambda >> 1$ the prehistory of the system and the resonance crossing are basically defined by the limit solution p_0 while the atom-molecule oscillations are described by the correction u.

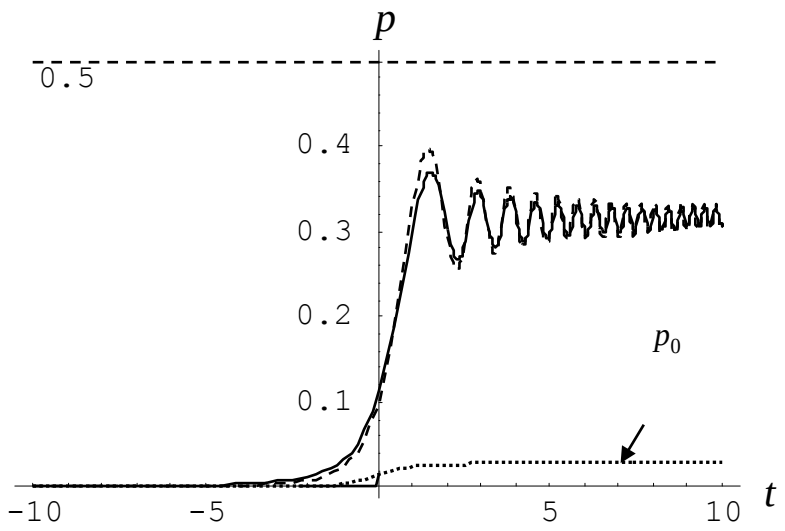

Fig. 2.7. Molecular state probability vs. time at $\lambda = 1$ (dashed line – approximate solution with parameters (2.40), (2.53), and (2.54), dotted line – limit solution). The limit solution p_0 is small so that it is the "correction" u that basically defines the time evolution of the system in the regime of moderate coupling $\lambda \geq 1$.

This is, indeed, a rather unexpected result, especially, if one notes that at moderate coupling $1 < \lambda < 1.5$ the function $p_0(t)$ is very far from the exact solution, as it is seen from Fig. 2.7. An immediate conclusion following from this result is that it is not the limit solution p_0 that basically defines the time evolution of the system in this regime but the "correction" u which was during our calculation envisaged to be small as compared with the limit solution.

Let us note in conclusion that the obtained formulas show that the final probability of the molecular state is given by the simple formula

$$p(+\infty) = \beta_1 + C^* . \tag{2.55}$$

Hence, the formula derived in Refs. [59, 60] for the strong coupling limit $\lambda >> 1$ is modified to include also the intermediate regime of moderate coupling $\lambda \geq 1$ as follows

$$p(+\infty) = \frac{1}{2} - \left(\frac{\sqrt{2}}{3} - \frac{1}{4} \right) \frac{1}{\lambda} + \frac{1}{27\lambda^3} \approx \frac{1}{2} - \frac{0.2214}{\lambda} + \frac{1}{27\lambda^3} . \tag{2.56}$$

Thus, for the quadratic nonlinear interaction we have discussed here the final probability for the system to stay in its initial all-atom state, $|a_1(+\infty)|^2 = 1 - 2p(+\infty)$, is not given by an exponential as predicted by the linear Landau-Zener theory [24-27]. Instead, in the limit of strong coupling it is a linear function of the sweep rate $2\delta_0 \sim 1/\lambda$ if the leading order of the approximation is discussed [59, 60]. This linear dependence of the non-transition probability on the sweep rate is confirmed to occur also by many-body calculations [61-69]. Note, finally, that formula (2.56) suggests the next approximation term as $1/(27\lambda^3)$. The general formula for the final Landau-Zener transition probability applicable to the whole variation range of the Landau-Zener parameter, $\lambda \in [0, \infty)$, is derived in [89]. Remarkably, this formula is written in terms of elementary functions only.

Summary of Chapter 2

In this chapter, we have examined the second harmonic generation in a quadratic nonlinear optical medium and coherent photo- and magneto-association of cold atoms with formation of cold diatomic molecules in the framework of the nonlinear Landau-Zener two-state model. In the context of SHG, the Landau-Zener configuration models the situation when the second-order susceptibility doesn't change along the direction of propagation of the interacting waves, while the wave number mismatch varies linearly in this direction. For the cold molecule formation, the external field configuration is defined by linear-in-time term-crossing model, when the Rabi frequency is constant and the detuning linearly in time crosses the resonance.

For the weak interaction regime, we have proposed a basic functional form of the appropriate approximation, written in the form of a modification of the solution to the corresponding linear LZ problem with two scaling parameters involved. One of these parameters is a simple pre-factor while another one serves as an effective LZ parameter. We have shown that by an appropriate choice of these parameters the proposed solution well describes the main characteristics of the exact solution to the problem in the whole time domain.

We have constructed relevant equations for determination of the introduced auxiliary parameters. The approach for the derivation of these equations is as follows. The proposed zero-order initial approximation generates an inhomogeneous term (which is referred to as remainder) in the exact equation for the next approximation. The further idea was, first, to suppress the divergence of this remainder observed in the resonance-crossing point. Furthermore, second, we minimized the correction term by suppressing, as much as possible, the influence of the remainder on the forming of this next approximation term.

We have derived an accurate analytic approximation to the solution of the formulated equations for the scaling parameters. As expected, the pre-factor C_1 is a slowly varying, monotonically increasing function of the LZ parameter. In the meantime, the dependence of the effective LZ parameter λ_1 on the input LZ parameter λ turns to be non-trivial. As λ increases, the function $\lambda_1(\lambda)$ first monotonically increases ($\lambda_1 \approx \lambda$) starting from $\lambda_1(0) = 0$, reaches its maximal

value, $\lambda_{1\max} \approx 0.124$, at $\lambda \approx 0.454$ and further monotonically decreases reaching zero at $\lambda = \sqrt{2}$.

Using the constructed approximation, we have examined the weak coupling limit of the association process, which corresponds to the weak associating fields: $\lambda \leq 1$. This limit has been previously discussed by several authors. In particular, in Ref. [58, 88] a formula for the final transition probability at $t \to +\infty$ has been derived. Here we go beyond the previous studies and treat the whole time dynamics of the system. The results are inspiring. The constructed solution qualitatively correctly describes the main characteristics of the evolution of the molecular state probability as a function of time for the supposed range of variation of the LZ parameter: $\lambda \in [0,1]$. Furthermore, the behavior of the system before and during the resonance crossing and the frequency of the oscillations of the transition probability that start soon after crossing the resonance, as well as the final transition probability to the molecular state are determined with high accuracy. The present result for the final transition probability improves the accuracy of the previous approximation [58, 60] by order of magnitude.

Only the amplitude of the oscillations displays visible deviations from that of the numerical solution. The deviation is mostly pronounced for several first oscillation periods and becomes rather significant when the LZ parameter approaches unity.

Further, using an exact third-order nonlinear differential equation for the molecular state probability, we have presented an effective variational method for constructing the approximate solution to the problem in the strong coupling limit corresponding to the large values of the Landau-Zener parameter, $\lambda >> 1$. In the case of photoassociation this implies that the intensity of the applied laser field is large enough or, equivalently, the sweep rate across the resonance is sufficiently slow. In the case of SHG this limit supposes strong nonlinear susceptibility or, equivalently, slow variation rate of the phase mismatch.

We have shown that the approximation describing spatial dynamics of second harmonic's intensity and time evolution of the molecular state probability can be written as a sum of two distinct terms. In terms of cold molecule formation, in the strong coupling limit the first term, being a solution of a limit first-order *nonlinear* differential equation, effectively describes the process of

the molecule formation while the second one, being the scaled solution to the *linear* Landau-Zener problem (but now with *negative* effective Landau-Zener parameter as long as the strong coupling limit of high field intensities or, equivalently, slow sweeping rates is considered), describes the oscillation which comes up some time after the system has passed through the resonance. From this, one can conclude that in the strong coupling limit the time dynamics of the atom-molecule conversion consists of the essentially nonlinear process of resonance crossing followed by atom-molecular coherent oscillations that are principally of linear nature. The possibility to make such a decomposition is quite surprising since the Hamiltonian of the system is essentially nonlinear.

The constructed approximation describes the molecule formation process with high accuracy. For $\lambda > 3$ the produced graphs are practically indistinguishable from the exact numerical solution (Fig. 2.6). Interestingly, the approximation rather well works also in the regime of moderate coupling down to $\lambda = 1$ (Fig. 2.7) and slightly less: $0.95 < \lambda < 1$. It correctly describes many properties of the system's time evolution including the effective transition time, the final transition probability, and the period of the atom-molecule oscillations. The only noticeable discrepancy is that the approximate solution overestimates the amplitude of the oscillations [the largest deviation is observed at the points of maxima and minima of the probability $p(t)$ within the time interval covering several first periods of oscillation]. The applicability of the proposed approximation to the intermediate regime of moderate coupling is, indeed, a rather unexpected result because at $1 < \lambda < 1.5$ the limit solution $p_0(t)$ is very far from the exact solution, hence, it is not the limit solution that mostly defines the evolution of the system in this regime. Using the approximation one can find the main characteristics of the association process such as the tunneling time, the frequency of the oscillations of the transition probability that start soon after crossing the resonance, as well as the final transition probability to the molecular state. In particular, we have confirmed that the non-transition probability in the leading approximation order is a linear function of the sweep rate. In addition, we have found that the next approximation term is $1/(27\lambda^3)$.

Finally, we note that the presented approach is not restricted to the Landau-Zener model only [91]. It can be generalized to other time-dependent level-crossing and non-crossing models too

[92, 93]. Also, it can be adopted to explore other nonlinear regimes beyond by the Landau-Zener model [94-95]. Importantly, the developed approach allows one to treat the extended version of the nonlinear two-state problem, when higher-order nonlinearities involving functions of the transition probabilities of the states are added to the basic two-state system. For example, one can analyze the role of the inter-particle elastic scattering which is described by Kerr-type cubic nonlinear terms [96-98]. A successful example of such an application is presented in [98], where it is shown that the inclusion of the cubic-nonlinear terms results in modification of the limit equation to a *fifth* order polynomial equation for the transition probability, a root of which serves as a highly accurate generalized Landau-Zener transition formula applicable for the whole variation range of the involved scattering parameters [98]. Hence, the general conclusion is that the developed method may serve as a general strategy for attacking analogous nonlinear two-state problems involving the generic quadratic nonlinearity as discussed here.

CHAPTER 3. DEMKOV-KUNIKE MODEL FOR COLD ATOM ASSOCIATION

In the present chapter we study the spatial dynamics of SHG and the temporal dynamics of molecule formation for the case when system's configuration is defined by the quasi-linear level crossing Demkov-Kunike model. In nonlinear optics it describes a situation, when the second-order susceptibility varies with the spatial coordinate as hyperbolic secant, and the phase mismatch changes as hyperbolic tangent. In cold molecule formation via photoassociation the model is characterized by a bell-shaped pulse and finite variation of the frequency detuning.

We generalize the mathematical approach developed for the case of the weak interaction regime of the Landau-Zener model and apply it to the nonlinear Demkov-Kunike problem. The presented approximation, written as a scaled solution to the linear problem associated to the nonlinear one we treat, contains fitting parameters which are determined through a variational procedure. Assuming that the parameters involved in the solution of the linear problem are not modified, we suggest an analytical expression for the scaling parameter.

Analyzing the process in the weakly oscillatory regime, which models a situation when the peak value of the coupling is large enough and the resonance crossing is sufficiently fast, we construct a highly accurate ansatz to describe the spatial dynamics of second harmonic generation (temporal dynamics of the molecule formation) in the mentioned nonlinearity regime. The absolute error of the constructed approximation is less than $3 \cdot 10^{-5}$ *for the final second harmonic wave's intensity (transition probability) while at certain time points it might increase up to* 10^{-3}*. The proposed ansatz applies to all the values of the coupling constant, hence, it presents a unified description of weak, intermediate, and strong interaction limits of the fast sweep regime.*

Overview

As it was mentioned above, though the Landau-Zener model has several attractive features, the most important of which for us is the high conversion efficiency predicted by this model, it has some drawbacks. For instance, in the case of photoassociation the LZ model describes a situation when the two quantum states are coupled by an external optical field of constant amplitude and a variable frequency, which is linearly changed in time. But it is unrealistic to have a constant coupling that never turns off or infinite energies at $t \to \pm\infty$. A model that has all the virtues of the Landau-Zener model and is free from its shortcomings and can be considered as a *physical generalization* of the Landau-Zener model, is the first Demkov-Kunike quasi-linear level-crossing model of a bell-shaped pulse (vanishing at $t \to \pm\infty$) and finite detuning [28-29].

In this chapter, we analyze a level crossing process defined by the Demkov-Kunike model and compare the derived results with those for the Landau-Zener model.

We investigate the spatial dynamics of second harmonic generation and temporal dynamics of coherent molecule formation via photo- or Feshbach-association of ultracold atoms. We consider the common case when there is no initial seed of second harmonic. In cold atom association terminology, this situation corresponds to a condensate initially being in all-atomic state (under contemporary conditions one faces this case most frequently), while for SHG it means that there is only fundamental mode at the entrance of the medium with second order nonlinear suscectibility.

The weak interaction limit of the nonlinear DK problem, corresponding to small values of the coupling constant (second-order nonlinear susceptibility in the case of SHG and Rabi frequency of the associating field in the case of cold atom association), has been previously discussed in [99]. Applying Picard's successive approximations to the nonlinear Volterra integral equation, an analytical formula for the final conversion coefficient or probability of transition to the molecular state has been obtained. However, the temporal dynamics of the system has not been discussed in this study.

The strong interaction limit of the DK model, corresponding to large values of the coupling constant, has been studied in [94, 95, 100]. In [94, 95], it has been shown that the strong interaction limit of the DK problem is effectively subdivided into two different interaction regimes

corresponding to slow and fast sweep through the resonance. When the passage through the resonance is slow, the system exhibits large-amplitude Rabi-type oscillations between interacting waves' intensities or atomic and molecular states' populations. In the opposite limit, in the case of the fast enough crossing of the resonance, only weak, damped oscillations between the involved two states are observed. It should be mentioned here, that the Landau-Zener model reveals only one type of behavior: in this case only weak oscillatory regime occurs.

In Ref. [100], an approximate solution to the nonlinear DK problem in the large sweep rate regime of the strong interaction limit has been constructed. This approximation, defined as a solution of a first-order nonlinear equation, contains a fitting parameter which has been determined through a variational procedure. However, the constructed approximation misses several essential features of the association process such as the coherent oscillations between atomic and molecular populations which arise after the system has passed through the resonance. Here we further examine the model and construct the next approximation to the problem by using the previous solution as a zero-order approximation. The resultant approximation contains fitting parameters that we determine combining analytical and numerical methods. The numerical simulations show that the absolute error of the constructed formula is less than $3 \cdot 10^{-5}$ for the final transition probability while at certain time points it might increase up to 10^{-3}. The proposed approximation turns out to be of rather wide applicability: it equally applies to weak, intermediate and strong coupling cases of the fast sweep regime of the process.

3.1. A physically realizable crossing model

As we have already mentioned above, in the most of the theoretical developments the dynamics of the system has typically been treated by the constant-amplitude linear level-crossing Landau-Zener model. However, the actual external field configuration applied in the cold atom association experiments (see, e.g., also [101-105] and references therein) is different from that defined by the LZ model. Hence, for understanding of the physics underlying these experiments, it is important to study how the variation of the laser pulse's shape and the frequency detuning affects the nonlinear dynamics of the system. The field configuration we discuss below is the first Demkov-Kunike (DK) quasi-linear level-crossing model [28,29], characterized by a bell-shaped pulse and a finite variation of the detuning:

$$U(t) = U_0 \operatorname{sech}(t/\tau), \tag{3.1}$$

$$\delta_t(t) = 2\delta_0 \tanh(t/\tau), \tag{3.2}$$

where τ is a positive parameter. The DK model is considered as a natural physical generalization of the LZ model. Fig. 3.1 demonstrates that this model is a physical generalization of the LZ model. Without loss in generality we put $\tau = 1$ in what follows.

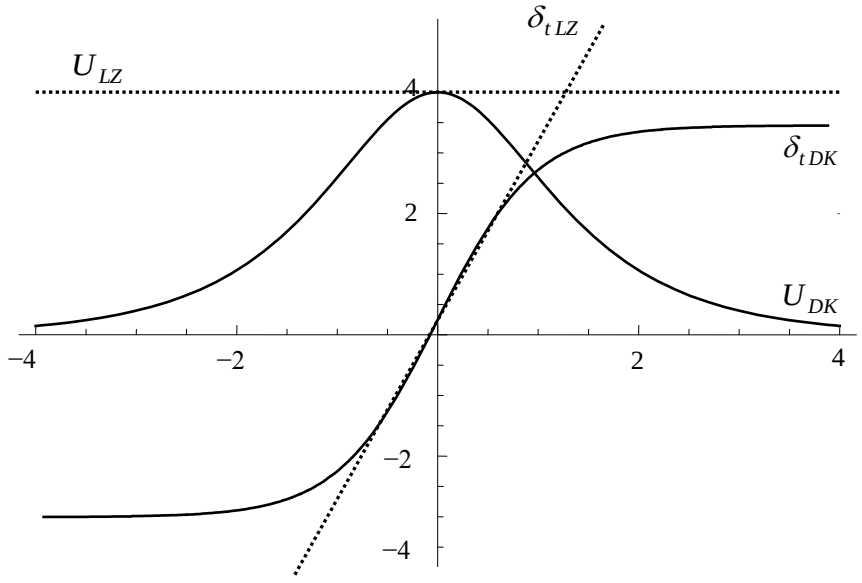

Fig. 3.1.a. Solid curves - the first Demkov-Kunike model: $U = U_0 \operatorname{sech}(t)$, $\delta_t = 2\delta_0 \tanh(t)$, dotted lines - the Landau-Zener model: $U = U_0$, $\delta_t = 2\delta_0 t$.

We start with a numerical simulation of the conversion efficiency. It is clearly seen from Fig. 3.1.b that for DK model there are two different regimes - oscillatory and non-oscillatory. The oscillatory regime is the case for very small phase mismatch $\delta_0 < 1$, while for $\delta_0 > 1$ the conversion efficiency reveals only weak (almost negligible) oscillations. Furthermore, for the latter weak-oscillatory regime one can distinguish two limits, one of which corresponds to relatively small second order nonlinear susceptibility (and large enough phase mismatch), while the other limit corresponds to large nonlinear susceptibility (again, provided large enough phase mismatch). Below we investigate these regions in details and present relevant analytic approximations for each of the non-oscillatory limits. Of particular interest is the region of the parameters where the conversion efficiency is close to unity (Fig. 3.1.c).

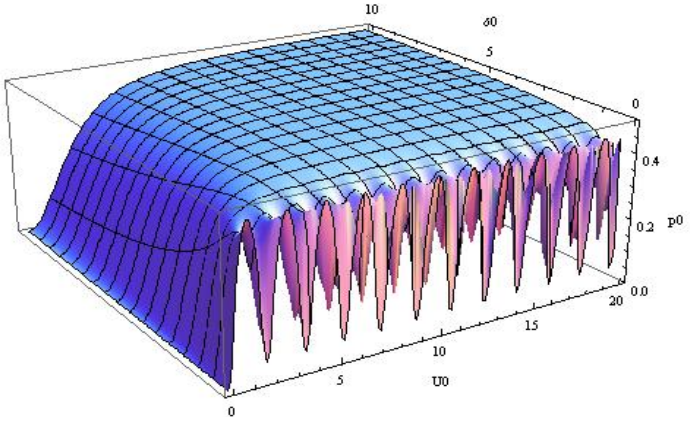

Fig. 3.1.b. Numerical simulation of conversion efficiency as a function of the second order nonlinear susceptibility U_0 and the phase mismatch δ_t for the Demkov-Kunike model.

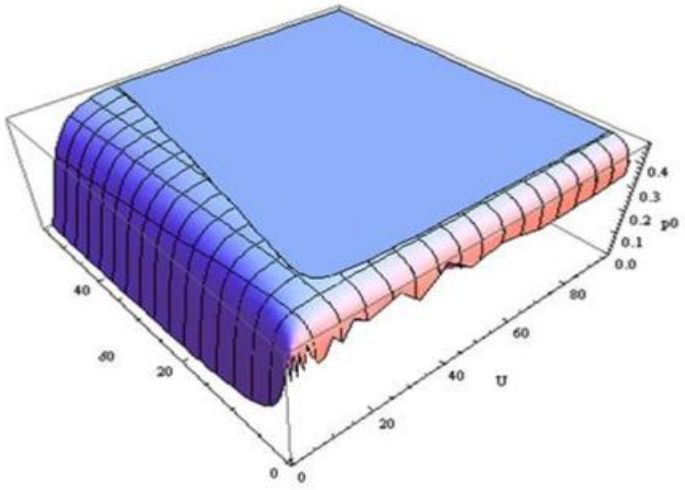

Fig. 3.1.c. Uniform layer represents the region for more than 95% conversion efficiency.

The treatment we present here is based on the following exact equation for the molecular state probability $p = |a_2|^2$:

$$p_{ttt} - \left(\frac{\delta_{tt}}{\delta_t} + 2\frac{U_t}{U}\right)p_{tt} + \left[\delta_t^2 + 4U^2(1-3p) - \left(\frac{U_t}{U}\right)_t + \frac{U_t}{U}\left(\frac{\delta_{tt}}{\delta_t} + \frac{U_t}{U}\right)\right]p_t + \\ + \frac{U^2}{2}\left(\frac{\delta_{tt}}{\delta_t} - \frac{U_t}{U}\right)(1-8p+12p^2) = 0. \tag{3.3}$$

First we simplify this equation, applying transformation of the independent variable

$$z(t) = \int_0^t \frac{U(t')}{U_0} dt', \tag{3.4}$$

reducing Eq. (3.3) to the following constant-amplitude form:

$$p_{zzz} - \frac{\delta_{zz}^*}{\delta_z^*} p_{zz} + \left[\delta_z^{*2} + 4U_0^2(1-3p)\right]p_z + \frac{U_0^2}{2}\frac{\delta_{zz}^*}{\delta_z^*}\left(1-8p+12p^2\right) = 0, \tag{3.5}$$

where the effective detuning δ_z^* is defined as

$$\delta_z^*(z(t)) = \delta_t(t)\frac{U_0}{U(t)}. \tag{3.6}$$

In the case of the DK model, the relations (3.4) and (3.6) take the following form:

$$z(t) = 2\mathrm{Arctan}(e^t) - \frac{\pi}{2}, \tag{3.7}$$

where $z \in \left(-\frac{\pi}{2}, \frac{\pi}{2}\right)$, and $\delta_z^* = 2\delta_0 \tan(z)$. (3.8)

If the physical variable t is used for δ_z^*, it becomes

$$\delta_z^*(z(t)) = 2\delta_0 \sinh(t). \tag{3.9}$$

Note that the resonance crossing point $t = 0$ is mapped into the point $z = 0$.

A linear problem associated to the nonlinear problem at hand can be defined by removing the nonlinear terms from equation (3.3). It can be checked that the obtained linear equation is obeyed by the function $p_L = |a_{2L}|^2$, where a_{2L} is determined from the linear set of equations

$$i\frac{da_{1L}}{dt} = U(t)e^{-i\delta(t)}a_{2L}, \quad i\frac{da_{2L}}{dt} = U(t)e^{i\delta(t)}a_{1L} \tag{3.10}$$

with the normalization constraint

$$|a_{1L}|^2 + |a_{2L}|^2 = I_L = 1/4. \tag{3.11}$$

From the quantum optics point of view this system describes coherent interaction of an isolated atom with an optical laser radiation.

Next, we write the exact solution of the linear set (3.10), satisfying the initial conditions $a_1(-\infty) = 1$ and $a_2(-\infty) = 0$, hence, normalized as

$$|a_{1DK}|^2 + |a_{2DK}|^2 = I_L = 1. \tag{3.12}$$

This solution is given as follows:

$$a_{1DK} = {}_2F_1(-i\delta_0 + \sqrt{U_0^2 - \delta_0^2}, -i\delta_0 - \sqrt{U_0^2 - \delta_0^2}; 1/2 - i\delta_0; x), \tag{3.13}$$

$$a_{2DK} = \frac{U_0}{i + 2\delta_0}(\cosh(t))^{-1+2i\delta_0}\ {}_2F_1(1 - i\delta_0 + \sqrt{U_0^2 - \delta_0^2}, 1 - i\delta_0 - \sqrt{U_0^2 - \delta_0^2}; 3/2 - i\delta_0; x), \tag{3.14}$$

where $x(t) = (1 + \tanh(t))/2$, and ${}_2F_1(\alpha, \beta; \gamma; x)$ is the Gauss hypergeometric function. Accordingly, the probability of transition to the second level is written as

$$p_{DK} = |a_{2DK}|^2, \tag{3.15}$$

and the final transition probability is given by the formula

$$p_{DK}(+\infty) = |a_{2DK}(+\infty)|^2 = 1 - \cos^2\left(\pi\sqrt{U_0^2 - \delta_0^2}\right)\mathrm{sech}^2\,\pi\delta_0. \tag{3.16}$$

It can be easily seen that the solution of the set (3.10), normalized to $1/4$ [according to the normalization condition (3.11)], is given as

$$a_{1L} = \frac{a_{1DK}}{2} \quad \text{and} \quad a_{2L} = \frac{a_{2DK}}{2}. \tag{3.17}$$

3.2. Weak interaction regime for the nonlinear DK model

Now we examine the *weak interaction regime* of the nonlinear DK problem [106]. This regime describes the case when the number of molecules, formed during the association process, is small. For the DK model, it corresponds to the weak coupling limit ($U_0 << 1,\ \forall \delta_0$) and the very large detuning regime of the strong coupling limit ($U_0 > 1,\ \delta_0 >> U_0$).

To develop better intuitive understanding of the problem at hand, we examine the exact equation for the molecular state probability (3.3). The nonlinearity is determined by the current value of the transition probability p. Hence, one may expect that if p remains small enough (note that, anyway, $p \le 1/2$) the role of the nonlinearity will be rather restricted. In this case, neglecting the nonlinear terms in equation (3.3), we get the linear equation, satisfied by the function $p_L = |a_{2L}|^2$ [see Eqs. (3.15) and (3.17)]. Studying now the solution of the linear two-state problem $p_L(t)$ we see that, if the dimensionless peak coupling U_0 is small enough ($U_0 << 1$), or if it is much smaller compared to the sweep rate through the resonance ($U_0 << \delta_0$) then the function p_L does not attain large values. From this one can infer that in these cases the transition probability defined by the nonlinear two-state problem is close to that defined by the linear two-state problem. This observation suggests that in the weak interaction regime the dynamics of the system could be described by the scaled solution of the linear problem, but, with some effective parameters $U_0^*,\ \delta_0^*$:

$$p_0 = C^* \frac{p_L(U_0^*, \delta_0^*, t)}{p_L(U_0^*, \delta_0^*, +\infty)}. \tag{3.18}$$

Such a conjecture for the weak coupling limit of the LZ model was made in Ref. [90] where an accurate analytic approximation written in terms of the scaled solution to an auxiliary linear LZ problem with some effective LZ parameter had been constructed and analytical expressions for the introduced parameters had been determined. Preliminary numerical analysis shows that the function (3.18) is capable to provide high enough accuracy without modification of the detuning parameter δ_0. Hence, hereafter we put $\delta_0^* = \delta_0$. Note that for the variational ansatz (3.18) the approximate expression for the final transition probability is defined by the value of C^* only.

To develop general principles from which the fitting parameters U_0^* and C^* could be determined, we insert the suggested ansatz p_0 into the transformed equation for the molecular state probability (3.5) and consider the behavior of the remainder

$$R = \left(\frac{d}{dz} - \frac{\delta_{zz}^*}{\delta_z^*} \right) r(z), \tag{3.19}$$

$$r(z(t)) = \frac{C^*}{p_{DK}(U_0^*,+\infty)} \frac{U_0^{*2}}{2} \left[4 - 8 p_{DK}(U_0^*,t) \right] - \frac{U_0^2}{2} \left[1 - 8 C^* \frac{p_{DK}(U_0^*,t)}{p_{DK}(U_0^*,+\infty)} + 12 \left(C^* \frac{p_{DK}(U_0^*,t)}{p_{DK}(U_0^*,+\infty)} \right)^2 \right]. \tag{3.20}$$

It is obvious that the better approximation p_0 is the smaller remainder R will become [it would be identically zero if p_0 is the exact solution to Eq. (3.5)]. Thus, we try to minimize the remainder via appropriate choice of the fitting parameters C^* and U_0^*. We first note that, since the function $p_{DK}(U_0^*,t)$ is bounded everywhere, the function R is bounded almost everywhere. The exceptions are the resonance crossing point $z = 0$ $(t = 0)$ and the points $z = \pm\pi/2$ $(t = \pm\infty)$, where, due to the term $\delta_{zz}^* / \delta_z^*$ in the operator $(d/dz - \delta_{zz}^* / \delta_z^*)$, in general, R diverges. Since when passing to the physical variable t the singularities of the remainder R at $z = \pm\pi/2$ disappear, we choose to eliminate divergence at the resonance crossing point $z = 0$, i.e., we require U_0^* and C^* to satisfy the equation $r(0) = 0$. Explicitly, this equation is written as

$$\frac{C^*}{p_{DK}(U_0^*,+\infty)} \frac{U_0^{*2}}{2} \left[4 - 8 p_{DK}(U_0^*,0) \right] = \frac{U_0^2}{2} \left[1 - 8 C^* \frac{p_{DK}(U_0^*,0)}{p_{DK}(U_0^*,+\infty)} + 12 \left(C^* \frac{p_{DK}(U_0^*,0)}{p_{DK}(U_0^*,+\infty)} \right)^2 \right]. \tag{3.21}$$

To find appropriate values for U_0^* and C^* we need to introduce one more equation. Of course, in order to construct an approximation as simple as possible, one may first try to avoid variation of both auxiliary parameters and try to get a simpler, one-parametric approximation instead. A natural choice is then to fix $U_0^* = U_0$ and vary C^* alone. Equation (3.21) then readily gives:

$$C^* = \lim_{t \to +\infty} p_0(t) = \frac{1 - \sqrt{1 - 3 p_{DK}(U_0,0)^2}}{6 p_{DK}(U_0,0)^2} p_{DK}(U_0,+\infty). \tag{3.22}$$

As it follows from Eqs. (3.13)-(3.14), the explicit expression for $p_{DK}(0)$ can be written as:

$$p_{DK}(0) = 1 - \left| {}_2F_1(-i\delta_0 + \sqrt{U_0^2 - \delta_0^2}, -i\delta_0 - \sqrt{U_0^2 - \delta_0^2}; 1/2 - i\delta_0; 1/2) \right|^2 . \quad (3.23)$$

Numerical analysis shows that the constructed approximation (3.18), with $\delta_0^* = \delta_0$, $U_0^* = U_0$ and C^* defined according to Eq. (3.22), accurately describes the temporal dynamics of the molecule formation in the weak coupling limit. Further, we compare the derived approximate expression for the final transition probability (3.22) with that calculated in Ref. [99]:

$$\lim_{t \to +\infty} p(t) \approx \frac{p_{DK}(U_0, +\infty)}{4} \left(1 + \frac{3U_0^2}{64} \frac{1 + 2\delta_0^2}{1 + \delta_0^2} \, | B(1/2 + i\delta_0, 1/2 + i\delta_0) |^2 \; p_{DK}(U_0, +\infty) \right). \quad (3.24)$$

The derived formula (3.22) for the final transition probability, approximation (3.24) of Ref. [99], and the result of numerical simulation are shown in Fig. 3.2. As we see, in the weak coupling limit $U_0 < 1$ the derived formula works slightly well than the one defined by Eq. (3.24). On the other hand, numerical analysis shows that in the very large detuning regime of the strong coupling limit ($U_0 > 1$, $\delta_0 >> U_0$), the formula (3.24) has wider applicability range than formula (3.22). However, importantly, in addition to providing an expression for the final transition probability in the weak interaction regime, the presented method also accurately treats the temporal dynamics of the molecule formation (Figs. 3.3 and 3.4).

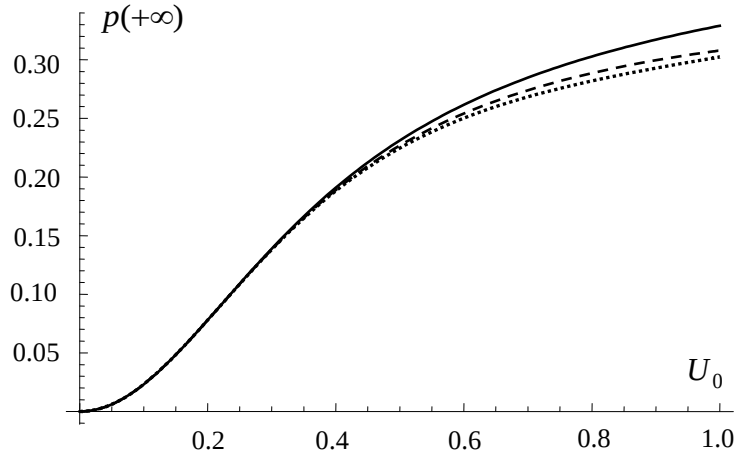

Fig. 3.2. Final transition probability for $\delta_0 = U_0$. Solid line – numerical result, dashed line – approximate formula (3.22), dotted line - formula (3.24).

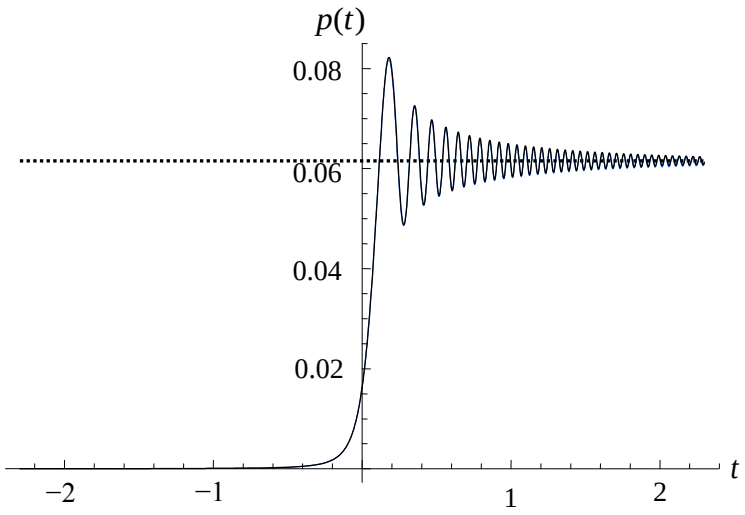

Fig. 3.3. Molecular state probability versus time for $U_0 = 2.5$, $\delta_0 = 70$.

For considered values of parameters, the numerical result and the approximate formula (3.22) are undistinguishable. Dotted line is the final transition probability given by Eq. (3.24).

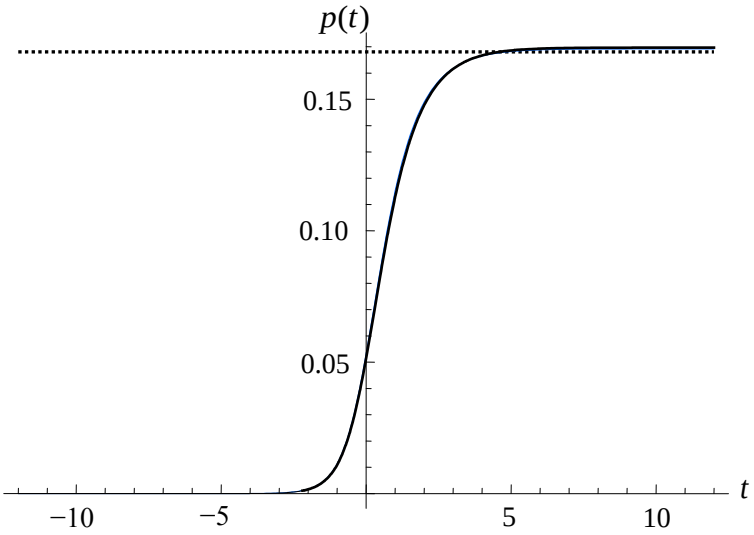

Fig. 3.4. Molecular state probability versus time for $U_0 = 0.3$, $\delta_0 = 0.01$.

The numerical solution and the approximate formula (3.22) produce practically undistinguishable graphs. Dotted line is the final transition probability given by Eq. (3.24).

3.3. An ansatz for the nonlinear DK model

Though the maximal value attained by the function p is equal to $1/2$, we conventionally refer to p as to the molecular state probability. For gaining a better intuitive understanding of the molecule formation in the large sweep rate regime of the strong interaction limit ($\lambda > 1$, $1 < \delta_0 < \sqrt{\lambda}$), in Fig. 3.5 we show the numerical plot of the molecular state probability in the mentioned interaction regime as a function of time.

In Ref. [100], the approximate solution of the exact equation for the molecular state probability (Eq. 3.3) has been constructed by neglecting the two higher order derivate terms and adding to the truncated equation a term of the form $A\delta_{zz}^*/\delta_z^*$, where A is an adjustable parameter. Thus, the zero-order approximation to the problem has been chosen as a solution of the following nonlinear equation of the first order:

$$\left[\delta_z^{*2} + 4\lambda(1-3p_0)\right]p_{0z} + \frac{\lambda}{2}\frac{\delta_{zz}^*}{\delta_z^*}\left(1-8p_0+12p_0^2\right) - A\frac{\delta_{zz}^*}{\delta_z^*} = 0. \tag{3.25}$$

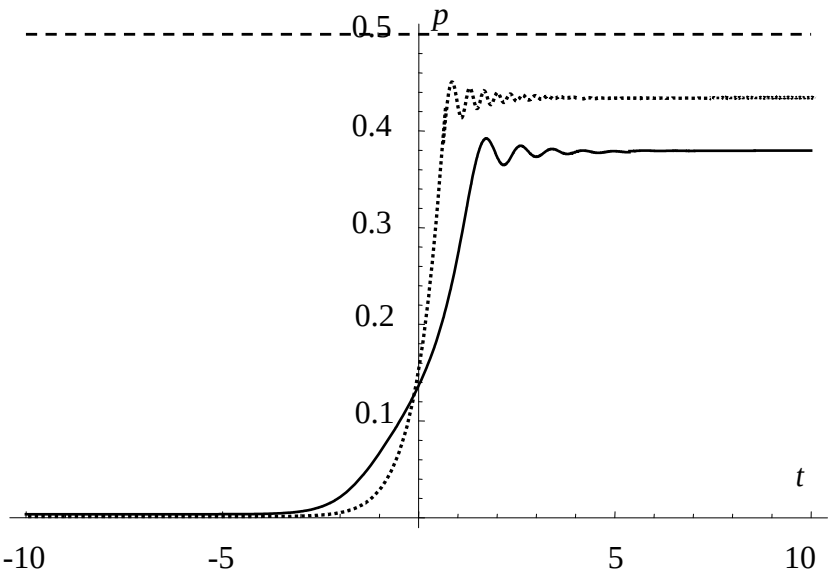

Fig. 3.5 The probability of the molecular state versus time for the DK model in the large sweep rate regime of the strong interaction limit.

Solid line - $\lambda = 100$, $\delta_0 = 10$, dotted line - $\lambda = 100$, $\delta_0 = 4$.

The arguments to construct this approximation have been based on the fact that in the large sweep rate regime of the strong interaction limit the parameters λ and δ_0 are supposed to be large. As it has been shown in [100,107], the exact solution of the augmented limit equation (Eq. 3.25), satisfying the imposed initial condition $p_0(t=-\infty)=0$, is given as a solution of the following polynomial equation of the fourth order:

$$\frac{\lambda}{\delta_z^{*2}(z(t))}=\frac{p_0(p_0-\beta_1)(p_0-\beta_2)}{9(p_0-\alpha_1)^2(p_0-\alpha_2)^2}, \tag{3.26}$$

where

$$\alpha_{1,2}=\frac{1}{3}\mp\frac{1}{6}\sqrt{1+\frac{6A}{\lambda}}, \quad \beta_{1,2}=\frac{1}{2}\mp\sqrt{\frac{A}{2\lambda}}. \tag{3.27}$$

Eq. (3.26) defines a *quartic algebraic equation* for determination of $p_0(t)$. Note that

$$p_0(0)=\alpha_1 \quad \text{and} \quad p_0(+\infty)=\beta_1. \tag{3.28}$$

The limit solution $p_0(z(t),A)$ is a monotonically increasing function that starts from zero at $t=-\infty$, reaches some value less than $1/6$ at $t=0$ and tends to a finite positive value less than $1/2$ for $t\to+\infty$ when $0<A<\lambda/2$ (see Fig. 3.6). An analytical expression for the parameter A has been suggested. However, in the present development we do not specify the value of A, but consider it as a fitting parameter.

To proceed further, we now try to construct the first-order approximation to the problem using the limit function p_0 as a zero-order approximation. To do that, we make the change of the dependent variable

$$p=p_0+u \tag{3.29}$$

in the exact equation for the molecular state probability (Eq. 3.5). This transformation leads to the following exact equation for the correction term u:

$$\left(\frac{d}{dz}-\frac{\delta_{zz}^*}{\delta_z^*}\right)\left(u_{zz}+4\lambda(1-3p_0)u+p_{0zz}-A-6\lambda u^2\right)-\delta_z^{*2}u_z=0. \tag{3.30}$$

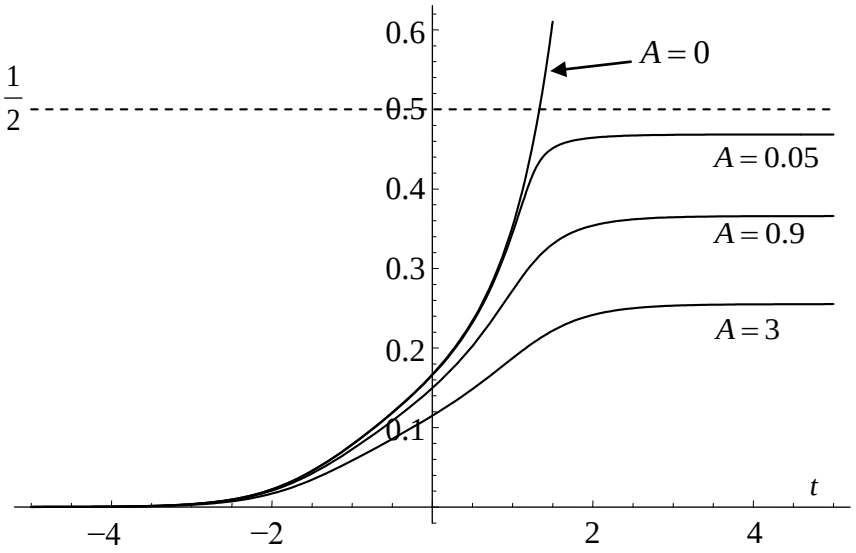

Fig. 3.6. The limit solution $p_0(t)$ [Eqs. (3.26)-(3.27)] vs. time for $A = 0, 0.05, 0.9, 3$ and $\lambda = 25$.

Since the function p_0 is supposed to be a good approximation for the molecular state probability p, the correction u is supposed to be small. Thus, if we neglect the nonlinear term $-6\lambda u^2$, the exact equation (3.30) for u will be linearized. By comparing the resultant linear equation with that obeyed by the second state probability P_{DK}, calculated within the linear theory of nonadiabatic transitions, we see that if we consider p_0 as a constant, the solution of the linearized equation will be given as a scaled solution to the *linear* DK problem with modified parameters. This observation gives an argument to make a conjecture that the exact solution of Eq. (3.30) can be approximated as

$$u = C^* \frac{P_{DK}(\lambda^*, \delta_0^*, t - t_{ph})}{P_{DK}(\lambda^*, \delta_0^*, \infty)}, \tag{3.31}$$

where $P_{DK}(\lambda^*, \delta_0^*, t)$ is the solution to the linear DK problem with effective parameters λ^*, δ_0^*, and t_{ph} being an extra temporal shift.

By combining Eqs. (3.29) and (3.31) we arrive at the following principal conjecture [107-109]: an accurate approximation describing the time evolution of the molecular state probability can be written as a sum of the solution of the limit equation (3.25) and a scaled solution to the *linear*

DK problem with *modified* parameters:

$$p = p_0(A,t) + C^* \frac{P_{DK}(\lambda^*, \delta_0^*, t - t_{ph})}{P_{DK}(\lambda^*, \delta_0^*, \infty)} , \tag{3.32}$$

This conjecture is well confirmed by numerical analysis; the numerical simulations show that one can always find A, C^*, λ^*, and t_{ph} such that the function (3.32) accurately fits the numerical solution of the exact equation for the molecular state probability (3.3). Furthermore, the simulations indicate that there is no need to modify the detuning parameter δ_0. It also turns out that we may put $t_{ph} = 0$. Further numerical analysis shows that the absolute error of formula (3.32) is less than $3 \cdot 10^{-5}$ for the final transition probability. For arbitrary times, its absolute error is commonly of the order of $10^{-5} - 10^{-4}$, and for the points of the first few maxima and minima of the function $p(t)$ (at certain values of the input parameters λ and δ_0) the deviation may increase up to 10^{-3}.

Examining the role of the two terms in the approximate expression for the molecular state probability (3.32), we see that the first term, being a solution of the nonlinear equation (3.25), effectively describes the process of the molecule formation while the second one, being the scaled solution to the *linear* DK problem, describes the oscillations which arise some time after the system has passed through the resonance (see Fig. 3.7). From this, one can conclude that in the strong coupling limit the dynamics of the atom-molecule conversion effectively consists of the nonlinear resonance crossing followed by atom-molecular coherent oscillations that are principally of linear nature. The possibility to make such decomposition is not trivial since the governing set of equations is essentially nonlinear.

One of the essential virtues of Eq. (3.32) is that it provides a simple expression for the final transition probability written in terms of the parameters A and C^*:

$$p(+\infty) = p_0(+\infty) + C^* . \tag{3.33}$$

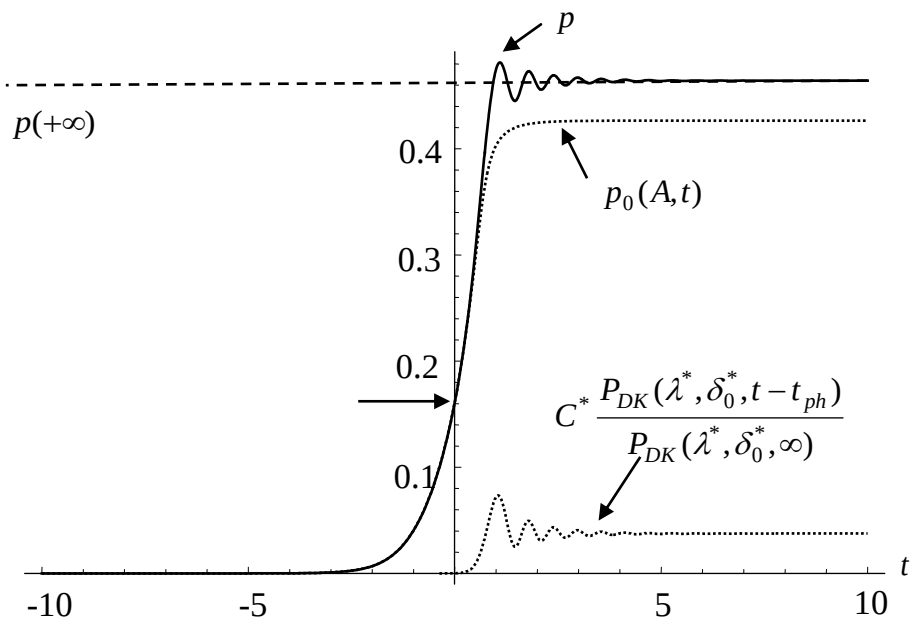

Fig. 3.7. Molecular state probability p, the limit solution p_0 determined from Eq. (3.25), and the scaled solution to the linear DK problem with modified parameters ($\lambda = 49$ and $\delta_0 = 5.5$).

To study the asymptotic behavior of the fitting parameters A and C^* in the limit $\lambda \to \infty$, we substitute the trial function (3.32) into the exact equation for the molecular state probability (3.5) and consider the behavior of the remainder

$$R = \left(\frac{d}{dz} - 2\csc(2z)\right)\left\{4\left[\lambda(1-3p_0) - \lambda^*\right]C^* \frac{p_{DK}(\lambda^*, z(t))}{p_{DK}(\lambda^*, z(+\infty))} + C^* \frac{2\lambda^*}{p_{DK}(\lambda^*, z(+\infty))} + \left(p_{0zz} - A\right) - 6\lambda C^{*2} \frac{p_{DK}^2(\lambda^*, z(t))}{p_{DK}^2(\lambda^*, z(+\infty))}\right\}. \tag{3.34}$$

It is seen that for $\lambda >> 1$ the first term of the remainder is highly suppressed if we choose the fitting parameter λ^* as

$$\lambda^* = \lambda(1 - 3p_0(+\infty)). \tag{3.35}$$

Then taking into account the value of $p_0(+\infty)$ [see Eqs. (3.27)-(3.28)], we have:

$$\lambda^* = -\frac{\lambda}{2} + 3\sqrt{\frac{A\lambda}{2}}. \tag{3.36}$$

Hence, we conclude that for $\lambda >> 1$, λ^* is a (large) *negative* parameter.

Regarding the two last terms of Eq. (3.34), one should minimize them with respect to the parameter C^*. This implies the condition

$$\frac{\partial(R/C^*)}{\partial C^*} = \left(\frac{d}{dz} - 2\csc(2z) \right) \left(-\frac{1}{C^{*2}} \left(p_0'' - A \right) - 6\lambda \frac{P_{DK}^2(\lambda^*, z(t))}{P_{DK}^2(\lambda^*, z(+\infty))} \right) = 0 . \tag{3.37}$$

Since the last term is proportional to (large) λ and $P_{DK}(\lambda^*, t)$ is an increasing function of time, the "worst" point is $t = +\infty$. Hence, we look for a minimization at $t = +\infty$. This immediately leads to the following value for C^*:

$$C^* = \sqrt{\frac{A}{6\lambda}} . \tag{3.38}$$

Thus, we have constructed approximate expressions for the fitting parameters C^* and λ^* in the case of large values of the peak laser field intensity and large values of the sweep rate through the resonance ($\lambda >> 1$, $1 < \delta_0$). Note that the parameters C^* and λ^* still depend on of the fitting parameter A.

Summarizing the presented analysis, we have arrived at the following limit expressions for the fitting parameters:

$$\lambda << 1, \qquad C^* \approx P_{DK}(\lambda^*, \infty)/4, \quad \lambda^* \approx \lambda, \quad A \approx \lambda/2 \tag{3.39}$$

$$\lambda >> 1, \qquad C^* = \sqrt{A/6\lambda}, \quad \lambda^* = \lambda(1 - 3p_0(+\infty)), \quad A \approx \frac{\lambda}{27\delta_0^{\sqrt{3}}} . \tag{3.40}$$

These are the starting asymptotes that we want to generalize to achieve a uniformly valid description of the process applicable for the all values of involved input parameters of the problem.

3.4. Unified description

In the present section, we make an attempt to construct unified expressions for the fitting parameters A, C^*, and λ^*, that is, we try to determine the functions $A(\lambda,\delta_0)$, $C^*(\lambda,\delta_0)$, and $\lambda^*(\lambda,\delta_0)$ such that the ansatz

$$p = p_0(A,t) + C^* \frac{P_{DK}(\lambda^*,t)}{P_{DK}(\lambda^*,+\infty)} \tag{3.41}$$

provides an appropriate approximation to the solution of the problem in the whole range of variation of the input Landau-Zener parameter λ.

We first try to construct a general expression for the principal parameter A (it is shown afterwards that all other introduced parameters are expressed in terms of this parameter). So far, we have succeeded in gaining information about the asymptotic behavior of the function A at small and large limiting values of the parameter λ. Having in the mind the asymptotes discussed above, a possible version is the following smooth function:

$$A = \left(\frac{\delta_0}{\sqrt{2\lambda}} + \frac{\lambda}{27\delta_0{}^{\sqrt{3}}} \right) \tanh\left(\frac{\lambda^{3/2}}{\sqrt{2}\delta_0} \right). \tag{3.42}$$

Obviously, this choice of the function $A(\lambda,\delta_0)$ is not unique. It is also possible to choose it, e.g., as

$$A = \left(\frac{\lambda}{2} + \frac{\lambda^3}{27\delta_0{}^{\sqrt{3}}} \right) \tanh\left(\frac{1}{\lambda^2} \right). \tag{3.43}$$

What is the best choice remains a question. It turns out that an appropriate function can be proposed using the Gauss hypergeometric function. Below we address this question in detail.

As regards the determination of function $C^*(\lambda,\delta_0)$, we note that a possibility comes up when one considers a function of the following structure:

$$C^* \approx \frac{P_{DK}(\lambda^*,\infty)}{4} \sqrt{\frac{A}{f(\lambda,\delta_0)\lambda}}, \tag{3.44}$$

where $f(\lambda,\delta_0)$ should be a slowly varying function such that $f(\lambda,\delta_0) \to 1/2$ at $\lambda \to 0$, in order to fulfill the limit given by Eq. (3.39).

As we show here, it is possible to considerably improve the suggested phenomenological formulas (3.42)-(3.44) for the fitting parameters by means of a combination of analytical methods and numerical simulations. This allows us to determine specific forms for the functions $A(\lambda,\delta_0)$, $C^*(\lambda,\delta_0)$, and $\lambda^*(\lambda,\delta_0)$ such that the ansatz (3.41) provides a highly accurate approximation.

To do this, we replace the hyperbolic tangent by a Gauss hypergeometric function which has a behavior qualitatively similar to that of the function $\tanh\left(\lambda^{3/2}/\sqrt{2}\delta_0\right)$ but contains some adjustable parameters which we could define via fitting suggested functions $A(\lambda,\delta_0)$, $C^*(\lambda,\delta_0)$, and $\lambda^*(\lambda,\delta_0)$ to the numerical data. Extensive simulations lead to the following result:

$$A=\left(\frac{\lambda}{2}+\frac{2\lambda^2}{27\delta_0{}^{\sqrt{3}}}\right)_2F_1\left(\frac{5}{4},\frac{1}{2},\gamma,\frac{-\lambda^2}{1.25\delta_0{}^{3/2}}\right), \tag{3.45}$$

$$C^*=\frac{P_{DK}(\lambda,+\infty)}{4}\sqrt{\frac{2}{\lambda}\left(\frac{\lambda}{2}+\frac{2\lambda^2}{27\delta_0{}^{\sqrt{3}}}\right)_2F_1\left(\frac{5}{4},\frac{1}{2},\gamma_1,\frac{-\lambda^2}{1.5\delta_0{}^{3/2}}\right)}, \tag{3.46}$$

and $$\lambda^*=\lambda\,(1-3\beta_1-3C^*)=\lambda\,(1-3p(+\infty))\,, \tag{3.47}$$

where γ and γ_1 are some parameters which depend on the value of the detuning parameter δ_0. The behavior of A, C^*, and λ^* as a function of the input parameter λ is shown in Figs. 3.8-3.10.

Let us first discuss the behavior of the fitting parameter A. Fig. 3.8 suggests that there exist three distinct interaction regimes: weak, intermediate and strong interaction regimes. In the weak interaction regime, corresponding to small values of the input parameter λ, the fitting parameter A abruptly increases reaching its maximal value at a point $\lambda=\lambda_{\max}$. At sufficiently small values of λ the behavior of the parameter A is given by the linear asymptote $\lambda/2$. With increasing values of λ, the parameter A starts to deviate from this asymptote, always remaining smaller than $\lambda/2$. Such a behavior is observed also in the case of the Landau-Zener model, and it can be shown that this behavior is common for all the level-crossing models. Hence, we conclude that the specific character of the models is not much revealed in the weak coupling regime. For this reason, we will refer to the weak interaction limit $\lambda<<1$ as the fundamental limit of weak coupling regime.

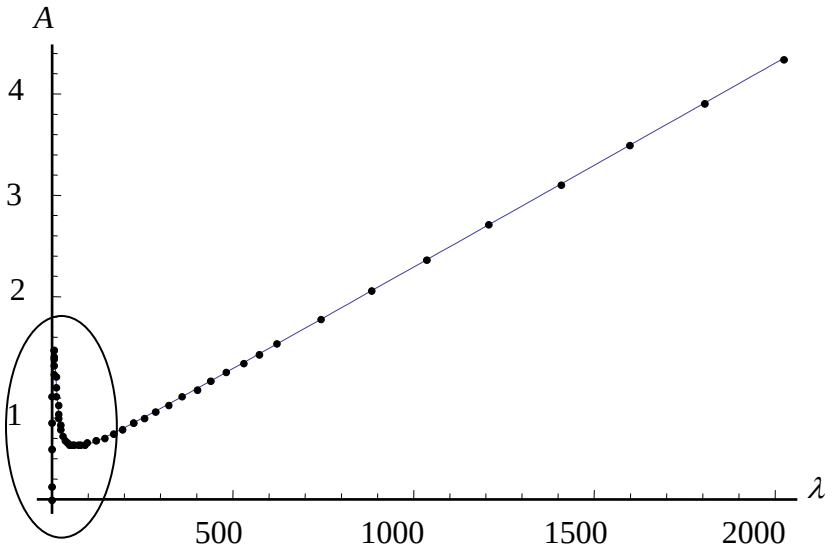

Fig. 3.8a. Fitting parameter A as a function of λ for $\delta_0 = 5.5$.

Filled circles are the result of the fit while the solid line corresponds to the formula (3.45). Linear dependence at large lambda is observed. The circled region is shown in Fig. 3.8b.

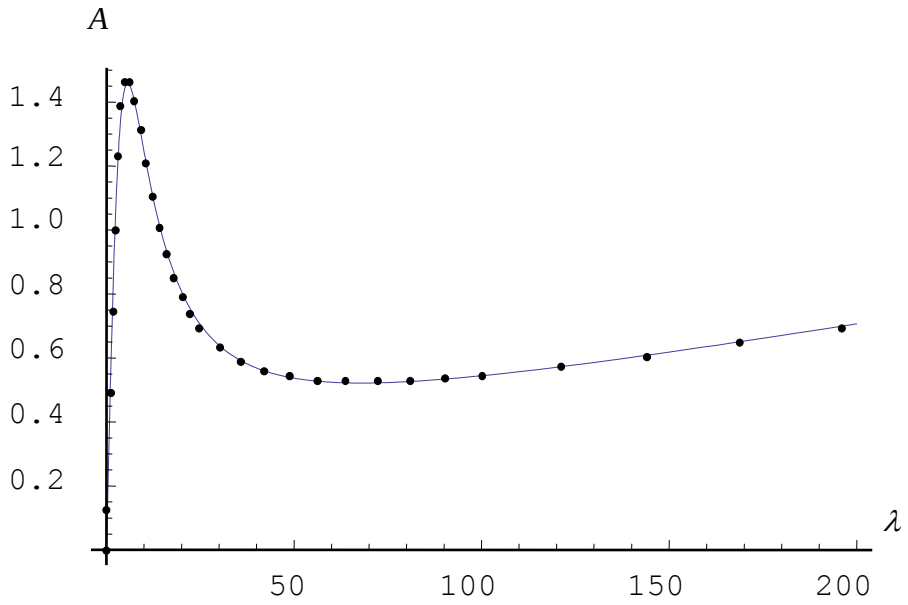

Fig. 3.8b. Parameter A as a function of λ for $\delta_0 = 5.5$. Weak coupling corresponds to $\sqrt{\lambda} < \delta_0$.

Filled circles are the result of numerical fit while the solid line corresponds to the formula (3.45).

Further, for $\lambda_{\max} < \lambda < \lambda_{\min}$, where $\lambda = \lambda_{\min}$ is the point where the function A has a minimum, the function $A(\lambda)$ rapidly decreases. We refer to this regime as the intermediate interaction regime. Finally, for $\lambda > \lambda_{\min}$, which corresponds to the strong interaction regime, the function A increases with λ. To gain a better insight into the behavior of the function A in the strong interaction regime, let us consider the asymptotic expansion of the function A at $\lambda >> \delta_0^2$:

$$A \approx \frac{0.173456\ \Gamma(\gamma)}{\delta_0^{0.982051}\ \Gamma(\gamma - 0.5)}\lambda + \alpha_0 + \frac{\beta_0}{\lambda}. \tag{3.48}$$

The structure of Eq. (3.45) suggests that for $\lambda >> \lambda_{\min}$ the leading asymptotic term of this expansion is determined by the product of the second term in the brackets and the hypergeometric function. Numerical simulations show that for $\lambda >> \lambda_{\min}$ the slope of the term linear in λ is always positive. In particular, for $\delta_0 = 5.5$, we have $\gamma = 0.5365$, hence, for $\lambda >> \lambda_{\min}$ $A \approx 0.00192897\lambda$. An important observation now concerns the very structure of Eq. (3.48). We see that in the transitional region between the weak and strong interaction regimes the function $A(\lambda)$ is approximated as a sum of the hyperbola β_0 / λ, a constant and a linear function. It is known that in the case of the LZ model the asymptotic behavior of the parameter A for $\lambda >> 1$ is given by a hyperbola, $4/(9\lambda)$, only. For this reason, the hyperbola in the asymptotic expansion (3.48) can be interpreted as the LZ "imprint", while the particular character of the DK model is related to the term linear in λ in Eq. (3.48). This term is mostly expressed in the strong interaction limit $\lambda >> \lambda_{\min}$ where it becomes the leading asymptotic term.

Consider now the behavior of the function $C^*(\lambda)$ (Fig. 3.9). From Eq. (3.46) one readily gets that for $\lambda >> \delta_0^2$

$$C^* \approx P_{DK}(\lambda, +\infty)\sqrt{\frac{\Gamma(\gamma_1)}{\Gamma(\gamma_1 - 1/2)}}\left(\frac{0.147248}{\delta_0^{0.491025}} + \frac{0.496962\delta_0^{1.24103}}{\lambda}\right). \tag{3.49}$$

The dependence of the fitting parameter λ^* as a function of λ is shown in Fig. 3.10.

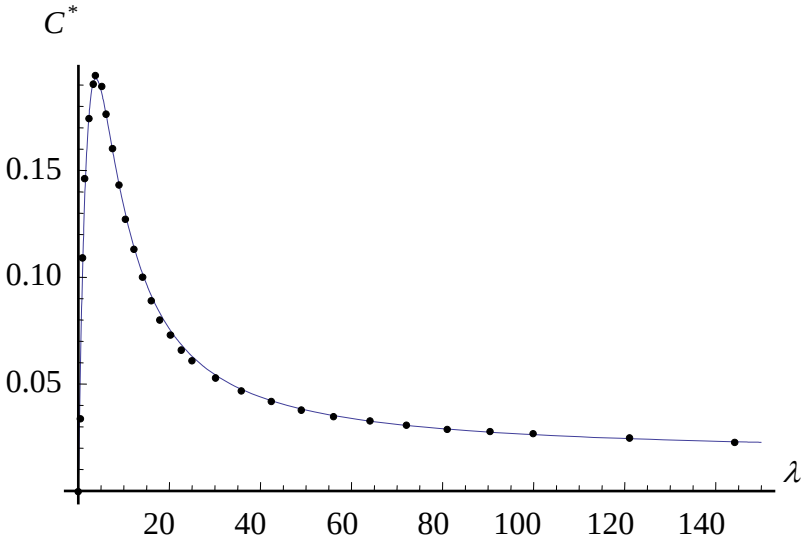

Fig. 3.9. Fitting parameter C^* as a function of λ for $\delta_0 = 5.5$.

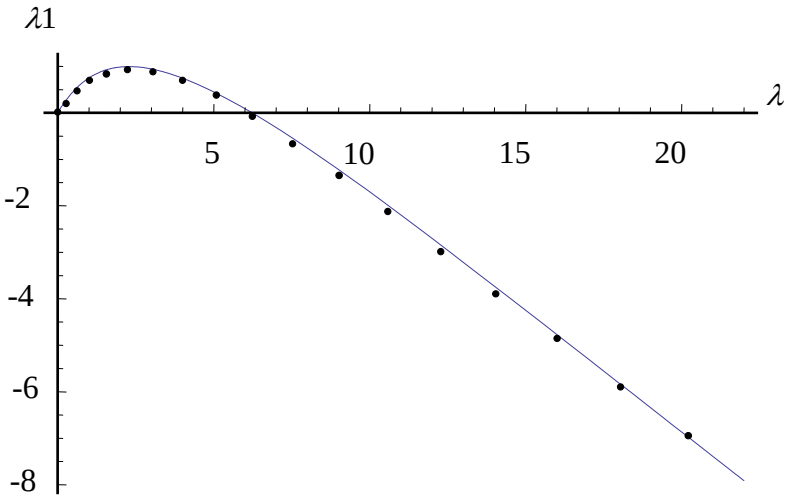

Fig. 3.10. Fitting parameter λ^* as a function of λ for $\delta_0 = 5.5$.

Now we discuss the dependence of the final transition probability $p(+\infty)$ on the parameter λ (see Fig. 3.11). Taking into account Eqs. (3.27), (3.33), (3.45), and (3.46), we arrive at the following asymptotic expression for large values of λ ($\lambda >> \lambda_{\min}$):

$$p(+\infty) = \frac{1}{2} - \frac{0.142782}{\delta_0^{0.491025}} \left(2\sqrt{\frac{\Gamma(\gamma)}{\Gamma(\gamma - 0.5)}} - P_{DK}(\lambda, +\infty) \sqrt{\frac{\Gamma(\gamma_1)}{\Gamma(\gamma_1 - 0.5)}} \right). \qquad (3.50)$$

Numerical simulations show that the fitting parameters γ and γ_1 are of the same order, hence, the expression in the brackets is a positive quantity. This remarkable result shows that in the case when the external field configuration is defined by the DK model, it is impossible to convert all the atoms of the system into molecules. Further, we compare the obtained expression (3.50) with the formula describing the final transition probability in the linear case (3.16). As we see, in the linear case for any value of the detuning parameter δ_0 there exist values of the parameter $\lambda = \lambda_n$ such that $P_{DK}(\lambda_n, +\infty) = 1$. These values λ_n are defined from the condition $\lambda_n = \delta_0^2 + n/2$, where n is an integer number. In contrast to the linear case, in the nonlinear case, it follows from formula (3.50) that for any given δ_0 (recall that $\delta_0 > 1$), it is impossible to find a value of the parameter $\lambda = \lambda_n$ such that $p(\lambda_n, +\infty) = 1$. This limitation in the conversion efficiency can be interpreted as a saturation effect due to the nonlinearity.

Comparison of the suggested analytic formulae for A, C^*, and $p(+\infty)$ with numerically fitted values for $\delta_0 = 5.5$ are shown in the Figures Fig. 3.12-3.14. It is seen that the proposed approximation provides absolute error of the order of 10^{-3} for the final transition probability $p(+\infty)$ (we should keep in mind that this is the result produced by *analytic* approximations (3.45)-(3.47) for the variation parameters A, C^*, λ^*, not the *ansatz* (3.32); the ansatz itself provides much better fit, of the order of 10^{-5}, if the parameters are properly chosen numerically).

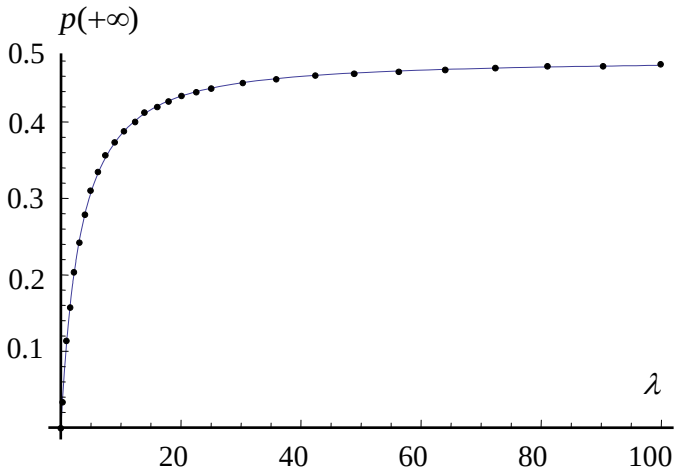

Fig. 3.11. Final transition probability $p(+\infty)$ versus λ for $\delta_0 = 5.5$.

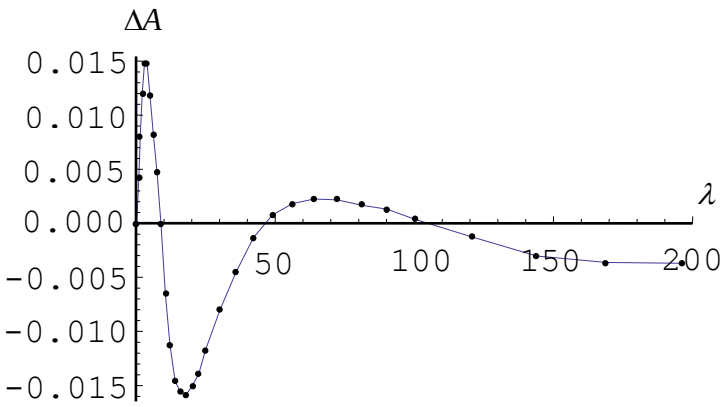

Fig. 3.12. Comparison of formula (3.45) for A with numerically fitted values for $\delta_0 = 5.5$.

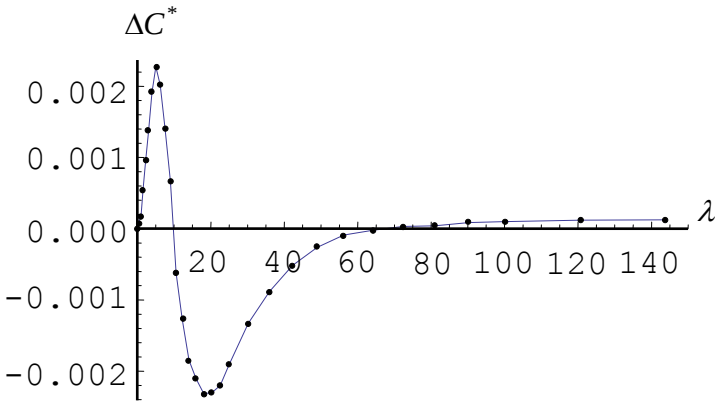

Fig. 3.13. Comparison of formula (3.46) for C^* with numerically fitted values for $\delta_0 = 5.5$.

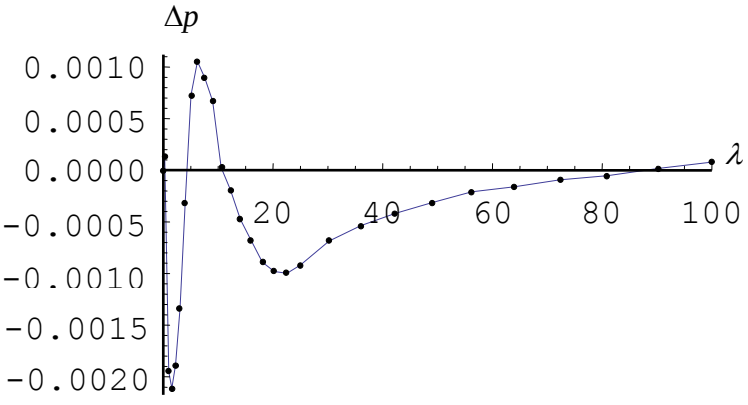

Fig. 3.14. Comparison of formula (3.50) for final transition probability with numerical results.

Summary of Chapter 3

In this chapter, we have studied the second harmonic generation and cold molecule formation using the quasi-linear level-crossing Demkov-Kunike model, characterized by a bell-shaped coupling constant and finite variation of the detuning. Within the framework of the second harmonic generation, the Demkov-Kunike model implies that both second-order susceptibility and wave-number mismatch change along the direction of propagation of interacting waves; while the former function changes according to a hyperbolic-secant law, the latter one varies according to a hyperbolic-tangent law.

Using cold molecule formation terminology, analyzing the case of *large detuning* ($\delta_0 > 1$), we have shown that there exist three different interaction regimes: the *weak coupling* (corresponding to the case when the intensity of the applied laser field is small, $\sqrt{\lambda} << \delta_0$), the opposite *strong coupling* (corresponding to the case of large field intensity, $\sqrt{\lambda} >> \delta_0$) limits, and the intermediate regime, when the detuning and the field amplitude are of the same order. A common feature of the three interaction regimes is that in all these cases the time dynamics of molecule formation is weakly-oscillatory if initially the system consists of only atomic Bose-Einstein condensate (only weak, damped oscillations between the atomic and molecular populations are observed and that occurs only after the resonance has been crossed). Using an exact third-order nonlinear differential equation for the molecular state probability, we have developed an effective variational method which has enabled us to construct a highly accurate approximate solution of the problem, which is equally applicable for the description of the association process in all the mentioned interaction regimes of the large-detuning case.

We have shown that the approximate expression for the molecular state probability can be represented as a sum of two distinct terms. The first term is defined as a solution to the limit first-order *nonlinear* differential equation, while the second one is a scaled solution to the *linear* DK problem with modified parameters. The constructed solution incorporates three auxiliary fitting parameters, A, C^*, and λ^*, the appropriate choice of which ensures that it provides an accurate approximation. First, we have analytically found asymptotic expressions for these parameters in the

case of vanishingly weak ($\lambda << 1$) and very strong laser field intensity ($\lambda >> 1$). Further, taking into account the obtained asymptotic expressions, we have combined analytical and numerical methods to find expressions for the fitting parameters $A(\lambda, \delta_0)$, $C^*(\lambda, \delta_0)$, and $\lambda^*(\lambda, \delta_0)$, valid in the whole range of variation of λ.

Studying the behavior of the fitting parameter A, we have revealed the main characteristics of the three interaction regimes. In the weak interaction regime, corresponding to small values of the input parameter λ, the fitting parameter A abruptly increases first following the linear asymptote $\lambda/2$ and then deviates from it, always remaining smaller than $\lambda/2$. It can be shown that such a behavior of the parameter A is common for all the level-crossing models. Hence, we conclude that the specific character of a model is not strongly revealed in the weak coupling regime. For this reason, we refer to the weak interaction limit $\lambda << 1$ as the *fundamental limit* of weak coupling regime. Studying further the behavior of the function $A(\lambda)$ we see that there exists an interval $\lambda \in (\lambda_{\max}, \lambda_{\min})$ where the parameter A rapidly decreases. We refer to this regime as the intermediate interaction regime. Finally, we have seen that for $\lambda > \lambda_{\min}$ which corresponds to the strong interaction regime the function A increases linearly with λ.

Further analysis of the function $A(\lambda)$ has shown that the transitional region between the weak and strong interaction limits can be approximated as a sum of the hyperbola β_0/λ, a constant, and a linear function. Comparing this decomposition with the results for the LZ model, we see that in the case of the LZ model the asymptotic behavior of the parameter A for $\lambda >> 1$ is given as a hyperbola, $4/(9\lambda)$, only. For this reason, the hyperbola in the asymptotic expansion of A can be interpreted as the LZ "imprint", while the "true individuality" of the DK model is related to the linear in λ term of the asymptotic expansion for $A(\lambda)$. This term mostly manifests itself in the strong interaction limit $\lambda >> \lambda_{\min}$ where it becomes the leading asymptotic term.

Examining the role of the different terms in the approximate expression for the molecular state probability, we have seen that in the strong coupling limit the first term, being a solution to the limit nonlinear equation, effectively describes the process of the molecule formation while the

second one, being a scaled solution to the *linear* DK problem (but now with *negative* effective λ^* in the strong coupling limit), describes the oscillations which come up some time after the system has passed through the resonance. From this, one can conclude that in the strong coupling limit the dynamics of the system consists of the process of nonlinear resonance crossing followed by coherent oscillations that are principally of linear nature. The possibility to make such decomposition is not trivial since the Hamiltonian of the system is essentially nonlinear.

The constructed approximation describes the process with high accuracy. The ansatz provides an approximation whose absolute error is less than $3\cdot10^{-5}$ for the final transition probability. For arbitrary time points, its absolute error is commonly of the order of 10^{-4}, and for the points of the first few maxima and minima of the function $p(t)$ (at certain values of the input parameters λ and δ_0) it may increase up to 10^{-3}.

Using the constructed approximation one can readily find the main characteristics of the process such as the tunneling time, the frequency of the oscillations that start soon after the crossing of the resonance, as well as the conversion efficiency. For example, studying the final conversion efficiency, we have seen that in the case when the external field configuration is defined by the Demkov-Kunike model, it is impossible to achieve 100% conversion. This limitation on the conversion efficiency can be interpreted as saturation caused by the nonlinearity. In this connection it is interesting to recall the predictions made by the constant-amplitude linear level-crossing Landau-Zener model according to which the conversion efficiency asymptotically tends to 100% with coupling growing infinitely or, equivalently, sweep rate decreasing infinitesimally. It might be concluded that this substantial difference in the obtained results is caused by the configuration effects. Since the configuration defined by the Demkov-Kunike model is physically realizable, in contrast to that defined by the Landau-Zener model, we conclude that the Demkov-Kunike model provides more accurate description of system's dynamics.

MAIN RESULTS

- An analytical theory describing second harmonic generation with high accuracy was constructed for the Landau-Zener model characterized by phase mismatch linearly varying in the direction of fundamental mode propagating through infinite medium with constant nonlinearity.
- It was shown, that the growth of the conversion coefficient is mostly governed by an essentially nonlinear first order differential equation, while the damped oscillations of harmonics' intensities occurring after the resonance crossing are characterized by a scaled solution of an analogous linear problem.
- It was demonstrated, that, despite expectations, the scaled solution of the analogous linear problem, which is the part of the approximate solution of the nonlinear Landau-Zener model for SHG, in the strong interaction region is described by a negative effective Landau-Zener parameter.
- It was shown, that the scaling factor of the linear solution involved in the variational ansatz is determined by the auxiliary parameter of the solution of the nonlinear limit equation, which indicates that the nonlinearity of the problem is directly expressed in this term as well.
- A two-term ansatz describing, with high accuracy, the spatial dynamics of the conversion coefficient at second harmonic generation through the first Demkov-Kunike configuration is constructed for the relatively large finite values of phase mismatch.
- The appropriate choice of the variational parameters involved in the proposed ansatz ensures that the constructed approximation describes the numerical solution of the problem with absolute accuracy higher than 10^{-3}.
- It was shown, that in the case of large nonlinearities one of the terms of the ansatz effectively describes the resonance crossing, and the other term describes the damped oscillations of second harmonic's intensity, which are observed soon after the resonance crossing
- It was revealed, that during second harmonic generation through the Demkov-Kunike model with large finite values of phase mismatch, the spatial dynamics of conversion coefficient has three distinct behavioral regions corresponding to weak, medium and strong nonlinearities.

APPENDIX 1

Any electromagnetic process in the medium is described by Maxwell's equations:

$$\nabla \times \mathbf{E} = -\frac{1}{c}\frac{\partial \mathbf{B}}{\partial t}, \quad \nabla \cdot \mathbf{B} = 0 \tag{A1.1}$$

$$\nabla \times \mathbf{H} = \frac{4\pi}{c}\mathbf{j} + \frac{1}{c}\frac{\partial \mathbf{D}}{\partial t}, \quad \nabla \cdot \mathbf{D} = 4\pi\rho \tag{A1.2}$$

where $\mathbf{E}$ and $\mathbf{H}$ are intensities of electric and magnetic fields, $\mathbf{D}$ and $\mathbf{B}$ are electric and magnetic field inductions, ρ is electric charge density, $\mathbf{j}$ is current density. The constitutive relations, which specify the response of bound charge and current to the field are:

$$\mathbf{D} = \mathbf{E} + 4\pi\mathbf{P}, \tag{A1.3}$$

$$\mathbf{B} = \mathbf{H} + 4\pi\mathbf{M}, \tag{A1.4}$$

$$\mathbf{j} = \sigma\mathbf{E}, \tag{A1.5}$$

where $\mathbf{P}$ and $\mathbf{M}$ are polarization and magnetization of medium.

If we neglect the magnetic response of the medium, that is if we consider $\mathbf{M} = 0$, the optical response of a material is characterized in terms of the induced polarization $\mathbf{P}$. For a linear material the relation between the polarization and the electric field $\mathbf{E}$ of the incident radiation is linear:

$$\mathbf{P} = \varepsilon_0 \chi^{(1)}\mathbf{E}, \tag{A1.6}$$

where $\chi^{(1)}$ is the linear susceptibility. In nonlinear optics, the response of the material can be described as a Taylor expansion of the material polarization $\mathbf{P}$ in powers of the electric field $\mathbf{E}$:

$$\mathbf{P} = \varepsilon_0 \sum_n \chi^{(n)}\mathbf{E}_n = \varepsilon_0 \chi^{(1)}\mathbf{E} + \varepsilon_0 \chi^{(2)}\mathbf{E}^2 + \varepsilon_0 \chi^{(3)}\mathbf{E}^3 + ..., \tag{A1.7}$$

where $\chi^{(n)}$ corresponds to the tensor of the n-th order nonlinear process.

Now we derive the equation for the generation of second harmonic. From Eq. (A1.4) we have $\mathbf{B} = \mathbf{H}$. Applying ∇ operation to both left-hand and right-hand sides of equation (A1.1), we get

$$\nabla \times \nabla \times \mathbf{E} = -\frac{1}{c}\frac{\partial \nabla \mathbf{B}}{\partial t} = -\frac{1}{c}\frac{\partial \nabla \mathbf{H}}{\partial t} \tag{A1.8}$$

Combining equations A1.2, A1.3 and A1.8, and considering $\mathbf{j} = 0$, we obtain:

$$\nabla \times \nabla \times \mathbf{E} = -\frac{1}{c^2}\frac{\partial^2 \mathbf{E}}{\partial t^2} - \frac{4\pi}{c^2}\frac{\partial^2 \mathbf{P}}{\partial t^2} \tag{A1.9}$$

Let us decompose the polarization into two parts:

$$\mathbf{P} = \mathbf{P}^{\mathrm{L}} + \mathbf{P}^{\mathrm{NL}}, \tag{A1.10}$$

where $\mathbf{P}^{\mathrm{L}}$ depends linearly on the electric field, and $\mathbf{P}^{\mathrm{NL}}$ term is a nonlinear part of polarization.

Considering $\mathbf{P}^{\mathrm{L}} = \chi_0 \mathbf{E}$ and $\varepsilon_0 = 1 + 4\pi\chi_0$, we obtain:

$$\frac{1}{c^2}\frac{\partial^2 \mathbf{E}}{\partial t^2} + \frac{4\pi}{c^2}\frac{\partial^2 \mathbf{P}^{\mathrm{L}}}{\partial t^2} = \frac{1}{c^2}\frac{\partial^2 (\mathbf{E} + 4\pi \mathbf{P}^{\mathrm{L}})}{\partial t^2} = \frac{1}{c^2}\frac{\partial^2 \mathbf{E}(1 + 4\pi\chi_0)}{\partial t^2} = \frac{\varepsilon_0}{c^2}\frac{\partial^2 \mathbf{E}}{\partial t^2}. \tag{A1.11}$$

Then Equation A1.9 is rewritten as follows:

$$\nabla \times \nabla \times \mathbf{E} + \frac{\varepsilon_0}{c^2}\frac{\partial^2 \mathbf{E}}{\partial t^2} = -\frac{4\pi}{c^2}\frac{\partial^2 \mathbf{P}^{\mathrm{NL}}}{\partial t^2}. \tag{A1.12}$$

Let the spatial variation of the electric field and nonlinear polarization be only in direction of one of the axes (for instance, *z* axis). Then

$$\nabla \times \nabla \times \mathbf{E} = -\frac{\partial^2 \mathbf{E}}{\partial z^2} \tag{A1.13}$$

and equation (A1.12) becomes

$$\frac{\partial^2 \mathbf{E}}{\partial z^2} - \frac{\varepsilon_0}{c^2}\frac{\partial^2 \mathbf{E}}{\partial t^2} - \frac{4\pi}{c^2}\frac{\partial^2 \mathbf{P}^{\mathrm{NL}}}{\partial t^2} = 0. \tag{A1.14}$$

Let us assume we have a monochromatic wave of frequency ω perpendicularly falling on the surface $z = 0$ of the half-infinite medium $z > 0$. We suppose that waves with a fundamental frequency ω and its harmonics can propagate in the medium.

The propagating waves in the medium can be written in the following form:

$$\mathbf{E}_r = \mathbf{E}^{(r)}(z)e^{-i\omega t} + \mathbf{E}^{(-r)}(z)e^{i\omega t}, \tag{A1.15}$$

where $\mathbf{E}^{(-r)}(z) = (\mathbf{E}^{(r)}(z))^*$, and the dependence of polarization and electric field are given by equation (A1.2). Considering only the second order dependence, for polarization components we

have:

$$P_k^{\mathrm{NL}} = \sum_{j,k,r,s} \chi_{ijk}(\omega_r, \omega_s) E_i^{(s)} E_j^{(r)} e^{-i(\omega_s+\omega_r)t}, \tag{A1.16}$$

where ω_s and ω_r can have both negative and positive values, indexes r and s differ the waves in the medium by their frequencies.

For second harmonic generation we are interested in the polarization components on the fundamental ω and second harmonic 2ω frequencies. For clarity we will consider, that the field with the fundamental frequency is along some direction b, and the field of second harmonic is along the direction a. Then from the equation A1.16, we will obtain that the non-linear polarization on the second harmonic is:

$$P_a^{\mathrm{NL}} = \chi_{abb}(\omega,\omega)(E_b^{(1)})^2 e^{-2i\omega t} + \chi_{abb}(-\omega,-\omega)(E_b^{(-1)})^2 e^{2i\omega t}, \tag{A1.17}$$

and non-linear polarization on the fundamental frequency:

$$P_b^{\mathrm{NL}} = 2\chi_{bab}(-2\omega,\omega) E_a^{(-2)} E_b^{(1)} e^{i\omega t} + 2\chi_{bab}(2\omega,-\omega) E_a^{(-2)} E_b^{(-1)} e^{-i\omega t}. \tag{A1.18}$$

In A1.18 the factor 2 arises due to the existence of two similar terms containing $e^{i\omega t}$ and $e^{-i\omega t}$ in the equation (A1.16), when we take $\omega_s = \omega,\ \omega_r = 2\omega,$ and $\omega_r = -\omega,\ \omega_s = 2\omega.$

After incorporating new quantities $A_r(z)$ and $A_r^*(z)$:

$$\begin{aligned} E^{(r)} &= A_r(z) e^{ik_r z}, \\ E^{(-r)} &= A_r^*(z) e^{-ik_r z}, \end{aligned} \tag{A1.19}$$

then instead of (A1.15) we should write:

$$\mathbf{E}_r = \mathbf{e}_r \left(A_r(z) e^{i(k_r z - \omega_r t)} + A_r^*(z) e^{-i(k_r z - \omega_r t)} \right), \tag{A1.20}$$

where $\mathbf{e}_r$ is an elementary vector in the direction of $\mathbf{E}_r$.

If to write the complex quantity $A_r(z)$ as $A_r(z) = |E_r| e^{i\varphi_r(z)}$, where $|E_r|$ is the real value, then for the wave propagating in the medium, we will obtain the following equation:

$$\mathbf{E}_r = \mathbf{e}_r |E_r| \cos[k_r z - \omega_r t + \varphi_r(z)]. \tag{A1.21}$$

In the isotropic case by inserting equations (A1.17) and (A1.18) into the (A1.14) and considering waves in the form of (A1.15), we will obtain the following equations for amplitudes of

wave and its second harmonic by equating the terms for exponents with the same indexes:

$$\frac{\partial^2 E_b^{(-1)}}{\partial z^2} + k_1^2 E_b^{(-1)} + \frac{8\pi}{c^2}\omega^2 \chi_{bab}(-2\omega,\omega) E_a^{(-2)} E_b^{(1)} = 0, \tag{A1.22}$$

$$\frac{\partial^2 E_a^{(2)}}{\partial z^2} + k_2^2 E_a^{(2)} + \frac{16\pi}{c^2}\omega^2 \chi_{abb}(\omega,\omega)(E_b^{(1)})^2 = 0, \tag{A1.23}$$

where $k_1 = \frac{\omega}{c}\sqrt{\varepsilon_0}$, $k_2 = \frac{2\omega}{c}\sqrt{\varepsilon_0}$.

It should be noted, that in this case we obtain two pairs of equations complex conjugated with each other.

Taking into account, that $\chi_{abb}(\omega,\omega) = \chi_{bab}(-2\omega,\omega)$, and incorporating new coefficient $k_\chi = \frac{2\pi}{c^2}\chi_{abb}(\omega,\omega)$, we obtain more compact equations (A1.22)-(A1.23):

$$\frac{\partial^2 E_b^{(-1)}}{\partial z^2} + k_1^2 E_b^{(-1)} + 4\omega^2 k_\chi E_a^{(-2)} E_b^{(1)} = 0, \tag{A1.24}$$

$$\frac{\partial^2 E_a^{(2)}}{\partial z^2} + k_2^2 E_a^{(2)} + 8\omega^2 k_\chi (E_b^{(1)})^2 = 0, \tag{A1.25}$$

Now we will replace complex amplitudes E with corresponding indexes according to the equation (A1.19) and considering that complex amplitudes $A_r(z)$ are varying quite slowly, so that $\frac{\partial A_r}{\partial z} << kA_r$.

By substitution of (A1.19) into the equations (A1.24), (A1.25), we can neglect the second derivatives $\frac{\partial^2 A_r}{\partial z^2}$. Resultant two equations for complex amplitudes could be obtained in the form of a system:

$$\begin{cases} \frac{dA_1^*}{dz} = -i\frac{2\omega^2 k_\chi}{k_1} A_2^* A_1 e^{+i(2k_1-k_2)z}, \\ \frac{dA_2}{dz} = +i\frac{4\omega^2 k_\chi}{k_2} A_1^2 e^{+i(2k_1-k_2)z}. \end{cases} \tag{A1.26}$$

The condition $\frac{\partial A_r}{\partial z} << kA_r$ means quasistationary approximation; meaningful deviation of

the field is noticeable on the distances, far larger than the wavelengths.

Equation (A1.26) can be written the following way:

$$\begin{cases} \dfrac{dA_1}{dz} = i\dfrac{4\pi}{c^2}\dfrac{\omega^2\chi_{abb}(\omega,\omega)}{k_1}A_2A_1^*e^{-i(2k_1-k_2)z}, \\ \dfrac{dA_2}{dz} = i\dfrac{8\pi}{c^2}\dfrac{\omega^2\chi_{abb}(\omega,\omega)}{k_2}A_1^2e^{+i(2k_1-k_2)z}. \end{cases} \quad \text{(A1.27)}$$

APPENDIX 2

Consider equation (2.27) obeyed by the correction term u:

$$\left(\frac{d}{dt}-\frac{1}{t}\right)\left(u_{tt}-\frac{\lambda}{2}(-8u+24p_0u+12u^2)+r\right)+4t^2u_t=0. \qquad \text{(A2.1)}$$

The initial conditions for u are

$$u(-\infty)=0,\quad u_t(-\infty)=0,\quad u_{tt}(-\infty)=0. \qquad \text{(A2.2)}$$

Now, examining Eq. (2.24), we see that since the solution p_{LZ} to the linear LZ problem is a quasi-step-wise function, the remainder r can be presented as a sum

$$r=r_1+r_2+r_3, \qquad \text{(A2.3)}$$

where $r_1=r(-\infty)=\text{const}$, $r_2=r_{20}(1+\tanh(t))/2$ with $r_{20}=r(+\infty)-r(-\infty)=\text{const}$. It is then understood that the last term, r_3, is a relatively small, oscillating quantity. Therefore, supposedly, this term can be neglected.

Furthermore, if the approximate solution p_0 is supposed to be good enough so that $|u|<<p_0\le 1/2 \;\Rightarrow\; |u|<<0.1 \;\Rightarrow\; u^2<<|u|$, then we can linearize equation (2.27) by neglecting the quadratic term $12u^2$. Then, since the remaining equation is linear, we may expect that $u(r)\approx u_1(r_1)+u_2(r_2)+u_3(r_3)$, where u_1, u_2 and u_3 are the solutions to the linearized equations written for the remainders r_1, r_2 and r_3, respectively, satisfying the same initial conditions (A2.2). We have mentioned above that r_3 is expected to be small as compared to r_1 and r_2. Moreover, since it is also an oscillating function, then $u_3(r_3)$ should be small as compared to $u_1(r_1)$ and $u_2(r_2)$. Numerical experiments confirm this assumption. Therefore, we neglect the term $u_3(r_3)$.

The auxiliary linear differential equations for u_1 and u_2 are

$$\left(\frac{d}{dt}-\frac{1}{t}\right)\left(u_{1tt}-\frac{\lambda}{2}(-8u_1+24p_0u_1)+r_1\right)+4t^2u_{1t}=0, \qquad \text{(A2.4)}$$

$$\left(\frac{d}{dt}-\frac{1}{t}\right)\left(u_{2tt}-\frac{\lambda}{2}(-8u_2+24p_0u_2)+r_2\right)+4t^2u_{2t}=0. \qquad \text{(A2.5)}$$

In the weak interaction limit the probability of molecule formation p is small, hence, the

approximate solution p_0 is also relatively small. This means that we can neglect the term $24p_0u_1$ in equation (A2.4), and, as a result, we will get an equation for u_1 [compare with equation (2.21)]:

$$\left(\frac{d}{dt}-\frac{1}{t}\right)\left(u_{1tt}-\frac{\lambda}{2}\left(-\frac{2r_1}{\lambda}-8u_1\right)\right)+4t^2u_{1_t}=0. \qquad \text{(A2.6)}$$

The exact solution to this equation is $u_1=-r_1p_{LZ}(\lambda)/2\lambda$, therefore $u_1(+\infty)\approx -r_1/(2\lambda)p_{LZ}(\lambda,+\infty)$.

It is also possible to construct a good approximation for the solution to equation (A2.5) for the function u_2. As a result of the construction (using the method "from the inverse") we arrive at the approximation

$$u_2(+\infty)\approx -r_{20}/(4\lambda)p_{LZ}(\lambda,+\infty). \qquad \text{(A2.7)}$$

The behavior of functions $u_1(t)$ and $u_2(t)$ is shown on Fig. A2.1. As it is seen, the correction $u\approx u_1+u_2$ will be significantly suppressed and, hence, u will be essentially suppressed if we require canceling of $u_1(+\infty)$ and $u_2(+\infty)$:

$$u_1(+\infty)+u_2(+\infty)\approx \lim_{t\to+\infty}u\approx 0. \qquad \text{(A2.8)}$$

This condition is equivalent to the relation $r_1/(2\lambda)+r_{20}/(4\lambda)\approx 0$. The latter means that the following equation should hold:

$$r(+\infty)+r(-\infty)\approx 0. \qquad \text{(A2.9)}$$

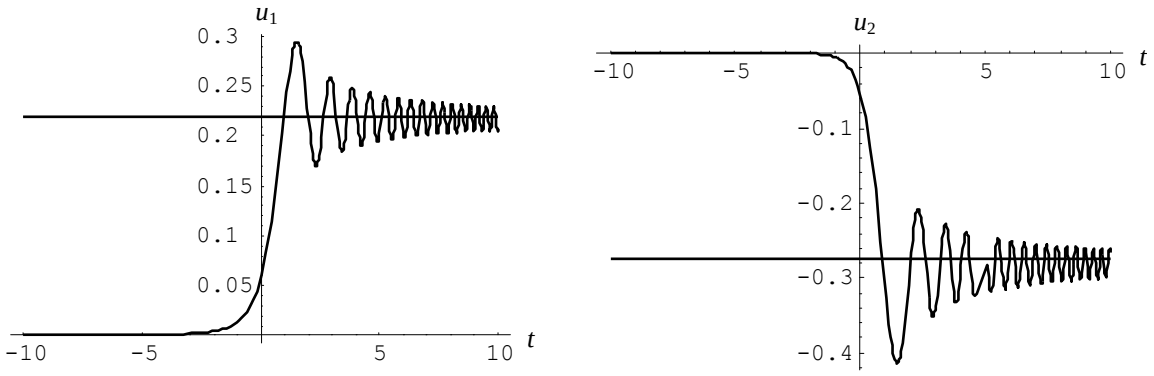

Fig. A2.1. Functions $u_1(t)$ and $u_2(t)$ for $\lambda=0.0625$.

More detailed examination of the roles of r_1, r_2 and r_3 in formation of the correction u shows that for further suppression of the latter we should add in the derived equation a small correction that is of the order of λ^3. Finally, we arrive at the following relation:

$$r(+\infty) + r(-\infty) \approx \frac{\lambda}{2} p_{LZ}^2(+\infty). \tag{A2.10}$$

Explicitly, this equation is written as

$$\begin{aligned} &\left(C_1 \frac{\lambda_1}{2} (4 - 8 p_{LZ}(\lambda_1, +\infty)) - \frac{\lambda}{2} \left(1 - 8 C_1 p_{LZ}(\lambda_1, +\infty) + 12 (C_1 p_{LZ}(\lambda_1, +\infty))^2 \right) \right) + \\ &+ \left(2 C_1 \lambda_1 - \frac{\lambda}{2} \right) - \frac{\lambda}{2} p_{LZ}^2(\lambda_1, +\infty) = 0. \end{aligned} \tag{A2.11}$$

The derived equation is the second equation required for determination of the auxiliary parameters λ_1 and C_1.

PUBLICATIONS

The main results of this dissertation are presented in the following publications

1. H. Azizbekyan, “An ansatz for the nonlinear Demkov-Kunike problem for cold molecule formation”, *J. Contemp. Physics* (Arm. Acad. Sci.), **45** (3), 162-172 (2010).
2. R. Sokhoyan, H. Azizbekyan, C. Leroy, and A. Ishkhanyan, “Demkov-Kunike model for cold atom association: weak interaction regime”, *J. Contemp. Physics* (Arm. Acad. Sci.) **44** (6), 272-277 (2009).
3. N. Sahakyan, H. Azizbekyan, H. Ishkhanyan, R. Sokhoyan, and A. Ishkhanyan, “Weak coupling regime of the Landau-Zener transition for association of an atomic Bose-Einstein condensate”, *Laser Physics* **20** (1), 291-297 (2009).
4. R. Sokhoyan, H. Azizbekyan, C. Leroy and A. Ishkhanyan, “Strong-coupling regime of the nonlinear Landau-Zener problem for photo- and magnetoassociation of cold atoms”, *J. Exp. Theor. Phys.* **112** (4), 543-550 (2011).
5. H. Azizbekyan, T. Shahverdyan, H. Ishkhanyan, R. Sokhoyan, A. Ishkhanyan, “A physically realizable term-crossing model for cold atom association”, Proc. of Conf. Laser Physics-2009, Ashtarak-2, pp. 54-57 (2010).
6. S. Karapetyan, T. Shahverdyan, H. Ishkhanyan, H. Azizbekyan, R. Sokhoyan, A. Ishkhanyan “First Demkov-Kunike model in cold molecule formation: Strong interaction limit of the large detuning regime”, Proc. of Intern. Advanced Research Workshop on "MPOP-2009", pp. 48-52, Yerevan, (2010).
7. N. Sahakyan, H. Azizbekyan, R. Sokhoyan, C. Leroy, Y. Pashayan-Leroy, and A. Ishkhanyan, “Landau-Zener transition for association of an atomic Bose-Einstein condensate with inter-particle elastic interactions included”, Proc. of Conf. Laser Physics-2008, Ashtarak-2, pp. 29-33 (2009).
8. H. Azizbekyan, B. Joulakian, J. Hanssen, A. Ishkhanyan, “Quadratic Nonlinear Landau-Zener problem for cold molecule formation: Strong interaction limit”, Book of Abstracts of Intern. Advanced Research Workshop "MPOP-2009", p. 31, Yerevan (2009).
9. H. Azizbekyan, “Cold molecule formation using Demkov-Kunike field configuration”, Control of Atom and Molecule Ensembles by Light IV, Varna, Bulgaria, pp. 1-2 (2010).
10. H. Azizbekyan, A. Manukyan, A. Ishkhanyan, “Second harmonic generation modeled by the Demkov-Kunike resonance-crossing configuration”, Book of Abstracts, p. 7, Laser Physics 2011, Ashtarak, Armenia (2011).

REFERENCES

1. P. Franken, A. E. Hill, C. W. Peters, and G. Weinreich, “Generation of optical harmonics”, Phys. Rev. Lett. **7**, 118-119 (1961).
2. N. Bloembergen, and P. S. Pershan, “Light Waves at the Boundary of Nonlinear Media”, Phys. Rev. **128**, 606-622 (1962).
3. J. A. Armstrong, N. Bloembergen, J. Ducuing, and P. S. Pershan, “Interaction between light waves in a nonlinear dielectric”, Phys. Rev. **127,** 1916-1939 (1962).
4. N. Bloembergen, and Y. R. Shen, “Quantum-theoretical comparison of nonlinear susceptibilities in parametric media, lasers, and raman lasers”, Phys. Rev. **133**, A37-A49 (1964).
5. A. J. Schell, and N. Bloembergen, “Laser studies of internal conical diffraction. III. Second-harmonic conical refraction in α-iodic acid”, Phys. Rev. A **18**, 2592-2602 (1978).
6. D. A. Kleinman, “Theory of second harmonic generation”, Phys. Rev. **128**, 1761-1775 (1962).
7. J. E. Bjorkholm, “Optical second harmonic generation”, Phys. Rev. **126**, 1452 (1966).
8. H. J. Simon and N. Bloembergen, “Second-Harmonic Light Generation in Crystals with Natural Optical Activity”, Phys. Rev. **171**, 1104–1114 (1968).
9. Y. R. Shen, “Optical Second Harmonic Generation at Interfaces”, Annu. Rev. Phys. Chem**. 50**, 327-350 (1989).
10. M. A. Dreger and J. K. McIver, “Second-harmonic generation in a nonlinear, anisotropic medium with diffraction and depletion”, J. Opt. Soc. Am. B **7**, 776-784 (1990).
11. Y. R. Shen, The Principles of Nonlinear Optics (Wiley, New York, 1984; Nauka, Moscow, 1989).
12. A. Yariv, Quantum Electronics (Wiley, New York, 1989. Sovetskoe Radio, Moscow, 1973);
13. P. N. Butcher and D. Cotter, The Elements of Nonlinear Optics (Cambridge Univ. Press, Cambridge, 1991).
14. A. Fioretti, D. Comparat, A. Crubellier, O. Dulieu, F. Masnou-Seeuws, and P. Pillet, “Formation of cold Cs_2 molecules through photoassociation”, Phys. Rev. Lett. **80**, 4402-4405 (1998).
15. A. N. Nikolov, E. E. Eyler, X. T. Wang, J. Li, H. Wang, W. C. Stwalley, and P. L. Gould, “Observation of Ultracold Ground-State Potassium Molecules”, Phys. Rev. Lett. **82**, 703-706 (1999).
16. J. Weiner, V. S. Bagnato, S. Zilio, and P. S. Julienne, “Experiments and theory in cold and ultracold collisions”, Rev. Mod. Phys. **71**, 1-85 (1999).
17. F. Masnou-Seeuws, and P. Pillet, “Formation of ultracold molecules $T \le 200\mu$K via photoassociation in a gas of lasercooled atoms”, Adv. At. Mol. Opt. Phys. **47**, 53 (2001).
18. W. C. Stwalley, “Stability of Spin-Aligned Hydrogen at Low Temperatures and High Magnetic Fields: New Field-Dependent Scattering Resonances and Predissociations”, Phys. Rev. Lett. **37**, 1628-1631 (1976).
19. E. Tiesinga, B. J. Verhaar, and H. T. C. Stoof, “Threshold and resonance phenomena in ultracold ground-state collisions”, Phys. Rev. A **47**, 4114-4122 (1993).
20. E. Tiesinga, A. J. Moerdijk, B. J. Verhaar, and H. T. C. Stoof, “Conditions for Bose-Einstein condensation in magnetically trapped atomic cesium”, Phys. Rev. A **46**, R1167 (1992).
21. A. J. Moerdijk, B. J. Verhaar, and A. Axelsson, “Resonances in ultracold collisions of ^{6}Li, ^{7}Li, and ^{23}Na,” Phys. Rev. A **51**, 4852 (1995).
22. S. Inouye, M. R. Andrews, J. Stenger, H. -J. Miesner, D. M. Stamper-Kurn, and W. Ketterle, “Feshbach resonances”, Nature (London) **392**, 151-154 (1998).

23. P. Courteille, R. S. Freeland, D. J. Heinzen, F. A. van Abeelen, and B. J. Verhaar, “Observation of a Feshbach Resonance in Cold Atom Scattering”, Phys. Rev. Lett. **81**, 69 (1998).
24. L. D. Landau, Phys. Z. Sowjetunion **2**, 46 (1932).
25. C. Zener, Proc. R. Soc. London, Ser. A **137**, 696 (1932).
26. E. C. G. Stuckelberg, Helv. Phys. Acta. **5**, 369 (1932).
27. E. Majorana, Nuovo Cimento **9**, 45 (1932).
28. N. Demkov and M. Kunike, Vestn. Leningr. Univ. Fis. Khim. **16**, 39 (1969).
29. K.-A. Suominen and B. M. Garraway, “Population transfer in a level-crossing model with two time scales”, Phys. Rev. A **45**, 374-386 (1992).
30. E. Cornell and C. Wieman, “Nobel Lecture: Bose-Einstein condensation in a dilute gas, the first 70 years and some recent experiments”, Rev. Mod. Phys. **74**, 875 (2002).
31. W. Ketterle, “Nobel lecture: When atoms behave as waves: Bose-Einstein condensation and the atom laser”, Rev. Mod. Phys. **74**, 1131 (2002).
32. C. J. Pethick and H. Smith, Bose-Einstein condensation in dilute gases (Cambridge University Press, Cambridge, 2002).
33. C. Chin, R. Grimm, P. Julienne, and E. Tiesinga, “Feshbach Resonances in Ultracold Gases”, Rev. Mod. Phys. **82**, 1225-1286 (2010).
34. L. D. Carr, D. DeMille, R. V. Krems, and J. Ye, “Cold and ultracold molecules: science, technology and applications”, New J. Phys. **11**, 055049 (2009).
35. S. Chu, “Nobel lecture – the manipulation of neutral particles”, Rev. Mod. Phys. **70**, 685-706 (1998).
36. C. N. Cohen-Tannoudji, “Nobel lecture: manipulating atoms with photons”, Rev. Mod. Phys. **70**, 707-719 (1998).
37. W. D. Phillips, “Nobel Lecture: Laser cooling and trapping of neutral atoms”, Rev. Mod. Phys. **70**, 721-741 (1998).
38. M. H. Anderson, J. R. Ensher, M. R. Matthews, C. E. Wieman, and E. A. Cornell, “Observation of Bose-Einstein Condensation in a Dilute Atomic Vapor”, Science **269**, 198-201 (1995).
39. K. B. Davis, M. -O. Mewes, M. R. Andrews, N. J. van Druten, D. S. Durfee, D. M. Kurn, and W. Ketterle, “Bose-Einstein Condensation in a Gas of Sodium Atoms”, Phys. Rev. Lett. **75**, 3969-3973 (1995).
40. C. C. Bradley, C. A. Sackett, J. J. Tollett, and R. G. Hulet, “Evidence of Bose-Einstein condensation in an atomic gas with attractive interactions”, Phys. Rev. Lett. **75**, 1687-1690 (1995).
41. S. Bose, Z. Phys. **26**, 178 (1924).
42. A. Einstein, Sitzungsber. Kgl. Preuss. Akad. Wiss. 3 **(**1925).
43. M. Greiner, C. A. Regal, and D. S. Jin, “Emergence of a Molecular Bose-Einstein Condensate from a Fermi Gas”, Nature **426**, 537-540 (2003).
44. S. Jochim, M. Bartenstein, A. Altmeyer, G. Hendl, S. Riedl, C. Chin, J. Hecker Denschlag, and R. Grimm, “Bose-Einstein condensation of molecules”, Science **302**, 2101-2103 (2003).
45. S. Jochim, M. Bartenstein, A. Altmeyer, G. Hendl, C. Chin, J. Hecker Denschlag, and R. Grimm, “Pure gas of optically trapped molecules created from fermionic atoms”, Phys. Rev. Lett. **91**, 240402 (2003).
46. M. W. Zwierlein, C. A. Stan, C. H. Schunck, S. M. F. Raupach, S. Gupta, Z. Hadzibabic, and W. Ketterle, “Observation of Bose-Einstein Condensation of Molecules”, Phys. Rev. Lett. **91**, 250401 (2003).
47. D. J. Heinzen, R. Wynar, P. D. Drummond, and K. V. Kheruntsyan, “Superchemistry: Dynamics of Coupled Atomic and Molecular Bose-Einstein Condensates”, Phys. Rev. Lett. **84**, 5029-5033 (2000).

48. D. DeMille, "Quantum Computation with Trapped Polar Molecules", Phys. Rev. Lett. **88**, 067901 (2002).
49. K.-A. Brickman Soderberg, N. Gemelke, and Ch. Chin, "Ultracold molecules: vehicles to scalable quantum information processing", New J. Phys. **11**, 055022 (2009).
50. S. Kotochigova, T. Zelevinsky, and J. Ye, "Prospects for application of ultracold $\mathbf{Sr}_2$ molecules in precision measurements", Phys. Rev. A **79**, 012504 (2009).
51. E. R. Meyer and J. L. Bohn, "Prospects for an electron electric-dipole moment search in metastable **ThO** and $\mathbf{ThF}^+$", Phys. Rev. A **78**, 010502(R) (2008).
52. N. R. Claussen, S. J. J. M. F. Kokkelmans, S. T. Thompson, E. A. Donley, E. Hodby, and C. E. Wieman, "Very-high-precision bound-state spectroscopy near a ^{85}**Rb** Feshbach resonance", Phys. Rev. A **67**, 060701(R) (2003).
53. B. C. Regan, E. D. Commins, C. J. Schmidt, and D. DeMille, "New Limit on the Electron Electric Dipole Moment", Phys. Rev. Lett. **88**, 071805 (2002).
54. T. Zelevinsky, S. Blatt, M. M. Boyd, G. K. Campbell, A. D. Ludlow, and J. Ye, "Highly Coherent Spectroscopy of Ultracold Atoms and Molecules in Optical Lattices", Chem. Phys. Chem **9**, 375 (2008).
55. H. R. Thorsheim, J. Weiner, and P. S. Julienne, "Laser-induced photoassociation of ultracold sodium atoms", Phys. Rev. Lett. **58**, 2420-2423 (1987).
56. E. A. Donley, N. R. Claussen, S. T. Thompson, and C. E. Wieman, "Atom–molecule coherence in a Bose–Einstein condensate", Nature **417**, 529-533 (2002).
57. C. A. Regal, C. Ticknor, J. L. Bohn, and D. S. Jin, "Creation of ultracold molecules from a Fermi gas of atoms", Nature **424**, 47-50 (2003).
58. A. Ishkhanyan, J. Javanainen, and H. Nakamura, "A basic two-state model for bosonic field theories with a cubic nonlinearity", J. Phys. A **38**, 3505 (2005); A. Ishkhanyan, J. Javanainen and H. Nakamura, "General approach to the semiclassical two-mode photoassociation theory", Proc. Conf. Laser Physics-2003, 112-115 (2003).
59. A. Ishkhanyan, J. Javanainen, and H. Nakamura, "Landau–Zener transition in photoassociation of cold atoms: strong interaction limit", J. Phys. A **39**, 14887 (2006).
60. A. Ishkhanyan, M. Mackie, A. Carmichael, P. L. Gould, and J. Javanainen, "Landau-Zener problem for trilinear systems", Phys. Rev. A **69**, 043612 (2004).
61. I. Tikhonenkov, E. Pazy, Y. B. Band, M. Fleischhauer, and A. Vardi, "Many-body effects on adiabatic passage through Feshbach resonances", Phys. Rev. A **73**, 043605 (2006).
62. A. P. Itin and P. Törmä, "Dynamics of a many-particle Landau-Zener model: Inverse sweep", Phys. Rev. A **79**, 055602 (2009).
63. E. Altman and A. Vishwanath, "Dynamic Projection on Feshbach Molecules: A Probe of Pairing and Phase Fluctuations", Phys. Rev. Lett. **95**, 110404 (2005).
64. R. A. Barankov and L. S. Levitov, "Dynamical projection of atoms to Feshbach molecules at strong coupling", cond-mat/0506323 (2005).
65. A. Altland and V. Gurarie, "Many body generalization of the Landau-Zener Problem", Phys. Rev. Lett. **100**, 063602 (2008).
66. A. Altland, V. Gurarie, T. Kriecherbauer, and A. Polkovnikov, "Nonadiabaticity and large fluctuations in a many-particle Landau-Zener problem", Phys. Rev. A **79**, 042703 (2009).
67. B. E. Dobrescu and V. L. Pokrovsky, "Production efficiency of Feshbach molecules in fermion systems", Phys. Lett. A **350**, 154-158 (2006).
68. A. P. Itin, A. A. Vasiliev, G. Krishna, and S. Watanabe, "Change in the adiabatic invariant in a nonlinear two-mode model of Feshbach resonance passage", Physica D **232**, 108 (2007).
69. A. P. Itin and P**.** Törmä, "Non-adiabaticity of a many-particle Landau-Zener problem: forward and backward sweeps", eprint arXiv: 0901.4778 (2009).
70. F. G. Tricomi, Integral Equations (Dover, New York, 1985).
71. L. Allen and J. H. Eberly, Optical Resonance and Two-Level Atoms (Willey, New York, 1975).

72. B. W. Shore, Theory of Coherent Atomic Excitation (Willey, New York, 1990).
73. I. I. Rabi, "Space Quantization in a Gyrating Magnetic Field", Phys. Rev. **51**, 652-654 (1937).
74. A. Ishkhanyan, G. P. Chernikov and H. Nakamura, "Rabi dynamics of coupled atomic and molecular Bose-Einstein condensates", Phys. Rev. A **70**, 053611 (2004).
75. N. Rosen and C. Zener, "Double Stern-Gerlach Experiment and Related Collision Phenomena", Phys. Rev. **40**, 502-507 (1932).
76. E. E. Nikitin, Opt. Spectrosk. **13**, 431 (1962); E. E. Nikitin, "Resonance and non-resonance intermolecular energy exchange in molecular collisions", Discuss. Faraday Soc. **33**, 14 (1962).
77. E. E. Nikitin and S. Ya. Umanskii, Theory of Slow Atomic Collisions (Springer, Berlin, 1984); E. E. Nikitin, Adv. Chem. Phys. **5**, 135 (1970).
78. A. Ishkhanyan, "New classes of analytic solutions of the two-level problem", J. Phys. A **33**, 5539–5546 (2000).
79. A. M. Ishkhanyan, "New analytically integrable models of the two-state problem", Optics Commun. **176**, 155-161 (2000).
80. T. Kohler, K. Goral, and P. S. Julienne, "Production of cold molecules via magnetically tunable Feshbach resonances", Rev. Mod. Phys. **78**, 1311-1361 (2006).
81. P. Naidon and F. Masnou-Seeuws, "Photoassociation and optical Feshbach resonances in an atomic Bose-Einstein condensate: Treatment of correlation effects", Phys. Rev. A **73**, 043611 (2006).
82. J. Javanainen and M. Mackie, "Coherent photoassociation of a Bose-Einstein condensate", Phys. Rev. A **59**, R3186 (1999).
83. M. Koštrun, M. Mackie, R. Cote, and J. Javanainen, "Theory of coherent photoassociation of a Bose-Einstein condensate", Phys. Rev. A **62**, 063616 (2000).
84. P. D. Drummond, K. V. Kheruntsyan, and H. He, "Coherent Molecular Solitons in Bose-Einstein Condensates", Phys. Rev. Lett. **81**, 3055-3058 (1998).
85. M. Mackie and J. Javanainen, "Quasicontinuum modeling of photoassociation", Phys. Rev. A **60**, 3174-3187 (1999).
86. A. Carmichael and J. Javanainen, "Mean-field stationary state of a Bose gas at a Feshbach resonance", Phys. Rev. A **77**, 043616 (2008).
87. M. Abramowitz and I. A. Stegun, Handbook of Mathematical Functions (Dover, New York, 1965).
88. A. Ishkhanyan, B. Joulakian, and K.-A. Suominen, "Variational ansatz for the nonlinear Landau–Zener problem for cold atom association", J. Phys. B **42**, 221002 (2009).
89. A.M. Ishkhanyan, "Landau-Zener transition in quadratic-nonlinear two-state systems", Phys. Rev. A **81**, 055601 (2010).
90. N. Sahakyan, H. Azizbekyan, H. Ishkhanyan, R. Sokhoyan, and A. Ishkhanyan, "Weak coupling regime of the Landau-Zener transition for association of an atomic Bose-Einstein condensate", Laser Phys. **20**, 1, 291-297 (2009).
91. R. Sokhoyan, H. Azizbekyan, C. Leroy, and A. Ishkhanyan, "Strong-coupling regime of the nonlinear Landau-Zener problem for photo- and magneto-association of cold atoms", J. Exp. Theor. Phys. **112**, 543-550 (2011).
92. A. Ishkhanyan and H. Nakamura, "Strong-coupling limit in cold-molecule formation via photoassociation or Feshbach resonance through Nikitin exponential resonance crossing", Phys. Rev. A **74**, 063414 (2006).
93. A. Ishkhanyan, A. Manukyan, and B. Joulakian, "Second-Harmonic Generation in a Layer with Variable Susceptibility", Laser Physics **18** (7), 886-893 (2008).
94. R. Sokhoyan, B. Joulakian and A. Ishkhanyan, "Strong nonlinearity regimes of two-mode photoassociation of atomic Bose-condensates", J. Contemp. Physics (Armenian Ac. Sci.), **41** (3), 23-28 (2006).
95. A. Ishkhanyan, B. Joulakian, and K.-A. Suominen, "Two strong nonlinearity regimes in cold molecule formation", Eur. Phys. J. D **48**, 397-404 (2008).

96. A. Ishkhanyan, R. Sokhoyan, K.-A. Suominen, C. Leroy, and H.-R. Jauslin, “Quadratic-nonlinear Landau-Zener Transition for Association of an Atomic Bose-Einstein Condensate with Inter-Particle Elastic Interactions Included”, Eur. Phys. J. D **56**, 421-429 (2010).
97. N. Sahakyan, H. Azizbekyan, R. Sokhoyan, C. Leroy, Y. Pashayan-Leroy, and A. Ishkhanyan, “Landau-Zener transition for association of an atomic Bose-Einstein condensate with inter-particle elastic interactions included”, Proc. of Conf. Laser Physics-2008, Ashtarak-2, pp. 29-33 (2009).
98. A.M. Ishkhanyan, “Generalized formula for the Landau-Zener transition in interacting Bose-Einstein condensates”, Eur. Phys. Lett. **90**, 30007 (2010).
99. V. R. Ghazaryan, “First Demkov-Kunike model in the theory of photoassociation of cold atoms”, J. Contemp. Phys. **40**, 1, 1 (2005).
100. R. Sokhoyan, “Demkov-Kunike model in cold molecule formation: the fast resonance sweep regime of the strong interaction limit”, J. Contemp. Physics (Armenian Academy of Sciences) **45** (2), 51-57 (2010).
101. S. Dürr, T. Volz, A. Marte, and G. Rempe, “Observation of molecules produced from a Bose-Einstein condensate”, Phys. Rev. Lett. **92**, 020406 (2004).
102. E. Hodby, S. T. Thompson, C. A. Regal, M. Greiner, A. C. Wilson, D. S. Jin, E. A. Cornell, and C. E. Wieman, “Production Efficiency of Ultracold Feshbach Molecules in Bosonic and Fermionic Systems”, Phys. Rev. Lett. **94**, 120402 (2005).
103. I. Bloch, J. Dalibard, and W. Zwerger, “Many-body physics with ultracold gases,” Rev. Mod. Phys. **80**, 885–964 (2008).
104. M. Inguscio, W. Ketterle, and C. Salomon, Eds., *Ultracold Fermi Gases*, Proc. the Int. School of Physics “Enrico Fermi”- 2006, Course CLXIV, Varenna (ISO, Amsterdam) 2008.
105. C. Chin, R. Grimm, P. Julienne, E. Tiesinga, “Feshbach resonances in ultracold gases”, Rev. Mod. Phys. **82**, 1225 (2010).
106. R. Sokhoyan, H. Azizbekyan, C. Leroy, and A. Ishkhanyan, “Demkov–Kunike Model for Cold Atom Association: Weak Interaction Regime”, J. Contemp. Phys. (Armenian Ac. Sci.) **44** (6), 272-277 (2009).
107. H. Azizbekyan, T. Shahverdyan, H. Ishkhanyan, R. Sokhoyan, A. Ishkhanyan, “A physically realizable term-crossing model for cold atom association”, Proc. of Conf. Laser Physics-2009, Ashtarak-2, pp. 54-57 (2010).
108. S. Karapetyan, T. Shahverdyan, H. Ishkhanyan, H. Azizbekyan, R. Sokhoyan, A. Ishkhanyan “First Demkov-Kunike model in cold molecule formation: Strong interaction limit of the large detuning regime”, Proc. of Intern. Advanced Research Workshop on "MPOP-2009", p. 48-52, Yerevan, (2010).
109. H. Azizbekyan, “An ansatz for the nonlinear Demkov-Kunike problem for cold molecule formation”, J. Contemp. Physics (Armenian Ac. Sci.), **45** (3), 162-172 (2010).